Copyright Warning & Restrictions

The copyright law of the United States (Title 17, United States Code) governs the making of photocopies or other reproductions of copyrighted material.

Under certain conditions specified in the law, libraries and archives are authorized to furnish a photocopy or other reproduction. One of these specified conditions is that the photocopy or reproduction is not to be "used for any purpose other than private study, scholarship, or research." If a, user makes a request for, or later uses, a photocopy or reproduction for purposes in excess of "fair use" that user may be liable for copyright infringement,

This institution reserves the right to refuse to accept a copying order if, in its judgment, fulfillment of the order would involve violation of copyright law.

Please Note: The author retains the copyright while the New Jersey Institute of Technology reserves the right to distribute this thesis or dissertation

Printing note: If you do not wish to print this page, then select "Pages from: first page # to: last page #" on the print dialog screen

ABSTRACT

DETERMINATION OF PHYSICAL PARAMETERS AFFECTING BIOFILTRATION OF VOCS

by
Steven Matthew Wojdyla

This study dealt with the determination of physical and design parameters affecting the transient behavior of classical biofilters employed in removal of VOCs from airstreams. The column packing material consisted of a mixture of peat and perlite particles (2:3, v:v). The design parameters investigated were the density of the packing material, its porosity, and the void fraction of the filter-bed. The physical parameters investigated were the characteristics of adsorption equilibrium between VOCs and packing material, and the mass transfer coefficients of VOCs to the packing material.

The density of the packing material was found to be 0.679×10^6 g-packing/ m^3-packing, while its capacity for water holding was 0.601 m^3-water/ m^3-packing (i.e., 60% porosity). The void fraction of the filter-bed was determined as 0.324 m^3-air/ m^3-bed.

Batch adsorption equilibrium experiments were performed with single and mixtures of two VOCs. With single compounds, it was found that hydrophobic compounds such as benzene and toluene follow an almost linear isotherm (i.e. a Freundlich isotherm with an exponent almost equal to unity). Hydrophilic compounds such as butanol and ethanol were found to follow a clear Freundlich isotherm with an exponent of approximately 0.5. The adsorption equilibrium of mixtures of benzene and toluene vapors was found to follow the Langmuir-Freundlich isotherm which implies that the two VOCs are involved in a competitive interaction.

Column experiments with airstreams containing benzene, toluene, and their mixtures were performed in the absence of biological activity. Transient data under various inlet concentrations and air flow rates were used in determining the mass transfer coefficient of VOCs to the packing material. The data were successfully described with a mathematical model.

DETERMINATION OF PHYSICAL PARAMETERS AFFECTING BIOFILTRATION OF VOCS

by
Steven Matthew Wojdyla

A Thesis
Submitted to the Faculty of
New Jersey Institute of Technology
in Partial Fulfillment of the Requirements for the Degree of
Master of Science in Chemical Engineering

Department of Chemical Engineering,
Chemistry, and Environmental Science

January 1996

APPROVAL PAGE

DETERMINATION OF PHYSICAL PARAMETERS AFFECTING BIOFILTRATION OF VOCS

Steven Matthew Wojdyla

Dr. Basil C. Baltzis, Thesis Advisor — Date
Professor of Chemical Engineering, NJIT

Dr. Dana E. Knox, Committee Member — Date
Associate Professor of Chemical Engineering, NJIT

Dr. Robert G. Luo, Committee Member — Date
Assistant Professor of Chemical Engineering, NJIT

BIOGRAPHICAL SKETCH

Author: Steven Matthew Wojdyla

Degree: Master of Science in Chemical Engineering

Date: January 1996

Undergraduate and Graduate Education:

Master of Science in Chemical Engineering,
New Jersey Institute of Technology, Newark, NJ, 1996

Bachelor of Science in Chemical Engineering,
New Jersey Institute of Technology, Newark, NJ, 1994

Major: Chemical Engineering

Publications and Presentations:

B.C. Baltzis and S.M. Wojdyla. "Towards a Better Understanding of Biofiltration of VOC Mixtures," 1995 Conference on Biofiltration (an Air Pollution Control Technology), Los Angeles, CA (October 5-6, 1995).

B. C. Baltzis and S. M. Wojdyla, "Characteristics of Biofiltration of Hydrophilic VOC Mixtures," 4th Conference on Environmental Science and Technology, Molyvos, Greece (September 4-7, 1995).

B. C. Baltzis, S. M. Wojdyla, and D. M. Tsangaris, "A Comparative Study on Biofiltration of Single and Mixed Solvent Vapors," AIChE Annual Meeting, Miami Beach, FL (November 12-17, 1995).

B.C. Baltzis and S.M. Wojdyla. "Towards a Better Understanding of Biofiltration of VOC Mixtures," pp. 131-138 in *Proceedings of the 1995 Conference on Biofiltration (an Air Pollution Control Technology)*, D.S. Hodge and F.E. Reynolds, Jr. (eds.), The Reynolds Group, Tustin, CA (1995).

B. C. Baltzis and S. M. Wojdyla, "Characteristics of Biofiltration of Hydrophilic VOC Mixtures," pp. 322-331 (vol. B) in *Proceedings of the 4th Conference on Environmental Science and Technology*, Th. Lekkas (ed.), University of the Aegean Press, Lesvos, Greece, (1995).

B. C. Baltzis, S. M. Wojdyla, and D. M. Tsangaris, "Transient Behavior of Biofilters Removing Hydrophilic Solvent Vapors," 3rd International Symposium on "In Situ and On-Situ Bioreclamation," San Diego, CA (April 24-27, 1995).

This thesis is dedicated to
Douglas Jarvis

ACKNOWLEDGMENT

The author would like to express his sincere gratitude and thanks to his thesis advisor, Dr. Basil C. Baltzis, for his encouragement, support, guidance, and friendship. The author would also like to express thanks to Dr. Kung-Wei Wang, Helen Androutsopoulou, and especially Dr. Zarook Shareefdeen for their expert training, tutelage, and friendship.

The author would like to express thanks to Dr. Robert G. Luo for serving as his committee member, and sincere gratitude to Dr. Dana E. Knox who served as his committee member, acted as his advisor for 4 years with the NJIT Ice Hockey Team, and most importantly was a special friend.

The author appreciates the timely help and support from his fellow students and friends including: Jennifer Stellenberg, Michael Cohen, Christos Mpanias, and Dilip Mandel. Finally the author would like to express his appreciation of the love and support of his family and Miss Sumita Bery, without whom this thesis would never have been finished.

TABLE OF CONTENTS

TABLE OF CONTENTS
(Continued)

LIST OF TABLES

LIST OF FIGURES

LIST OF FIGURES
(Continued)

Figure **Page**

LIST OF FIGURES
(Continued)

Figure **Page**

LIST OF FIGURES
(Continued)

Figure **Page**

NOMENCLATURE

A_S^* : surface area of solids per unit volume of the column (1/m)

C_{Bin} : inlet benzene concentration (g/m^3)

C_{ge} : equilibrium gas concentration of a substance in single compound adsorption (g/m^3)

$C_{k,ge}$: equilibrium gas concentration of substance k in competitive adsorption (g/m^3) (k = i, j)

$C_{k,se}$: equilibrium solids concentration for substance k (k = i, j) in competitive adsorption (g-pollutant/g-packing)

c_j : concentration of substance j in the air at a position h along the column (g/m^3)

c_j^* : equilibrium gas concentration of a pollutant j at the gas/solid interface (g/m^3)

$\bar{c}_j$: dimensionless gas concentration equal to c_j/c_{ji}

$\bar{c}_j^*$: dimensionless equilibrium concentration equal to c_j^*/c_{ji}

$\bar{c}_{j,0}$: dimensionless version of $c_{j,0}$

c_{ji} : value of c_j at h = 0 (g/m^3)

c_{jo} : value of c_j at t = 0 (g/m^3)

c_{jp} : concentration of substance j on the solid particles (g-pollutant adsorbed/ g-packing)

$\bar{c}_{jp}$: dimensionless concentration of the solids equal to $(1-\upsilon)\rho_p c_{jp}/\upsilon c_{ji}$

$c_{jp,0}$: value of c_{jp} at t = 0 (g-pollutant adsorbed/g-packing)

C_{se} : equilibrium concentration of substance j on the solid particles in single compound adsorption (g-pollutant/g-packing)

C_{Tin} : inlet toluene concentration (g/m^3)

D_j : diffusion coefficient of compound j in air (m^2/h)

F : flow rate of airstream (m^3/h)

h : position in the column (m); h = 0 at entrance, h = H at the exit

H : total height of the column (m)

k_ν : constant in Langmuir isotherm ($\nu = 1, 2$)

k_a : mass transfer coefficient of VOCs between gas and the solid surface (m/h)

k_a'' : effective mass transfer coefficient, equal to $A_S^* k_a$ (1/h)

k_d : Freundlich isotherm parameter $(m^3)^n$ $(g\text{-pollutant})^{1-n}$ /(g-packing)

K : inverse of the Freundlich isotherm parameter k_d

n : Freundlich isotherm parameter

N : number of solid particles

n' : parameter of the Langmuir-Freundlich isotherm

q : superficial velocity in a packed column (m/h)

R : effective radius of a solid particle (m)

Re : Reynolds number for packed beds

S : cross sectional area of column (m^2)

SA_{part} : surface area of particles (m^2)

Sc : Schmidt number

t : time (h)

V_{bed} : volume of bed (m^3)

V_p : volume of bed (m^3)

z : dimensionless position in the column (z = h/H)

GREEK SYMBOLS

β : dimensionless parameter, defined as: $k_a A_S^* H/q\upsilon$

δ : coefficient in mass transfer coefficient equation

λ : parameter in the Langmuir-Freundlich isotherm

μ : viscosity of air (kg/(m/h))

ρ : density of the carrier air through the bed (g-air/m^3-air)

ρ_p : density of the packing material (g-packing/m^3-packing)

υ : void fraction of the bed (m^3-air/m^3-bed)

τ : residence time (min)

ψ : dimensionless parameter, defined as: $(1/c_{ji})[nc_{ji}/(1-n)\rho_p k_d]^{(1/n)}$

ζ : dimensionless time, equal to: qt/H

CHAPTER 1

INTRODUCTION

One of the most serious aspects of air pollution is the problem of volatile organic compound (VOC) emissions. These compounds are key contributors to the formation of ground-level ozone and smog and are also potentially harmful to human health. Regulations regarding VOC emissions are becoming increasingly stringent, both at the national and international level. Because gasoline constituents and a wide variety of organic solvents are VOCs, emission regulations are currently affecting industrial operations. However, it is predicted that regulations will soon affect even small businesses such as dry cleaners, gasoline stations, and storage facilities [Baltzis and Wojdyla (1995b)] Two such solvents are benzene and toluene. Benzene and toluene (two compounds studied in the present thesis) are VOCs classified as priority environmental pollutants [EPA (1986)]. They are frequently encountered in industrial operations and contaminated sites, while they are also major components of unleaded gasoline [Baltzis and Shareefdeen (1994), Stuart et al. (1991)].

Biofiltration is a new technology for the elimination of, as well as a viable control option for, dilute concentrations of VOCs [Baltzis and Wojdyla (1995b), Ziminski and Yavorsky (1994)]. Biofiltration is defined as the removal and oxidation of pollutants present in contaminated air, by the use of microorganisms immobilized on a solid support [Androutsopoulou (1994)]. This process may be more accurately described as a gas/liquid phase biofilm process, since a true filtration mechanism does not occur [Shi et al. (1995)]. It has a range of potential applications such as in the flavor, fragrance, food and tobacco industries; solvent using industries; polymer and abrasives industries; soil remediation; pharmaceutical industry; chemical industries and ventilation from waste

water treatment facilities [Androutsopoulou (1994), Ziminski and Yavorsky (1994), Shareefdeen (1994)].

Biofiltration utilizes vapor-phase biological reactors known as biofilters. These are usually open or closed structures containing, in a packed bed configuration, porous solids around which biofilms of organisms are formed [Baltzis and Wojdyla (1995b)]. The process of biofiltration depends on many factors. These factors include: the kinetics of biodegradation of the pollutants, mass transfer of the pollutants and oxygen from the air stream to the biofilm and packing material, fluid flow characteristics in the bed, properties of the solid packing material, pH, moisture content of the bed, and temporal and spatial variation of the biomass in the filter bed [Baltzis and Wojdyla (1995a)].

In recent years, biofiltration has been intensively studied as a means of treating VOCs in an efficient and economical manner. A detailed process understanding is needed for deriving general and optimal engineering design criteria for biofilters. The optimization of biofiltration is facilitated by the use of experimentally validated mathematical models which should be capable of predicting the behavior of biofilters under both steady state and transient conditions [Baltzis and Wojdyla (1995a)].

Shareefdeen and Baltzis (1994) note that biofilter units (since they handle emissions) should be expected to be operating under transient conditions at all times, which makes the understanding of transient conditions essential for the implementation of biofiltration. Androutsopoulou (1994) states that it is the adsorption process which is primarily responsible for the long transients exhibited by biofilter columns. During the course of the study reported in the present thesis, parameters essential to the modeling of transient biofiltration of benzene and toluene were investigated. These included the characteristics of the solid packing material, the adsorption isotherm parameters, and the mass transfer coefficients of benzene and toluene to the packing materials.

The optimal packing material for biofilters is one which provides an optimal adsorption capacity, a good distribution of the gas along the filter bed, minimizes system

headloss and provides an environment suitable for the proliferation of microorganisms which oxidize VOCs [Tahraoui et al. (1994)]. The packing material can have a profound effect on overall removal rates. Devinny (1995) states that previous studies have suggested that the use of highly adsorptive media concentrates the contaminants at the surface of the material, making them more available for biodegradation. Peat has been found to be an effective bed material, and perlite has been added to reduce headloss and prevent formation of "hard clumps" of packing [Seed and Corsi (1994)]. A packing material of a peat and perlite mixture in a 2:3 volume ratio was developed by Shareefdeen et al. (1993), and was also used in the study presented here. The main concern in selecting the peat and perlite mixture was to provide a large surface area for microbial adhesion and efficient mass transfer, along with a minimal pressure drop. Microbial compatibility, low cost and ready availability of the material were also considered [Shareefdeen et al. (1993)].

The term adsorption is used loosely in this study, and it refers to both actual adsorption on the solid packing and absorption of VOCs in the water retained in the pores of the packing [Shareefdeen and Baltzis (1994)]. Under transient biofiltration, equilibrium conditions are not valid, and adsorption needs to be explicitly accounted for in the process modeling. The solution of transient biofiltration models requires knowledge of parameter values, such as the adsorption isotherm parameters and mass transfer coefficients, in addition to those needed for solving the steady state equations [Shareefdeen (1994)]. During transient conditions, the removal rates of the VOCs may be significantly higher, than those under steady-state conditions, due to adsorption, or lower, due to desorption. These phenomena, for single VOC adsorption, can be described by the use of the Freundlich isotherm [Rogers et al. (1980)].

In general, when multicomponent mixtures are considered, the adsorption isotherms of individual components must be supplemented by a quantitative description of the interference or competition for adsorption sites by the other components of the

mixtures [Jacobson et al. (1987)]. This is especially true at high concentrations. Competition phenomena should be explicitly described in deriving isotherms for mixed pollutants [Fritz et al. (1981)]. A way of expressing competitive adsorption is to use a modified version of the Langmuir isotherm [Jacobson et al. (1987), Yen and Singer (1984)]. This modification is known as the Langmuir-Freundlich isotherm [Robinson et al. (1991)].

A biofilter is a packed-bed reactor and can be viewed as such for determination of mass transfer coefficients. The mass transfer coefficient is a value used to describe the rate at which compounds in the gas phase (air) of the biofilter transfer into the solid phase (packing material). This constant depends on a number of physical/chemical properties of both the contaminant compound and the packing material [Hodge (1995)]. Most packed-bed mass transfer equations assume that the mass transfer coefficient of a compound varies with the Reynolds number, raised to a power and the superficial velocity [Kataoka et al. (1973), Jones et al. (1993), Onda et al. (1968), Jennings (1975), Weber, Jr. and Smith (1987)]. The equation used by Jones et al. (1993), is a modified version of the equation developed by Jennings (1975).

The study reported in the present thesis consists of two major parts. In the first part, batch experiments were performed for determining adsorption equilibrium isotherms of VOCs on a biofilter packing material identical to that used in earlier biofiltration studies [Shareefdeen (1994), Androutsopoulou (1994)]. This material was a 2:3 (v:v) mixture of peatmoss and perlite. Experiments were performed with single VOCs and a mixture of two VOCs. Vapors of ethanol, butanol, benzene and toluene were used in the experiments with individual (single) VOCs. Air containing mixtures of benzene and toluene were used in the experiments for determining isotherms of mixed pollutants.

The second part of the study dealt with determining the mass transfer coefficients for the VOCs to the packing material. These were flow through experiments with a small scale packed-bed reactor under various inlet VOC concentrations and air flowrates. The

experimental unit had all the characteristics of a biofilter except for the fact that no biomass was present as the intent was to separate physical from biological processes. These experiments were performed with airstreams containing benzene, toluene, and their mixtures.

Data from the column experiments were analyzed through the use of a modified version of a computer code originally developed by Shareefdeen (1994). Some of the model parameters, such as porosity of the bed, surface area and density of the packing material were also determined or measured during the course of this thesis.

CHAPTER 2

LITERATURE REVIEW

Biofiltration has the potential to become a low cost, effective technology for the elimination of VOCs from air streams [Seed and Corsi (1994), Moretti and Mukhopadhyay (1993), Ottengraf and van den Oever (1983), Ottengraf et al. (1986), Zilli et al. (1993)]. It has proven to be more environmentally friendly than conventional VOC abatement technologies, because it does not give rise to further environmental problems [Zilli et al. (1993)]. The pollutants do not enter another phase but are converted into harmless oxidation products. Zilli et al. (1993) also remark that biofiltration is relatively inexpensive because of low capital and operating costs. This technology has been successfully applied in Germany and the Netherlands in many full scale applications in a wide range of industrial and public sector uses [Leson and Winer (1991)].

Improvement of process conditions, construction of the filters, and composition of the packing materials have led to an extension of the uses of biofilters [Ottengraf et al. (1986)]. Due to a high porosity and hence a low pressure drop of the packing materials, high gas flow rates and high organic loads may be treated [Ottengraf et al. (1986)].

The type of filter bed material has a profound effect on the overall removal rates of the biofilter. Many materials can be used in filter beds including: compost, chicken manure, activated carbon, soil, humus, heather, or brush wood [Baltzis and Shareefdeen (1994), Ottengraf et al. (1986), Tahraoui et al. (1994), Zilli et al. (1993)]. Peat also has been found to be an effective filter bed material for both adhesion of microorganisms and inherent nutrient contents [Seed and Corsi (1994), Ottengraf and van den Oever (1983), Androutsopoulou (1994), Shareefdeen (1994), Ottengraf et al. (1986), Tahraoui et al.

(1994), Shareefdeen et al. (1993), Shareefdeen and Baltzis (1994)], but it also has pore spaces too small for even aeration, leading to channeling, pressure drop and poor contact with the gas phase [Shareefdeen et al. (1993)].

In order to increase bed porosity, inert materials need to be added when peat is used [Seed and Corsi (1994)]. These inert materials are "lightening" agents, which ensure uniform porosity, uniform gas flow, and low pressure drop [Ziminski and Yavorsky (1994)]. Lightening agents include: glass spheres, polystyrene spheres, heather, bark, gypsum and perlite [Ziminski and Yavorsky (1994), Tahraoui et al. (1994), Seed and Corsi (1994), Baltzis and Shareefdeen (1994)]. Perlite was selected by both Shareefdeen (1994) and Androutsopoulou (1994) in their biofilter studies. A peat and perlite mixture in a volume ratio of 2:3 was found to be optimal according to Shareefdeen et al. (1993). The addition of perlite assured that virtually every peat particle had good contact with the flow of the gas. The effectiveness of the air-media contact can be quantified by the actual bed detention time and the pressure drop. Both of these factors depend on the free air space of the biofilter media, which is a function of the porosity and the moisture content [Pinnette et al. (1995b)].

It has been proven essential to maintain a certain humidification level in biofilters. An insufficient supply of water, dries up the bed and results in deactivation of the microorganisms and channeling, while an excess of water promotes the development of anaerobic zones [Ottengraf and van den Oever (1983)]. A moisture content of less than 45% will limit microbial activity reducing treatment performance [Pinnette et al. (1995a)]. The most commonly recommended humidity range for a biofilter is 50-70% [Ottengraf and van den Oever (1983), Zilli et al. (1993), Shareefdeen (1994), Androutsopoulou (1994)]. To maintain a desired level of humidity in a filter bed is not an easy task. Factors such as insufficient humidification of the inlet air stream and temperature increases due to either weather variations or the exothermicity of the

biological oxidation of the pollutants can and do lead to a dry column. Complete humidification of the incoming airstream is imperative while periodic water addition to the filter packing has been also recommended.

Shareefdeen (1994) and Androutsopoulou (1994) humidified the biofilter inlet air stream by simply bubbling the air into a water reservoir. Others recommend using a counter-current humidification packed tower [Ottengraf and van den Oever (1983), Ziminski and Yavorsky (1994), Seed and Corsi (1994)]. Tahraoui et al. (1994) also recommend, in addition to the humidification tower, a down flow of the air stream in the biofilter to maximize the moisture content of the filter bed and to ease the addition of water, when such addition is needed. Androutsopoulou (1994) has reported that in most cases, prehumidification of the inlet air stream was enough to maintain proper moisture levels in the (experimental scale) filter-bed.

Baltzis and Shareefdeen (1994) state that future development of biofiltration models will need consideration of the adsorption process, if one wants to describe transient operation. They found that transient biofilter performance is significantly affected by adsorption/desorption effects [Baltzis and Wojdyla (1995b)]. Also in a theoretical study conducted by Cohen (1996), it was determined that the mass transfer coefficient and void fraction of the bed have an enormous impact on transient biofiltration. Under transient conditions, increases in the VOC concentration in the air stream directed to a biofilter lead to a temporarily high level of removal, higher than the eventual steady state level. This is due to adsorption of VOCs on the packing. Decreases in the VOC concentration in the air stream lead to the opposite behavior, i.e., temporarily low levels of removal. This occurs because at steady-state the adsorption of the pollutant is in equilibrium, but when the concentration is changed the adsorption equilibrium shifts and causes a change in the removal rate. In some cases of inlet concentration decrease, it has been observed that the removal rate is negative. This occurs because desorption leads to an exit concentration higher than the inlet concentration [Androutsopoulou (1994)].

Adsorption isotherms have long been a focus of investigation in chemical engineering for process design [Jacobson et al. (1987)]. The most useful way to present adsorption data is through the use of an adsorption isotherm. An adsorption isotherm is an expression of the equilibrium distribution between the concentration of a pollutant on the adsorbent surface and the concentration in the surrounding gas [Banerjee (1988)]. Many types of isotherms have been developed, but the ones most commonly used are the Langmuir and the Freundlich isotherms, which were introduced about 70 years ago [Kinniburgh (1986)]. The Langmuir isotherm may not well represent single component adsorption data [Golshan-Shirazi (1991)]. Shareefdeen (1994) used the Freundlich isotherm for his transient toluene biofiltration modeling. The Freundlich isotherm contains adjustable parameters which are normally determined through linear regression [Kinniburgh (1986)].

Adsorption of mixed pollutants is a topic which has not been widely studied in the literature. Jacobson et al. (1987) state that when several sorbable compounds are present in a mixture, they mutually influence the adsorption of one another in a competitive mode. This interference can be described by a modification of the isotherm of a compound. In biofiltration of mixtures one is interested in the competitive sorptive behavior of mixed pollutants under flow conditions. However, Stuart et al. (1991) have found that isotherms of mixtures obtained under batch conditions can be used in accurately predicting the competitive sorption under flow conditions. Competitive adsorption can be described by isotherms following either the competitive Langmuir equation [Yen and Singer (1984)] or a hybrid of the Freundlich and Langmuir equations [Robinson et al. (1991)].

A parameter which is essential in modeling the transient behavior of biofilters is the mass transfer coefficient of the VOCs to the solid packing material. This parameter is often calculated from one of a number of semi-empirical correlations. Most of these correlations involve the Reynolds, Sherwood, and Schmidt numbers [Weber and Smith

(1987)]. Specific to biofilters would be a relationship for mass transfer in a packed bed. Correlations for packed beds have been proposed by various researchers. Those proposed by Kataoka et al. (1973), Jennings (1975), Onda et al. (1968), and Jones et al. (1993) involve the void fraction of the bed, the superficial air velocity, and the Reynolds and Schmidt numbers raised to various powers. Other correlations discussed by Weber and Smith (1987) involve, in addition to the aforementioned parameters, the Sherwood number. It should be mentioned that the aforementioned correlations are for cases involving liquid phases and have never been tested for the case of biofilters, something which was done during the course of the work presented in this thesis.

CHAPTER 3

OBJECTIVES

The overall objective of this study was to determine parameter values needed for an accurate description and modeling of biofiltration of VOCs under transient conditions in a bed packed with peatmoss and perlite particles. As many of these parameters depend on the identity of the VOCs, model compounds had to be selected. Due to the wide interest in BTEX (benzene, toluene, ethylbenzene, xylene) mixtures, most of the work was performed with benzene and toluene. The specific objectives were as follows:

I. Determination of adsorption isotherms for single VOCs.

This objective was met by performing batch adsorption experiments with air containing vapors of one of the following compounds: benzene, toluene, ethanol, and butanol. As discussed in the first part of Chapter 5, it was found that all compounds follow the Freundlich isotherm.

II. Determination of adsorption isotherms for mixed VOCs.

This objective was met by selecting a case involving two pollutants. Mixtures of benzene and toluene were selected as the model system. Batch experiments have revealed that the two pollutants are involved in a competitive interaction. Their isotherms were described by the Langmuir-Freundlich equation which reduces to the Freundlich isotherm determined under objective I, when the concentration of the second pollutant is set equal to zero. This part of the study is presented in the second part of Chapter 5.

III. Determination of characteristics of the filter-bed.

Transient biofiltration as well as mere adsorption of VOCs depend on some physical characteristics of the filter bed. Such characteristics include the void fraction of the bed, surface area available for mass transfer, density of the packing material, capacity of the material for water holding (porosity packing), and effective radius of packing. Experiments discussed in the first part of Chapter 6 have led to the determination of all aforementioned parameters for the packing of interest (peat:perlite, 2:3, v:v).

IV. Determination of the mass transfer coefficient.

The objective here was to determine if existing correlations can be used in predicting the mass transfer coefficient of VOCs to the filter packing material of interest. It was met by performing experiments with an uninoculated and sterilized filter. This way, mass transfer to the packing was decoupled from biodegradation. Experiments were performed with air streams containing benzene, toluene, and their mixtures under various conditions for the air flowrate (or residence time) and concentration(s) of the pollutant(s) in the inlet air streams. Transient data were analyzed through a modification of a model and computer code developed by Shareefdeen (1994). For this analysis, mass transfer coefficient values were predicted through a modification of existing correlations. This part of the study is discussed in the second part of Chapter 6.

CHAPTER 4

MATERIALS AND METHODS.

4.1 Materials

All experiments were performed with mixtures of peat and perlite at 2:3 volume ratio. The perlite (Peter's Professional Perlite) was horticultural grade, and needed no additional maintenance. The peat (Canadian Sphagnum, Hyponex Corp., Marysville OH) was screened through a #20 standard wire mesh sieve. The resulting peat was autoclaved; the peat needed to be steam-sterilized because it contains considerable microbial activity.

Although experiments were performed in the absence of microbial activity, care was taken so that all other conditions were the same as in an actual biofilter. Hence, the solids were mixed with an amount of mineral medium equal -in volume- to 30% of the mixture of the solids. As discussed in Chapter 6, this amount of liquid fills 50% of the pore space of the solids.

The mineral medium consisted of two solutions: Solution A and Solution B (Table 4-1). After autoclaving both solutions separately, 1% of Solution B was added to Solution A.

Experiments were performed with butanol, ethanol, benzene and toluene. All were ACS certified, grade A obtained from Fisher Scientific (Springfield, NJ).

4.2 Analytical

Monitoring of VOC concentrations was performed through gas chromatographic (GC) analysis of air samples. Benzene and toluene concentrations were measured using a Hewlett Packard Model 5890 (series II, Paramus, NJ) gas chromatograph equipped with a 6' x 1/5" stainless steel column packed with 5%SP-1200/ 5% Bentone 34 on 100/120

Table 4-1 Medium composition

Compound	Amount
Solution A.	
Na_2HPO_4	4 g
KH_2PO_4	1.5 g
NH_4Cl	1 g
$MgSO_4 \cdot 7H_2O$	0.2 g
Distilled water	1 L
Solution B	
$FeNH_4$-citrate	0.05 g
$CaCl_2$	0.1 g
Distilled water	100 ml

Supelcoport packing (Supelco, Bellefonte, PA), and a flame ionization detector. Operating conditions were: injector temperature 120°C, oven temperature 90°C, detector temperature 200°C, and carrier gas (N_2) flow rate 21 mL/min. Under these conditions, the retention times of benzene and toluene were 1.8 and 3.2 minutes, respectively.

Ethanol and butanol concentrations were measured using a Hewlett Packard Model 5890 (series II, Paramus, NJ) gas chromatograph equipped with a 6' x 1/8"x 2 mm stainless steel Chromosorb 108 80-100 mesh column (Chrompack, Inc., Bridgewater, NJ), and a flame ionization detector. Operating conditions were: injector temperature 200°C, oven temperature 180°C, detector temperature 220°C, and carrier gas (N_2) flow rate 40 mL/min. Under these conditions, the retention times of ethanol and butanol were 1.8 and 5.1 minutes, respectively.

Calibration curves were prepared by injecting precise amounts of each solvent into sealed 160 mL serum bottles with a 10 or 50 μL liquid syringe (Hamilition Co., Reno, NV). The bottles were sealed with gray butyl Teflon faced stoppers (224100-175, Wheaton Glass, Millville, NJ) and aluminum crimp caps (224183-01, Wheaton Glass, Millville, NJ). The solvents were allowed to evaporate, and then 0.25 mL samples were taken using a 1 mL Pressure-Lok® syringe (Series A-2, Supelco, Bellefonte, PA) and

injected into the GC. GC calibration was repeated every two weeks or as necessary. A sample set of calibration curves for benzene, toluene, ethanol, and butanol is given in Appendix A-1.

4.3 Batch Adsorption Experiments

For the determination of adsorption isotherms, several serum bottles were prepared by loading 10 g of the packing material (peat, perlite, and medium) and injecting the head space of the bottle with different amounts of the solvent or solvent mixture of interest. These solvents were removed from sealed ("concentration") serum bottles (prepared as in the case of GC calibration discussed above) containing known amounts of vapor of the solvent(s) of interest. "Concentration" bottles containing benzene/toluene mixtures needed - in some cases- to be warmed slightly in order to evaporate the solvents.

After injection, the packing material containing bottles were left to come to equilibrium (5-7 days), and then 0.25 mL gas samples were taken using a 1 mL Pressure-Lok® syringe and injected into the GC. Several samples were taken over two days to ensure that equilibrium was achieved.

Each experiment was performed in duplicates. It was also determined that benzene, toluene, ethanol, and butanol do not adsorb to the surface of the walls of the serum bottles, from experiments where the solvents were injected into empty bottles and no change in concentration occurred over the duration of the experiment.

4.4 Column Experiments

Determination of mass transfer coefficients was based on transient VOC concentration data obtained in a unit the schematic of which is given in Figure 4.1.

The heart of the unit was a glass manifold with 4 evenly spaced sampling ports (Ace Glass Inc., Vineland, NJ). Its dimensions were 5 cm diameter and 60 cm

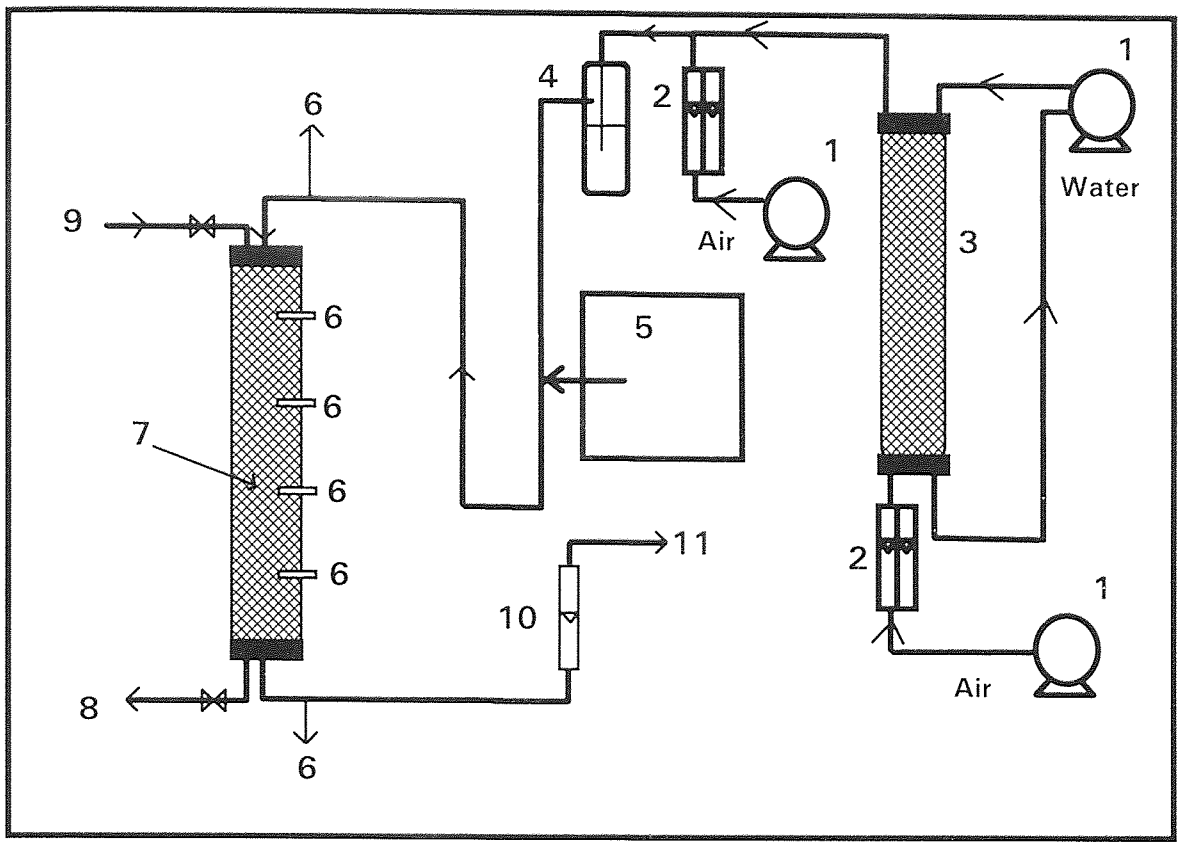

Figure 4.1. Schematic of the experimental packed-bed unit: (1)pump; (2) rotameter assembly; (3) humidification tower; (4) water tank; (5) syringe pump; (6) sampling ports; (7) column packing material; (8) water drain; (9) water supply (when needed); (10) air flowmeter; (11) exhaust.

height, with Teflon heads (top and bottom). The column (manifold) was packed with a mixture of peat, perlite, and medium having the composition mentioned earlier. The column was supplied with a humidified airstream carrying the solvent vapors of interest (i.e., benzene or toluene and benzene/toluene mixtures).

A countercurrent humidification tower was used to moisten the carrier air to the column. The tower consisted of 2 glass segments connected together, with a seal of stopcock grease. Each segment (Ace Glass Inc., Vineland, NJ) had a diameter of 15.2 cm and a height of 30.5 cm. The humidification tower also included two head-top/bottom segments which were custom made (Ace Glass Inc., Vineland, NJ). The tower was packed with 3/4" porcelain saddles (Norton, Akron, OH). A rotameter assembly (75-350,

Gow Mac Instrument Co., Bound Brook, NJ) was used to control the compressed oil free air flow, and a Masterflex pump (Cole Parmer, Niles, IL) was used to control the water flow to maintain a constant water level within the humidification tower. In cases where the air pump was not capable of generating enough air flow for the desired residence time, the humidified air was mixed with another air line, and that subsequent mixture was then bubbled into water in a 1 liter flask. The resulting stream was then injected with the solvent through the use of a syringe pump (G-74900-30, Cole Parmer, Niles, IL). For the experiments with benzene/toluene mixtures, two syringes were used to inject the solvents into the airstream.

The solvent concentration in the airstream was varied by changing the rate of injection of the syringe (500 μL, Pressure-Lok® , Series A-2, Supelco, Bellefonte, PA). The rate of injection was maintained between 100-1100 μL/h, and the air flow rate was maintained between 0.3 and 1.1 L/min. These conditions resulted in the solvent concentration values of up to 1.7 g/m^3. The resulting air/solvent mixture was then passed through a static mixer (21 element, Cole Parmer, Niles, IL).

The humidified air stream carrying the solvent was supplied to the top of the column containing the bed of solids. The top to bottom flow of the gas in the bed was used in order to simulate conditions used in biofiltration.

A soap film flow meter (1-10-100 mL, Hewlett Packard, Paramus, NJ) was used to measure the air flow rate at the exit of the bed of solids. The pressure drop in the bed was found to be negligible. A U-tube filled with water, with one end connected to the inlet stream of the column, and the other end to the atmosphere was used to measure the pressure drop (the exit of the column was open to the atmosphere). The difference in heights was measured. The average pressure drop was determined to be 0.10 " water/m packing.

All tubing used in the unit was Teflon (Nalgene 890, Fisher Scientific, Springfield, NJ). With the exception of the humidification tower, the unit was installed in an exhaust hood, and the temperature was maintained between 20-25°C.

During experiments, air samples were taken every 3-5 minutes sequentially from all sampling ports on the manifold containing the bed of solids. Samples were taken by 1 mL Pressure-Lok® syringes and immediately injected to the GC for analysis. For each experiment, the conditions (air flow rate or inlet concentration) were not changed until the concentration at the outlet of the bed was greater than 95% of that at its inlet. Each run (for given inlet concentration and space time) was completed in 60-100 min. The fact that the steady state outlet concentration was almost equal to that at the inlet indicated that there was no loss due to biodegradation (microbial activity). The packing of the column was changed every two weeks. Air humidification and temperature were essentially constant in all runs.

CHAPTER 5

DETERMINATION OF ADSORPTION ISOTHERMS

As has been mentioned earlier in this thesis, one of the objectives was to determine adsorption isotherms of VOCs on a packing material consisting of a 2:3 (v:v) mixture of peat and perlite. The interest in determining adsorption isotherms stems from the fact that transient biofiltration is highly affected by adsorption phenomena.

In this chapter the work performed for determining the isotherms of single and mixed VOCs is presented.

Adsorption isotherms are relations between concentrations of a species (VOC, chemical) in two phases under constant temperature. For the cases considered here, the species of interest are VOCs while the phases are the air and packing material.

As mentioned in Chapter 4 the concentration of VOCs in the air was measured through GC analysis of samples. The concentration of VOCs on the packing material was not directly measured. It was determined as follows. Each serum bottle was charged with amounts of solids and VOCs which were accurately determined. When equilibrium was reached and the gas (air) phase concentration of the VOCs measured, the amount of VOCs lost from the air was calculated by multiplying the concentration with the (known) volume of the headspace of the serum bottle, and then subtracting this number from the (known) total amount of VOCs that the bottle was charged with in the beginning of the experiment. It should be mentioned here that even though the volume of the solids was small when compared to the total volume of the bottle, the volume of the headspace did take into account the volume of solids. For the hydrophilic solvents, differing amounts of solids needed to be added in order to obtain enough data for a relevant regression. Subsequently, the concentration of VOCs on the packing material was determined via

dividing the amount "lost" from the headspace of the bottle by the (known) weight of the packing material.

5.1 Isotherms for Single VOCs

Experiments were performed with two hydrophilic compounds (butanol and ethanol) and two hydrophobic compounds (benzene and toluene).

Isotherms for single VOCs are relations between C_{se} and C_{ge}, which are equilibrium concentrations of the VOC on the packing and in the gas headspace, respectively.

As has been mentioned earlier, adsorption isotherms for a single adsorbant follow either the Langmuir or the Freundlich equations. These equations, respectively, are:

$$C_{se} = \frac{k_1 C_{ge}}{k_2 + C_{ge}} \tag{5.1}$$

$$C_{se} = k_d C_{ge}^n \tag{5.2}$$

Equation (5.1) suggests that at high values of C_{ge} the value of C_{se} remains constant. For the concentration ranges tried in the experiments this was not valid (see Figures 5.1 and 5.2). For this reason, equation (5.2) was employed.

In order to determine the values of parameters k_d and n, equation (5.2) was brought into the form:

$$\ln C_{se} = \ln k_d + n \ln C_{ge} \tag{5.3}$$

The data from each set of experiments (i.e., for each VOC studied) were regressed to equation (5.3) through a linear least squares algorithm. The correlation for the regression was greater than 99% for benzene and toluene, and approximately 99% for ethanol and

butanol. Hence, it was concluded that the adsorption isotherms do indeed follow the Freundlich equation. The values for the parameters k_d and n obtained from the regression are listed in Table 5.1.

Table 5-1 Freundlich Isotherm Parameters.*

Compound	n	k_d
Benzene	0.983	3.7×10^{-5}
Toluene	0.985	2.8×10^{-5}
Butanol	0.508	4.2×10^{-3}
Ethanol	0.467	5.2×10^{-3}

* when C_{se} in g-VOC/ g-packing and C_{ge} in g-VOC/ m^3-air

Using the values for k_d and n, the isotherm curves were generated and plotted as shown in Figures 5.1 and 5.2. On the same graphs the experimental data are also shown (as symbols). As can be seen, the agreement is excellent as expected by the high degree of correlation obtained in the regressions. The points shown in Figures 5.1 and 5.2 are actually average values from two experiments. As the error bars indicate, the reproducibility was very high.

As can be seen from Table 5-1, the value of n is almost equal to 1 for benzene and toluene. These results compare very well with those obtained by Rogers et al. (1980), who studied benzene adsorption to soil and clay, and reported n-values in the range of 0.9 to 1.08.

For the VOCs studied, the n-values obtained suggest that for the case of hydrophobic solvents C_{se} is proportional to C_{ge}, while for the case of hydrophilic solvents C_{se} is proportional to the square root of C_{ge}. For the concentration ranges used in the experiments, one can also observe from Figure 5.2 that even for the case of hydrophilic solvents there is an almost linear relation between C_{se} and C_{ge} provided that the latter is higher than 0.6 g-VOC/ m^3-air.

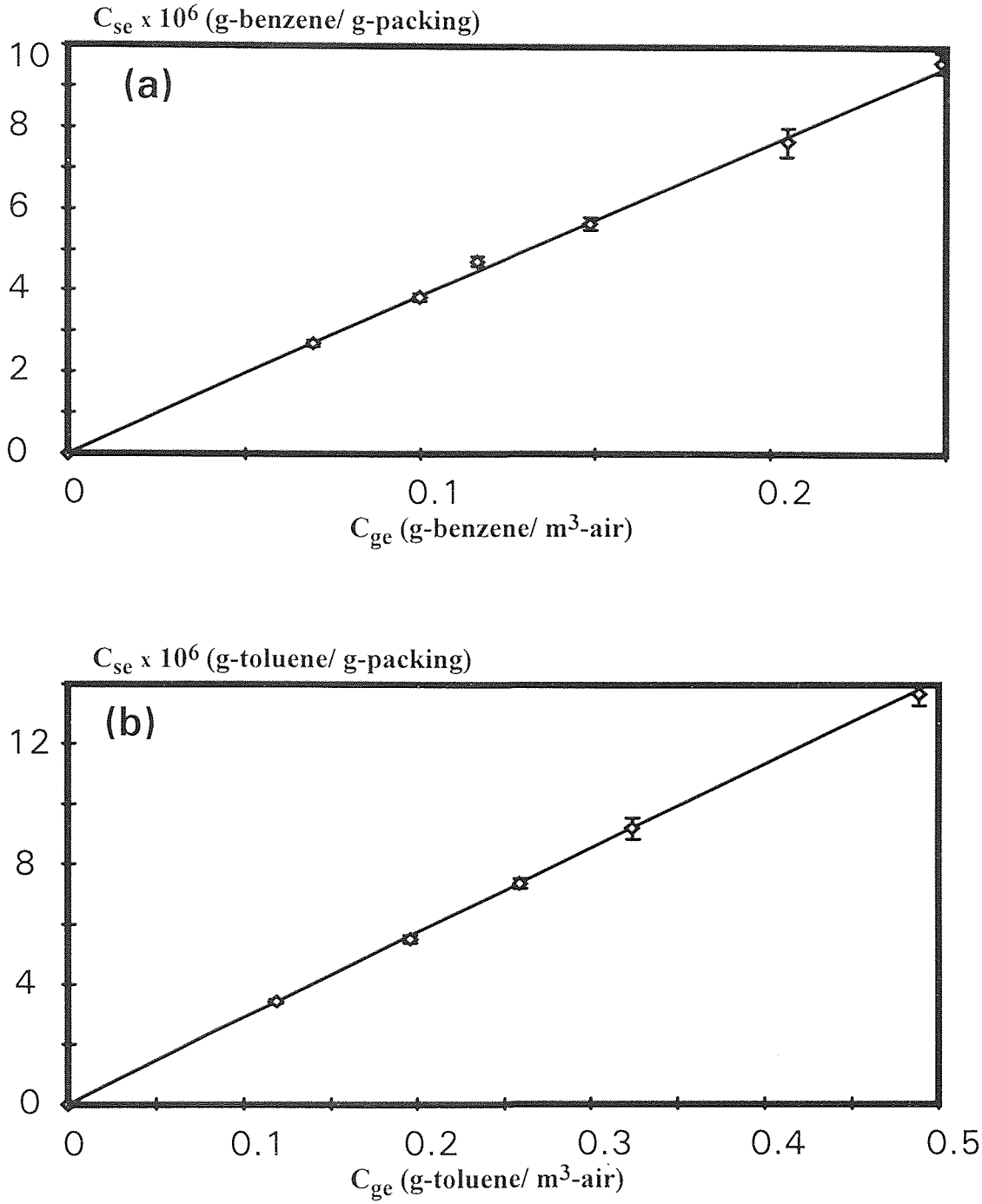

Figure 5.1 Adsorption isotherms of benzene (a) and toluene (b) on a mixture of peat and perlite (2:3 volume ratio). The symbols represent the average of two experimental values. The curve represents the Freundlich isotherm.

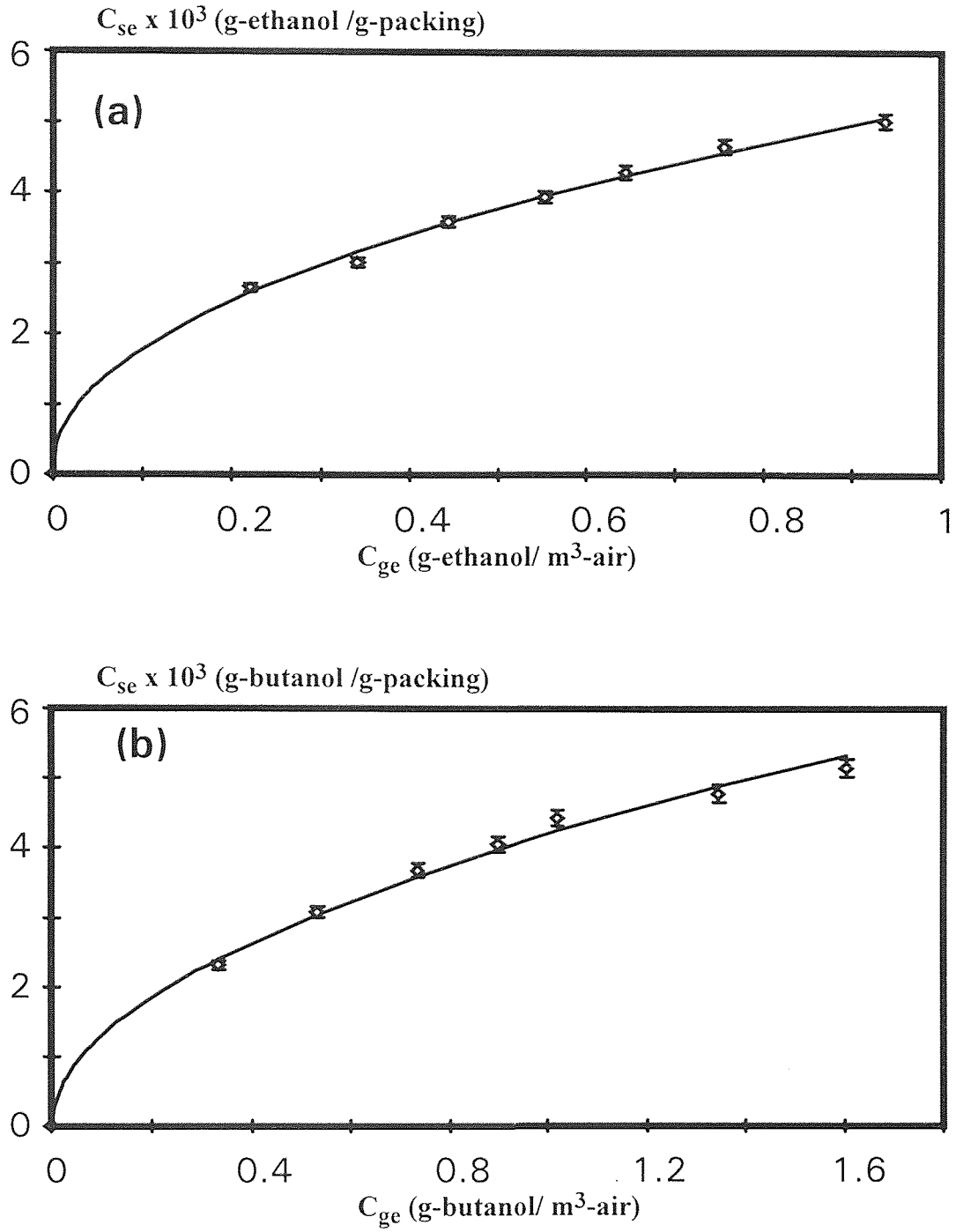

Figure 5.2 Adsorption isotherms of ethanol (a) and butanol (b) on a mixture of peat and perlite (2:3 volume ratio). The symbols represent the average of two experimental values. The curve represents the Freundlich isotherm.

If k_d is taken as a measure of the degree of strength of adsorption, the values in Table 5-1 suggest that the hydrophilic solvents adsorb more readily to the packing material than the hydrophobic solvents. In fact, for the same equilibrium gas concentration, the hydrophilic solvents adsorb 150 times more onto the solids than hydrophobic solvents. The increase in the adsorption capacity for the hydrophilic solvents could be due to the absorption of the solvents in the medium present in the pores of the packing material. As was mentioned in earlier chapters, adsorption in this study includes both absorption in the medium retained in the pores of the solids and actual adsorption on the solids themselves.

It should be mentioned that it was determined experimentally that the perlite does not adsorb either benzene or toluene. Hence, the peat does the actual adsorbing of the solvents. Experiments were performed on batch adsorption of perlite alone (with and without medium), and a very small amount of either benzene or toluene was adsorbed. The adsorption on perlite is 50 times less than that of the adsorption on peat. Similar experiments with ethanol and butanol were not performed.

5.2 Isotherms for a Mixture of Two VOCs

As mentioned in an earlier chapter, the model mixture selected for this part of the study involved benzene and toluene due to the interest in BTEX compounds. Two isotherms were obtained, one for benzene and one for toluene. The experimental protocol involved 18 experiments which could be grouped as follows: 1. Three series of experiments each one of which involved a single initial toluene concentration and six different initial benzene concentrations, or 2. Six series of experiments each one of which involved a single initial benzene concentration and three different initial toluene concentrations.

After equilibration, the concentrations of benzene and toluene in the headspace of the bottles were measured through GC analysis while the corresponding concentrations on the solids were determined as explained in the previous section. The equilibrium

concentrations of benzene on the solids were plotted against the corresponding benzene concentrations in the headspace as shown in Figure 5.3(a). The same was done for toluene and is shown in Figure 5.3(b). On the same diagrams, the curves predicted by the Freundlich isotherms determined in the preceding section were also plotted. If the data obtained from the experiments with benzene/toluene mixtures followed the Freundlich isotherms, the implication would be that benzene and toluene do not interfere with one another during their adsorption. However, as can be easily seen from Figure 5.3, this was not the case. In fact, the results suggest that for a given equilibrium concentration of benzene in the gas phase, the corresponding concentration on the solids is lower than what the Freundlich isotherm for benzene predicts. Furthermore, the higher the toluene presence, the higher is the deviation of the benzene concentration on the solids from the Freundlich prediction. These facts can be readily seen from Figure 5.3(a). Similar conclusions can be drawn for the case of toluene from Figure 5.3(b).

It was thus concluded that benzene and toluene are involved in a competitive interaction and was decided to fit the data to the Langmuir-Freundlich isotherm which accounts for competition and is given by the following form:

$$C_{j,se} = \frac{C_{j,ge}^{n}}{K + \lambda C_{i,ge}^{n'}} \qquad (5.4)$$

where parameters K, n, λ, and n' depend on the identity of compound j.

In the absence of compound i (i.e., when $C_{i,ge} = 0$) expression (5.4) should reduce to the Freundlich isotherm for compound j; thus the values of n and K for compound j should be those reported in Table 5.1. Consequently, four parameter values (two for λ and two for n') needed to be calculated, and this was done as follows.

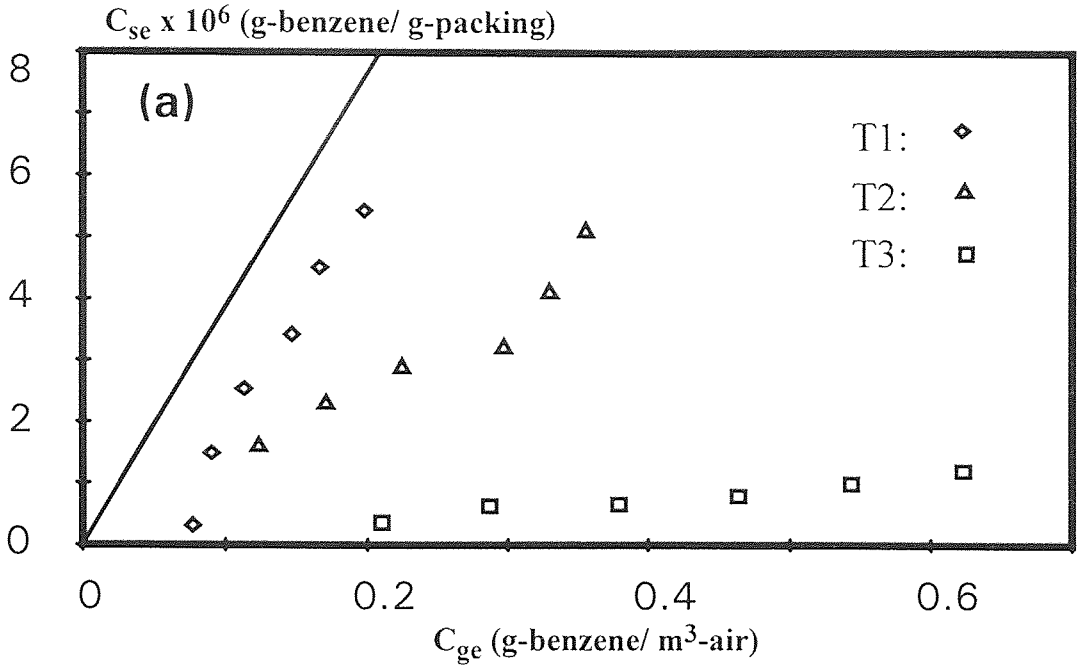

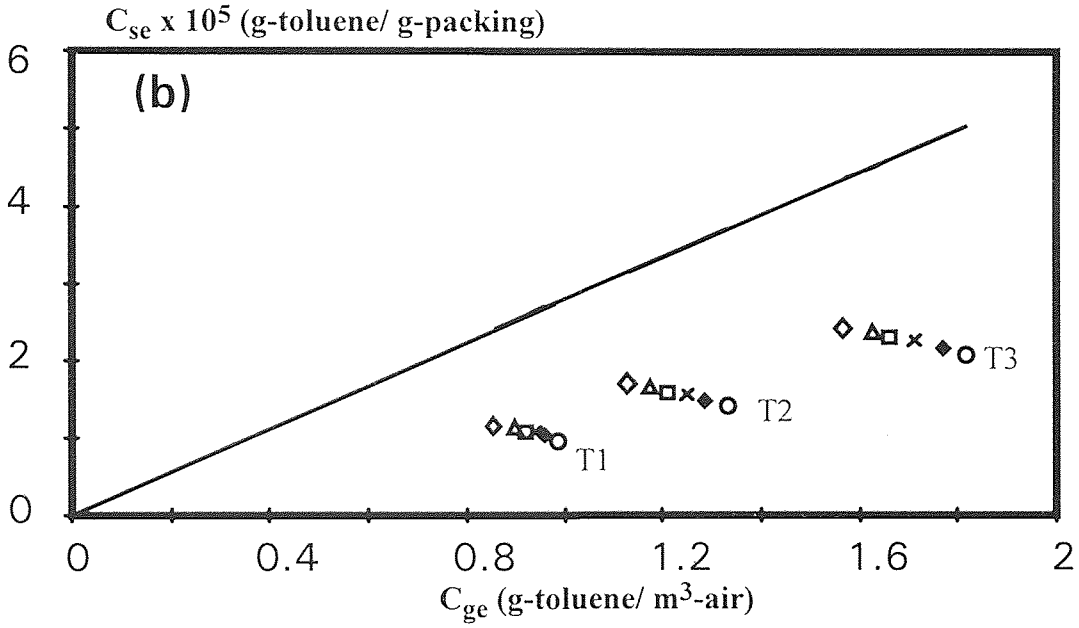

Figure 5.3 Equilibrium concentration data for benzene (a) and toluene (b), when both benzene and toluene are present in the system. The symbols represent the experimental data, and the curves represent the Freundlich isotherm assuming no competitive interference. Data in groups T1, T2, T3 correspond to initial toluene concentrations of 1.67, 2.32, and 3.25 g/m^3-air. Initial benzene concentrations are given in Table 5.3 (note).

Equation (5.4) was brought into the form,

$$\lambda C_{i,ge}^{n'} = \frac{C_{j,ge}^{n}}{C_{j,se}} - K \qquad (5.5)$$

or,

$$\ln\lambda + n' \ln\left[C_{i,ge}\right] = \ln\left[\frac{C_{j,ge}^{n}}{C_{j,se}} - K\right] \qquad (5.6)$$

With the values of n and K known, the data were regressed twice to equation (5.6) through the linear least-squares error method. In the first case, j was benzene and i was toluene while in the second regression j was toluene and i was benzene. The correlation was 95.8% when j was benzene, and 95.6% when j was toluene. A summary of all parameter values for the Langmuir Freundlich isotherms for benzene and toluene is given in Table 5-2.

Table 5-2 Langmuir-Freundlich Isotherm Parameter Values for Benzene and Toluene Mixtures.*

Parameter	j = Benzene i = Toluene	j = Toluene i = Benzene
λ	7.6×10^3	4.6×10^4
K	26954.2	35714.3
n'	8.0	0.06
n	0.983	0.985

* $C_{j,ge}$ and $C_{i,ge}$ in g-VOC/ m^3-air; $C_{j,se}$ in g-VOC/ g-packing.

The data obtained in the experiments as well as the predicted VOC concentrations on the solids are shown in Table 5-3. From the correlations given above, the agreement of the data is good but not perfect, as is also indicated in the parity plots of Figure 5.4.

As can be seen, the agreement is better in the benzene case than in the case of toluene. In the parity plots of Figure 5.4, the experimental values (symbols) are plotted against the predicted ones.

It is interesting to observe from the diagrams of Figure 5.3(a) that the equilibrium benzene data from experiments with the same initial toluene concentration fall on almost straight lines. The same is true for the toluene data (Figure 5.3(b)) corresponding to the same initial benzene concentration. This grouping does not seem to suggest anything more than the fact that competitive inhibition increases with the presence of the competitor.

Table 5-3 Initial and Equilibrium Concentration Data from Experiments with Benzene/Toluene Mixtures.*

$C_{B,gi}$	$C_{T,gi}$	$C_{B,ge}$	$C_{T,ge}$	$C_{B,se1}$ x 10^6	$C_{T,se1}$ x 10^5	$C_{B,se2}$ x 10^6	$C_{T,se2}$ x 10^5
<----------(g-VOC/ m^3-air)---------->				<----------(g-VOC/ g-packing)---------->			
0.705	1.67	0.198	0.982	7.41	1.00	6.07	1.26
0.611	1.67	0.166	0.957	6.50	1.04	5.31	1.24
0.517	1.67	0.147	0.931	5.41	1.08	4.85	1.21
0.423	1.67	0.113	0.920	4.53	1.09	3.8	1.21
0.329	1.67	0.090	0.903	3.49	1.12	3.1	1.19
0.235	1.67	0.077	0.857	2.31	1.19	2.76	1.14
0.705	2.32	0.356	1.33	5.11	1.44	3.54	1.67
0.611	2.32	0.329	1.29	4.12	1.50	3.86	1.63
0.517	2.32	0.297	1.25	3.22	1.56	4.2	1.58
0.423	2.32	0.224	1.21	2.90	1.62	3.71	1.54
0.329	2.32	0.171	1.17	2.31	1.68	3.26	1.51
0.235	2.32	0.123	1.13	1.63	1.74	2.72	1.47
0.705	3.25	0.623	1.82	1.20	2.08	0.654	2.23
0.611	3.25	0.544	1.77	0.986	2.15	0.707	2.18
0.517	3.25	0.464	1.72	0.781	2.24	0.771	2.13
0.423	3.25	0.379	1.66	0.644	2.32	0.815	2.07
0.329	3.25	0.287	1.63	0.616	2.37	0.725	2.05
0.235	3.25	0.211	1.57	0.356	2.45	0.687	2.00

* where $C_{B,gi}$ and $C_{T,gi}$ are the initial concentrations of benzene and toluene in the headspace, respectively; $C_{B,ge}$ and $C_{T,ge}$ are the experimental equilibrium headspace concentration of benzene and toluene, respectively; $C_{B,se1}$, $C_{T,se1}$ are the experimental equilibrium solids concentrations of benzene and toluene, respectively; $C_{B,se2}$, $C_{T,se2}$ are the model equilibrium solids concentrations of benzene and toluene, respectively.

Note: Initial benzene concentration (g/m^3) for Figure 5.3(b):
◇: 0.235, ▲: 0.329, □: 0.423, ×: 0.517, ◆: 0.611, ○: 0.705

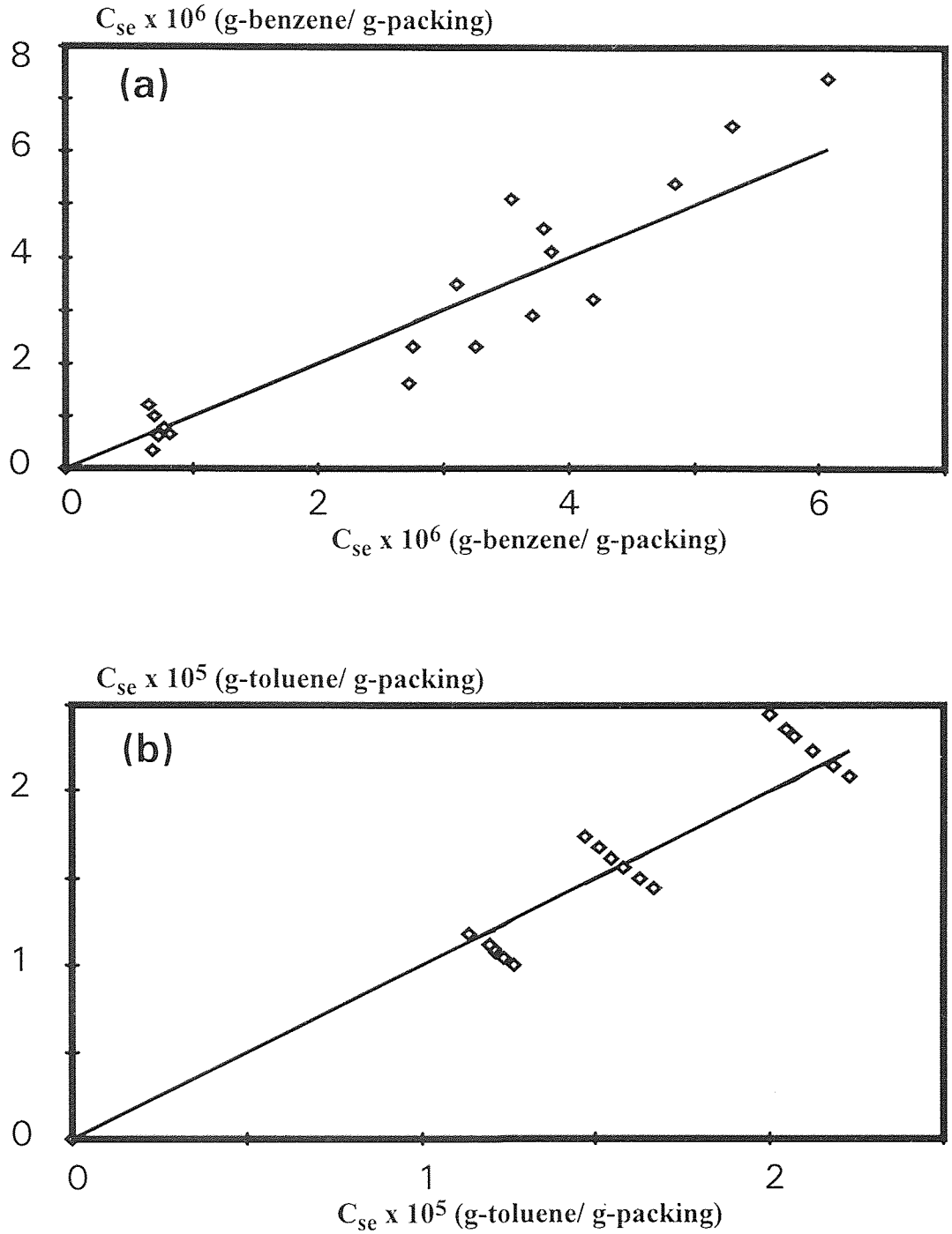

Figure 5.4 Parity plots of the Langmuir-Freundlich isotherm predicted equilibrium solids concentration (curve) versus the actual experimental equilibrium solids concentration (symbols), for benzene (a), and toluene (b).

CHAPTER 6

ADSORPTION OF BENZENE AND TOLUENE ON A PACKED COLUMN

In this chapter, results from experiments involving adsorption of benzene, toluene and their mixtures on a packed column are presented. These were flow experiments in which the air flow rate and/or the concentrations of VOCs at the inlet of the bed were varied. The intent was to determine the mass transfer coefficient. The latter was achieved through analysis of the transient data from experiments involving either benzene or toluene.

6.1 Development of the Mathematical Model

Data from experiments of adsorption of either benzene or toluene on a packed bed of peat and perlite were analyzed through a simplification of a transient biofiltration model originally developed by Shareefdeen and Baltzis (1994). The simplification involved elimination of the biological terms and the oxygen mass balances from the aforementioned model. This reduced it to a transient adsorption model. The assumptions involved in the transient adsorption model are:

1. Adsorption is a reversible process, and its characteristics are determined through the adsorption isotherms.
2. The airstream passes through the packed bed in plug flow.
3. The VOC is uniformly adsorbed on the particles; thus, there is no concentration variation within the particle. Pore diffusion resistance is neglible.

With this model, the adsorption of a pollutant j carried by the airstream is described by the following equations:

I. Mass Balance in the Gas Phase

$$\upsilon\frac{\partial c_j}{\partial t} = -q\frac{\partial c_j}{\partial h} - k_a A_S^*\left(c_j - c_j^*\right) \tag{6.1}$$

with initial and boundary conditions,

$$t = 0,\ h = 0,\ c_j = c_{ji,0} \tag{6.2}$$

$$t = 0,\ 0 < h \leq H,\ c_j = c_{j0}(h) \tag{6.3}$$

$$t > 0,\ h = 0,\ c_j = c_{ji} \tag{6.4}$$

II. Mass Balance in the Solid Phase (Particles)

$$(1-\upsilon)\rho_p\frac{dc_{jp}}{dt} = k_a A_S^*\left(c_j - c_j^*\right) \tag{6.5}$$

with initial condition,

$$t = 0,\ h \geq 0,\ c_{jp} = c_{jp,0}(h) \tag{6.6}$$

The adsorption of pollutant j on the packing material is described by the Freundlich isotherm:

$$c_{jp} = k_d\left(c_j^*\right)^n \tag{6.7}$$

After introducing the following dimensionless quantities,

$$\bar{c}_j = \frac{c_j}{c_{ji}} \qquad \bar{c}_j^* = \frac{c_j^*}{c_{ji}} \qquad \bar{c}_{jp} = \frac{(1-\upsilon)\rho_p c_{jp}}{\upsilon c_{ji}}$$

$$z = \frac{h}{H} \qquad \zeta = \frac{qt}{H}$$

$$\beta = \frac{k_a A_s^* H}{q\upsilon} \qquad \psi = \frac{1}{c_{ji}}\left[\frac{\upsilon c_{ji}}{(1-\upsilon)\rho_p k_d}\right]^{\frac{1}{n}}$$

the model is reduced to,

$$\frac{\partial \bar{c}_j}{\partial \zeta} = -\frac{1}{\upsilon}\frac{\partial \bar{c}_j}{\partial z} - \beta\left(\bar{c}_j - \bar{c}_j^*\right) \tag{6.8}$$

$$\frac{\partial \bar{c}_{jp}}{\partial \zeta} = \beta\left(\bar{c}_j - \bar{c}_j^*\right) \tag{6.9}$$

with initial and boundary conditions as follows:

$$\text{at} \quad \zeta = 0 \quad \text{and} \quad z = 0\text{:} \quad \bar{c}_j = 1 \quad \bar{c}_{jp} = \bar{c}_{jp,0}(0) \tag{6.10}$$

$$\text{at} \quad \zeta = 0 \quad \text{and} \quad 0 < z \le 1\text{:} \quad \bar{c}_j = \bar{c}_{j,0}(z) \quad \bar{c}_{jp} = \bar{c}_{jp,0}(z) \tag{6.11}$$

$$\text{at} \quad \zeta \ge 0 \quad \text{and} \quad z = 0\text{:} \quad \bar{c}_j = 1 \tag{6.12}$$

6.2 Correlation for the Mass Transfer Coefficient

The mass transfer coefficient, k_a, which is a parameter in the model equations presented in the preceding section was determined through the following relationship:

$$k_a = \delta q \, Re^{-3/4} \, Sc^{-2/3} \tag{6.13}$$

In the equation above, Re and Sc are the Reynolds number for packed beds and the Schmidt number, respectively, and are given by the following equations:

$$Re = \frac{4Rq\rho}{(1-\upsilon)\mu} \tag{6.14}$$

$$Sc = \frac{\mu}{\rho D_j} \tag{6.15}$$

The superficial velocity, q, in the above equations is based on an empty column (bed).

Equation (6.13) is a modification of the one proposed by Jones et al. (1993). These authors examined adsorption of a chemical from a liquid stream onto a packed bed, and the value for δ was 5.7. In the work presented here, the value of δ was determined by fitting concentration profiles to the solution of equations (6.8) through (6.12). As also discussed later, the value of δ was determined to be 3.56×10^{-2}.

The effective mass transfer coefficient is given by:

$$k_a'' = A_S^* k_a \tag{6.16}$$

6.3 Numerical Methodology

The model equations (6.8) through (6.12) were solved through a modification of a code originally developed by Shareefdeen (1994). The original code was developed for solving the transient biofiltration model of Shareefdeen and Baltzis (1994). As mentioned earlier, this model was reduced to the transient adsorption model for this thesis by deleting all terms pertaining to biological destruction of VOCs. The same was done with the computer code. The modified version of the original code which was used in the present study is given in Appendix B of the thesis.

The code is based on the use of finite differences in the z-direction and integration of the resulting system of ordinary differential equations (ODEs) by using the ODESSA (Ordinary Differential Equation Solver with explicitly Simultaneous Sensitivity Analysis) algorithm. ODESSA is a subroutine within the AUTO software package [Doedel

(1986)]. Twenty points were used for discretizing z (from z = 0 to z = 1), thus ODESSA solved a system of 40 simultaneous differential equations. The time step used was the dimensionless equivalent of one minute.

6.4 Determination of Model Parameters

In addition to the Freundlich isotherm parameters, n and k_d, which were determined in Chapter 5 and the mass transfer coefficient, k_a, which was estimated as explained in section 6.2, the model equations (6.8) through (6.12) also contain other parameters which were determined as follows.

6.4.1 Capacity of packing for water holding

A column was packed with dry peat and perlite (2:3, v:v). The amount of peat was 266.9 cm^3 and the amount of perlite was 400.3 cm^3. A 40-50 ml amount of water was added daily to the top of the column. The runoff was collected at the bottom of the column, and measured daily. This continued until the amount of water added was retained in the runoff for 3 days. The total amount of water that was equal to that in the packing was assumed to be the amount of water needed to completely saturate the pores of the packing pores, because in the dry peat and perlite mixture the void fraction is believed to be very small; thus no water would be retained in any interparticle space. The water retention of the packing material was 0.601 m^3-water/ m^3-packing. This implies a porosity of 60% for the packing material.

6.4.2 Void fraction of bed

A batch of packing material (2:3, v:v, peat: perlite) was mixed with an amount of water as determined in section 6.4.1 so that all pores of the packing were filled with water (401 cm^3-water was mixed with 667.2 cm^3-packing). The resulting mixture was packed into a column, and the volume of the bed was measured by taking the height of the bed and

multiplying it by the cross sectional area of the column. Then, water from a previously quantitized reservoir was pumped in through the bottom of the column. This was done until the level of the water equaled that of the top of the packing. Some settling occurred, so the volume of settling and the amount of water added was assumed to be the volume of the void of the bed. Its value was found to be 32.4%.

6.4.3 Density of packing material

The packing used in the experiments contained peat and perlite in a 2:3 ratio by volume. In addition, the packing contained an amount of medium as in actual cases of biofiltration. The amount of medium used is enough to fill approximately 50% of the pore space of the particles. Hence, the density of the packing refers to a mixture having the aforementioned properties (composition). This density was determined by taking the total mass and dividing by the total volume of the packing. The total mass was determined by summing the mass of the dry peat and perlite and the mass of the medium added. For this particular case, the mass of the dry peat and perlite was 153 g, and the mass of the medium was 300 g, making the total mass 453 g. The volume of particles was taken from measurements involving the column. It was determined that the total volume of bed was 987×10^{-6} m^3, and the volume of the void contained in that bed was 320×10^{-6} m^3. Hence, the volume of the particles was 667×10^{-6} m^3 which makes the resulting density, ρ_p , 0.679×10^6 g-packing/ m^3-packing. This value compares favorably with the value, 0.428×10^6 g-packing/ m^3-packing, previously used by Shareefdeen (1994).

6.4.4 Mass transfer coefficient and specific surface area

When the mass transfer coefficient is multiplied by the specific surface area, the effective mass transfer coefficient is determined. It is worth noticing from equations (6.1) and (6.5) that in the model it is the effective mass transfer coefficient which needs to be

known. However, the effective mass transfer coefficient cannot be predicted unless the specific surface area and the actual mass transfer coefficient are known.

Initially, two experimental runs (one for benzene and one for toluene) were selected. The experimentally obtained concentration profiles were fitted to the solution of the model equations by adjusting the value of the effective mass transfer coefficient. For the case of benzene, the optimal k_a" was found to be 2.85 (1/h) while for toluene it was found to be 3.04 (1/h). The fitting approach was such that the data would fit to the model not only at the exit of the bed but also at all sampling locations. These fitted profiles are shown in the diagrams of Figure 6.1 for the outlet concentrations and Figures A-2.1 through A-2.3 for other locations on the bed. It should be noticed that the residence time and thus, the superficial gas (air) velocity was different in the two experiments.

Subsequently, it was assumed that the particles are spheres. For a bed of volume V_p having a porosity υ and containing N particles of radius R the specific surface area is:

$$A_S^* = \frac{4\pi R^2 N}{V_p} \tag{6.17}$$

The following equality is also true,

$$(1-\upsilon)V_p = \frac{4}{3}N\pi R^3 \tag{6.18}$$

Using equations (6.17) and (6.18) one gets

$$A_S^* = \frac{3(1-\upsilon)}{R} \tag{6.19}$$

Since υ was found, as explained earlier, to be 0.324, expression (6.19) becomes:

$$A_S^* = \frac{2.03}{R} \tag{6.20}$$

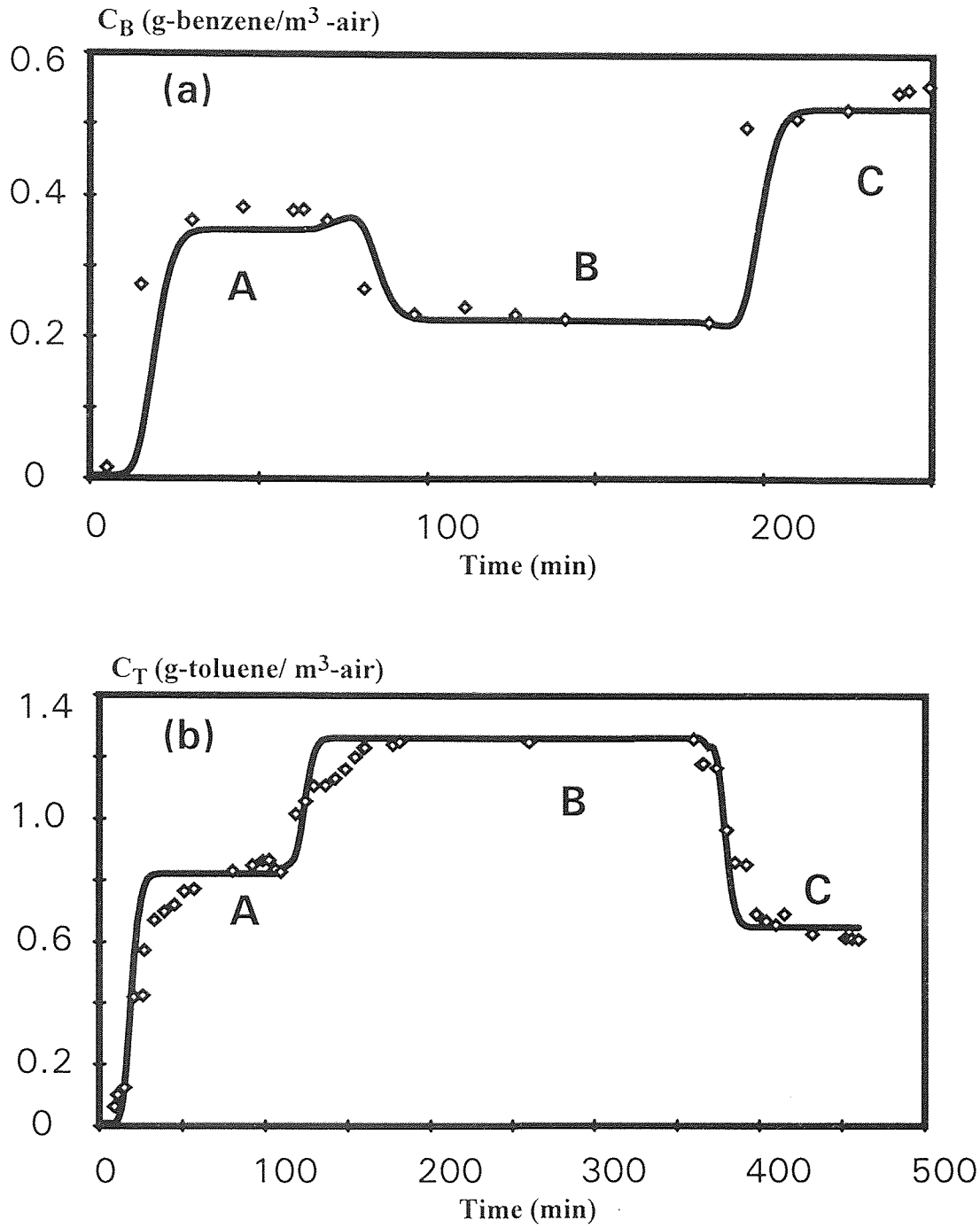

Figure 6.1 Experimental (symbols) and fitted (curves) profiles at the outlet of the column for determination of k_a" for benzene (a) and toluene (b). For benzene, the residence time was 2.2 min and the inlet concentrations (g/m^3) were **A**: 0.39, **B**: 0.21, **C**: 0.56. For toluene, the residence time was 1.6 min and the inlet concentrations (g/m^3) were **A**: 0.89, **B**: 1.30, **C**: 0.61.

Using equations (6.13), (6.16), and (6.20) one gets:

$$k_a'' = \delta q \, Re^{-3/4} \, Sc^{-2/3} \frac{2.03}{R} \qquad (6.21)$$

The value of δ in equation (6.13) is 5.7 when a liquid phase is involved [Jones et al. (1993)]. Using this value, equation (6.21) predicted an R of 1.85 cm when the fitted values of k_a'' (mentioned earlier) were used. This is not realistic since experimental observations indicated that when peat and perlite are mixed with the medium, clumps of about 2 mm in diameter are formed. Hence, it was decided to fix the value of R at 1 mm which, from equation (6.20), leads to a specific surface area of 1961 (1/m).

With the value of R known, the two k_a'' values were used in order to determine the value of δ in equation (6.21). This value was subsequently used in describing other data sets which are discussed in the next section of this chapter.

Equation (6.13) clearly indicates that the mass transfer coefficient depends on the superficial velocity q. This is also graphically shown in Figure 6.2 which has been prepared by using parameter values pertinent to the present study.

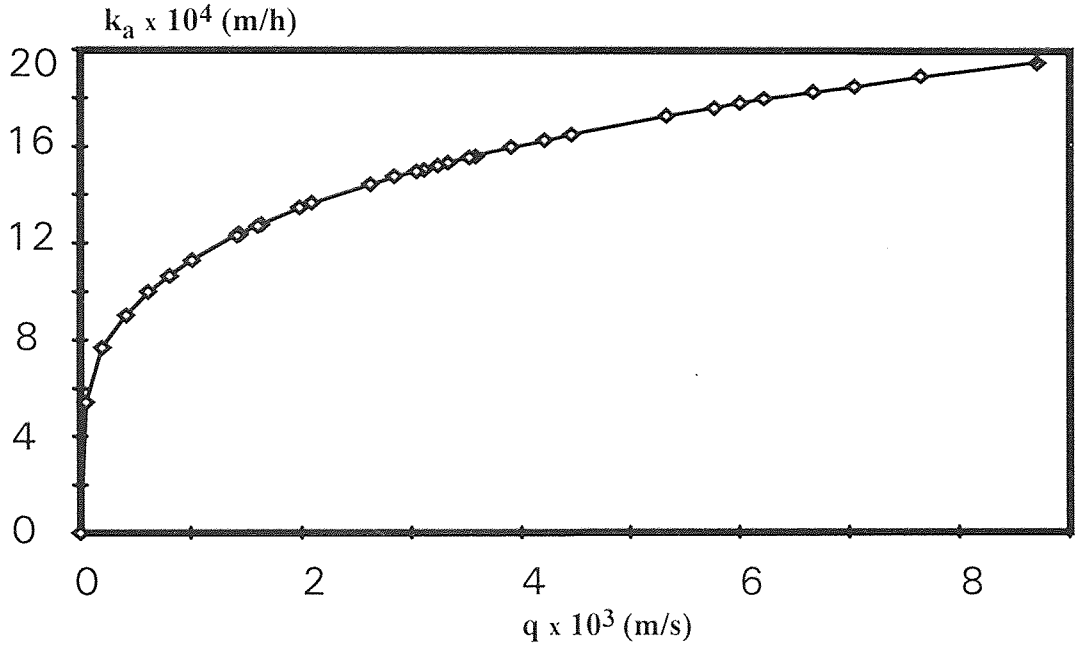

Figure 6.2 Dependence of the mass transfer coefficient on the superficial velocity of air.

6.5 Results and Discussion of Single Pollutant Adsorption

Results from experiments are presented in the form of graphs showing measured concentration values and model-predicted profiles. Parameter values used in solving the model equations are shown in Table 6.1. Values of parameters not obtained in this study were taken from literature [μ and ρ for air from Perry and Green (1984); D_j for benzene and toluene from Thibodeaux (1979)]. The values for the mass transfer coefficient were calculated by using equation (6.13) and are given in tabular form in Appendix C of this thesis.

Table 6-1 Parameter values.

Parameter	Value	Units
A_S*	1961	1/m
S	19.63×10^{-4}	m^2
V_p (Benzene)	834.5×10^{-6}	m^3
V_p (Toluene)	798.5×10^{-6}	m^3
V_p (Benzene/Toluene Mix)	834.5×10^{-6}	m^3
ρ_p	0.679×10^6	g-particle/m^3-particle
υ	0.324	m^3-air/m^3-bed
δ	3.56×10^{-2}	
ρ(air)	1.22×10^3	g/m^3
μ (air)	1.86×10^{-2}	g/m/s
D_j (Benzene)	0.00088	m^2/s
D_j (Toluene)	0.00088	m^2/s

Experiments were performed in two different ways. The first was to keep the volumetric flowrate of the air stream (residence time) constant and vary the concentration of either benzene or toluene in the stream fed to the bed. The second category of experiments dealt with cases where the concentration of the pollutant in the inlet stream was kept constant while the volumetric flow rate of the air stream was varied from run to run. Although as discussed in Chapter 4, data were collected at the inlet, outlet, and three ports on the column only the data from the outlet and the middle point of the bed are

presented here. Data from the non-reported ports had the same qualitative features as those reported here.

For the experiments reported in Figures 6.3 and A-2.4, the inlet concentrations were changed while the residence time was kept constant. As can be seen from the graphs, the model predicts the data very nicely both qualitatively and quantitatively. The agreement is very good both for inlet concentration shift-up (increase) and shift-down (decrease) experiments.

Results from other experiments under constant residence time are shown in the diagrams of Figures 6.4, A-2.5, A-2.9, and A-2.10. In these cases, the agreement between data and model predictions is qualitatively good, but at the quantitative level it is not as good as in the cases of Figures 6.3 and A-2.4. A difference between the sets is in the value of the residence time. For the case of Figures 6.3 and A-2.4, τ is low (less than 2 min) while for the case of Figures 6.4, A-2.5, A-2.9, and A-2.10 the residence time value is high (3.4 - 4.9 min).

One possible explanation of the discrepancy between experimental and model-predicted values is the following. One of the model assumptions is that the air stream passes through the column in plug flow. However, experimentally there may be channeling effects leading to deviations from the predictions. For example, the very initial data in Figure 6.4(a) do show that there is no breakthrough, and the agreement with the model is very good. On the other hand, Figures 6.4(b), A-2.9 and A-2.10 show a VOC presence in the outlet at very low times. This is most likely indicative of channeling and the deviation from the predications can be explained. Observe that once steady-state (equilibrium) is reached the quantitative agreement between data and model predictions is excellent in most cases since at steady-state channeling effects are not playing any role (in the absence of reaction as was the case for the experiments). Similar observations can be made from the diagrams of Figures 6.3 and A-2.4. Observe that at very low times the

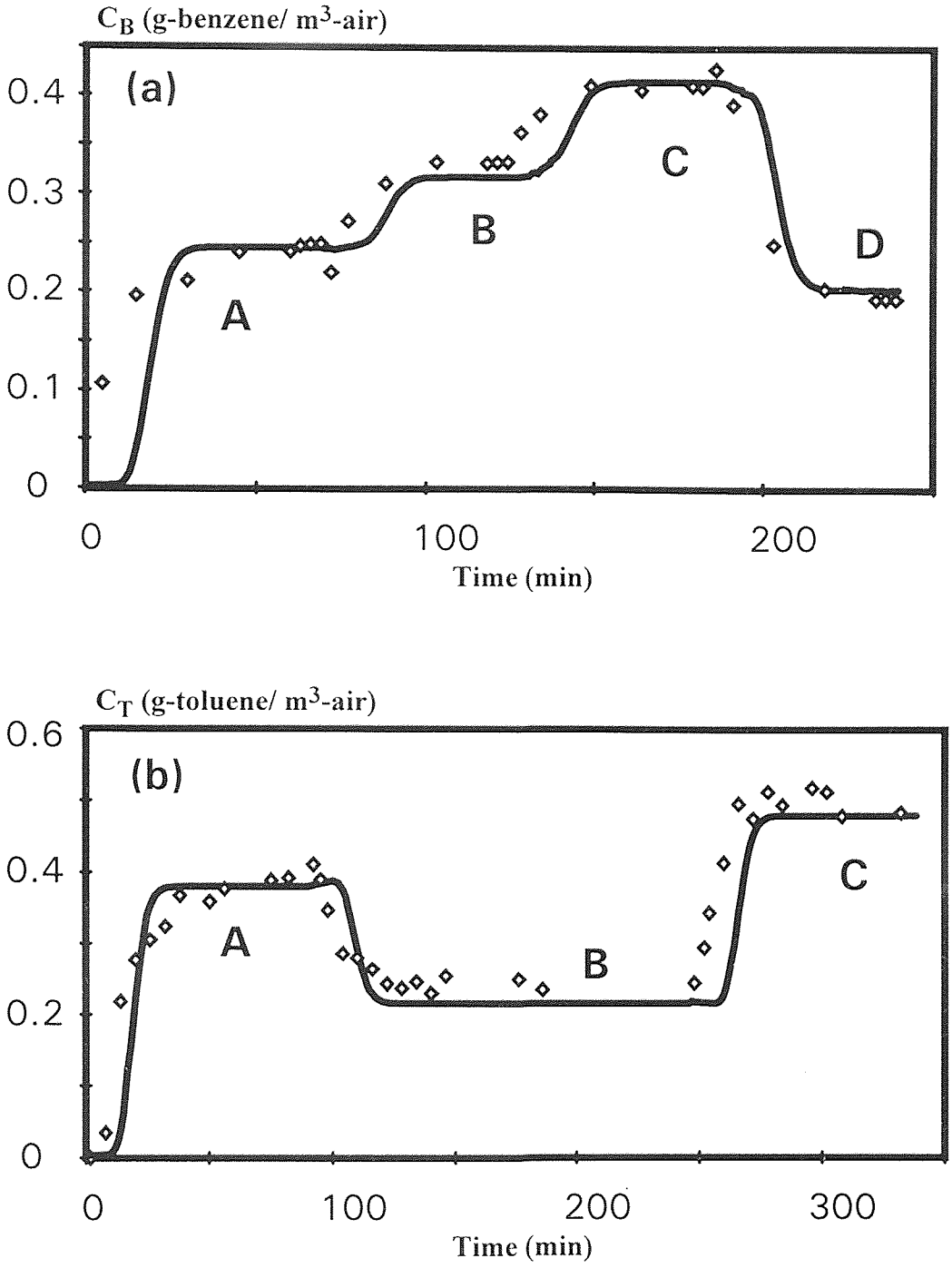

Figure 6.3 Experimental (symbols) and model-predicted (curves) benzene (a) and toluene (b) concentration profiles at the exit of the bed at constant low residence times. Experimental conditions are (a): τ = 1.0 min; F = 0.05 m^3/h, and $C_{Bin}(g/m^3)$ = 0.26, 0.32, 0.41, 0.19, for **A**, **B**, **C**, **D**, respectively; (b): τ = 0.80 min; F = 0.06 m^3/h, and $C_{Tin}(g/m^3)$ = 0.40, 0.21, 0.49, for **A**, **B**, **C**, respectively.

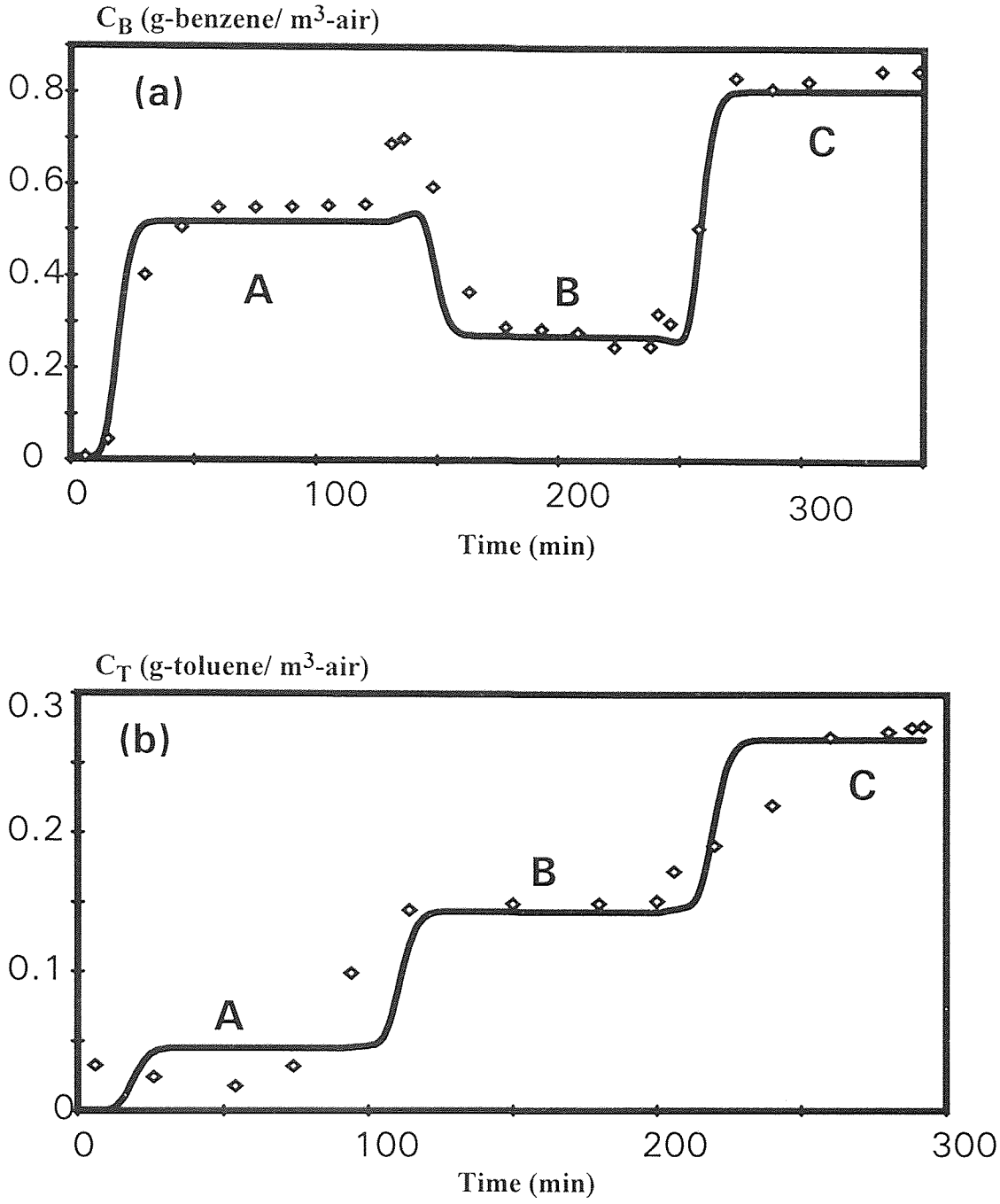

Figure 6.4 Experimental (symbols) and model-predicted (curves) benzene (a) and toluene (b) concentration profiles at the exit of the bed at constant high residence times. Experimental conditions are (a): τ = 4.9 min; F = 0.01 m^3/h, and $C_{Bin}(g/m^3)$ = 0.56, 0.15, 0.21, for **A**, **B**, **C**, respectively; (b): τ = 4.8 min; F = 0.01 m^3/h, and $C_{Tin}(g/m^3)$ = 0.05, 0.15, 0.21, for **A**, **B**, **C**, respectively.

agreement between experimental and predicted concentration values is much better in Figure 6.3(b) than in Figure 6.3(a). In the latter, channeling may had been present (as the initial breakthrough indicates). One could speculate that channeling effects impact the process more at high residence time something which could explain the difference in quantitative agreement between (as an example) Figures 6.3(a) and 6.4(b). A small flow "escapes" easier through the channels than a higher flow which possibly leads to a better air distribution in the bed.

Since adsorption is a reversible phenomenon, it is expected that if equilibrium has been reached a decrease in the VOC concentration in the inlet air should lead to temporarily high VOC presence in the outlet since desorption has to occur before equilibrium is reached again at a lower level. This has in fact been seen in a number of experiments and its best demonstration is shown in Figure 6.4(a) (transition from A to B). Observe that the model does have the ability to qualitatively describe this overshoot in concentration although it fails to describe it quantitatively. One possible explanation of this feature is the following. Experimentally, much higher concentrations are obtained. This means that the packing has a capability for adsorption much less than what is predicted. This may be due to the fact that the adsorption isotherms were obtained from batch experiments with VOC concentrations in the air much lower than those in many of the flow experiments. In fact, at high concentrations the model predicts attainment of steady-state at times much higher than those experimentally observed. This can be easily seen from the extreme case of Figures A-2.7(b) and A-2.8(b).

Results from experiments performed under constant VOC concentration in the inlet air and varying air flow rates are presented in the graphs of Figures 6.5, A-2.6, A-2.7(a), and A-2.8(a). In all cases the model captures the trend of the data very nicely while the quantitatively agreement is varying from relatively good to poor. If equilibrium (steady-state) has been in fact reached, a change in residence time under constant VOC concentration in the inlet air should make absolutely no difference in the concentration

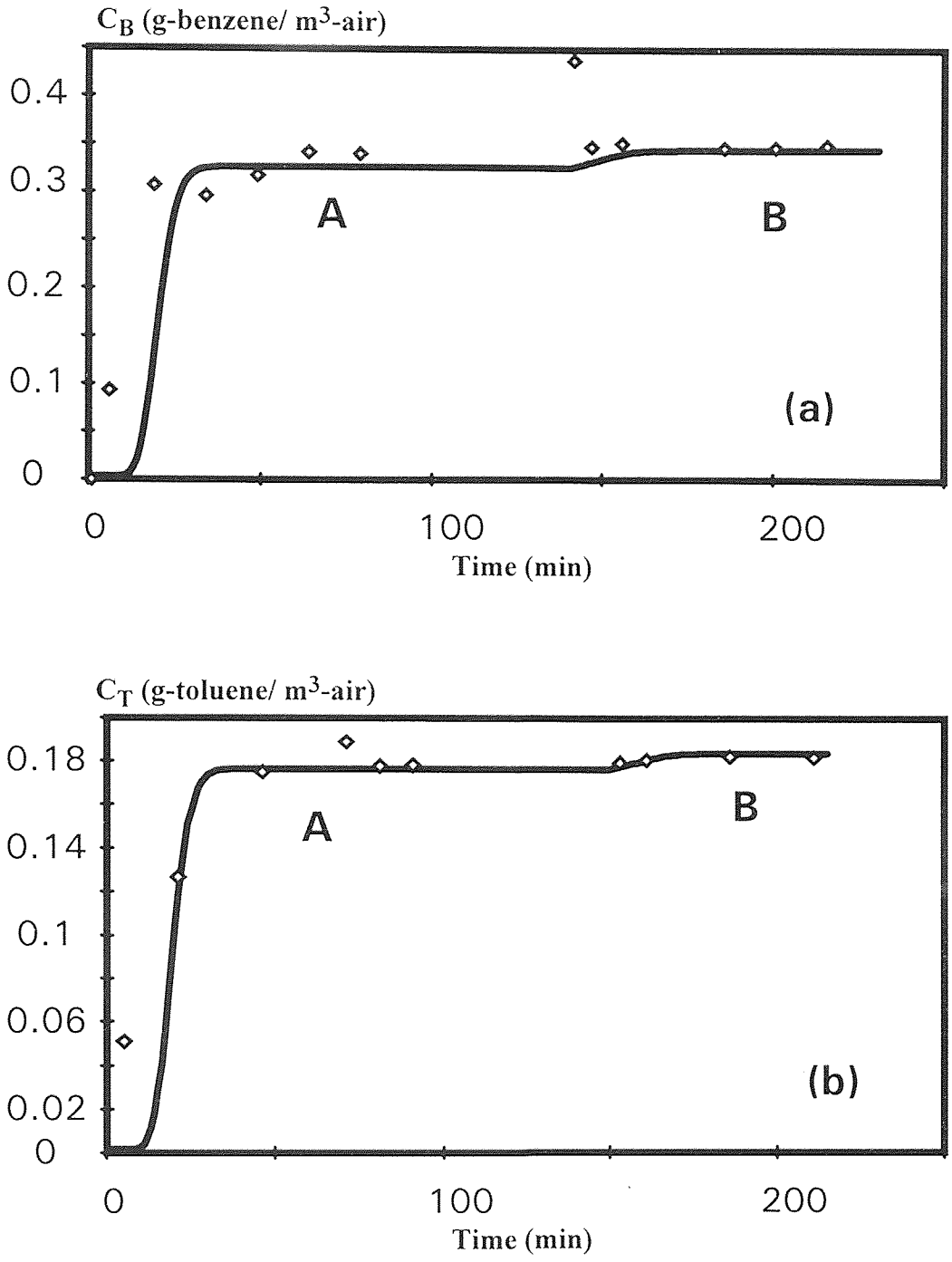

Figure 6.5 Experimental (symbols) and model-predicted (curves) concentration profiles at the outlet of the bed for benzene (a) and toluene (b). Experiments under constant inlet concentrations are (a): $C_{Bin}(g/m^3) = 0.35$, τ (min)= 1.3, 3.4, for **A** and **B**, F (m^3/h) = 0.04, 0.015, for **A** and **B**, respectively. (b): $C_{Tin}(g/m^3) = 0.19$, τ (min)= 0.8, 2.1, for **A** and **B**, F (m^3/h) = 0.06, 0.02, for **A** and **B**, respectively.

profiles (flat in this case) obtained from the column. This is the general trend observed from the figures. However, in some cases (e.g. Figures 6.5(a) and A-2.7(a)) there is a temporarily high concentration. This is due to the experimental methodology. Since the VOC-containing airstream was always created by injection of the VOC to humidified air, a change in air flow rate required a change in the rate of VOC injection so that the concentration remained constant. To ensure that the inlet air concentration was in fact constant, the flow to the column was briefly disconnected (between conditions A and B in Figures 6.5 and A-2.7(a)). For the experiments shown in Figures 6.5(a) and A-2.7(a) (benzene) the column was left open in the hood while it was covered (capped) for the toluene case (Figure 6.5(b)). The open columns may have experienced a desorption due to the high velocity of the hood vent. This may possibly explain the temporarily high experimental concentration values.

In general, one could say that the adsorption behavior of the columns was as expected and that it has been successfully modeled. The latter is especially true when one considers the difficulties in doing the experiments. One such difficulty was mentioned in the preceding paragraph. Others include the difficulty in ensuring plug flow conditions, the unavoidable fluctuations in flowrate and inlet VOC concentration, and the fact that stepwise changes in either concentration (e.g. Figure 6.3) or flowrate (e.g. Figure 6.5) are hard -if not impossible- to experimentally realize. What are considered (for the model) stepwise changes are at best ramp changes.

6.6 Results and Discussion of Adsorption of a Mixture of Pollutants

Results from column experiments performed with airstreams containing vapors of both benzene and toluene are presented in graphical form in Figures 6.6 through 6.8 and A-2.11 through A-2.15. The curves appearing in the aforementioned figures constitute model-predicted concentration profiles assuming that benzene and toluene are not

involved in a competitive interaction during their adsorption. In the absence of interaction, adsorption of benzene is decoupled from that of toluene and vice versa. Hence, the profiles for each compound were obtained by integrating equations (6.1) through (6.7), or (6.8) through (6.12) twice, once for each compound.

The diagrams of Figure 6.6 show results from a series of experiments performed under constant (and low) residence time but varying inlet concentrations of benzene and toluene. It can be observed that the agreement between data and model predictions is generally good, with the noticeable exception of region C. This good agreement may be due to the fact that the concentrations of the two compounds are low and thus, the intensity of competition is small. Another example of an experiment performed under low residence time is given in Figure A-2.11. Here, although one could again say that the data agree reasonably well with the predictions, one could see some trends indicating potential competition. For example, the model predicts that steady-state is attained faster than what the data seem to indicate. In addition, in region B transient concentrations are significantly (especially for benzene) higher than those predicted by the model, something which may indicate that lower than predicted VOC quantities are adsorbed due to inhibition (competition). It is worth observing that the concentrations in the case of Figure A-2.11 are significantly higher than those in the case of Figure 6.6, thus the possibility of competitive inhibition is higher.

Experiments similar to those shown in Figures 6.6 and A-2.11 were also performed under high residence times. An example is shown in Figure A-2.12. The trends are the same as those discussed earlier. It is worth observing the significant overshoot of experimental concentration values during the transition from conditions B to C. Both benzene and toluene concentrations are reduced significantly in the inlet stream and this causes desorption. As also discussed in the preceding section, the model does qualitatively depict this overshoot but fails to describe it quantitatively.

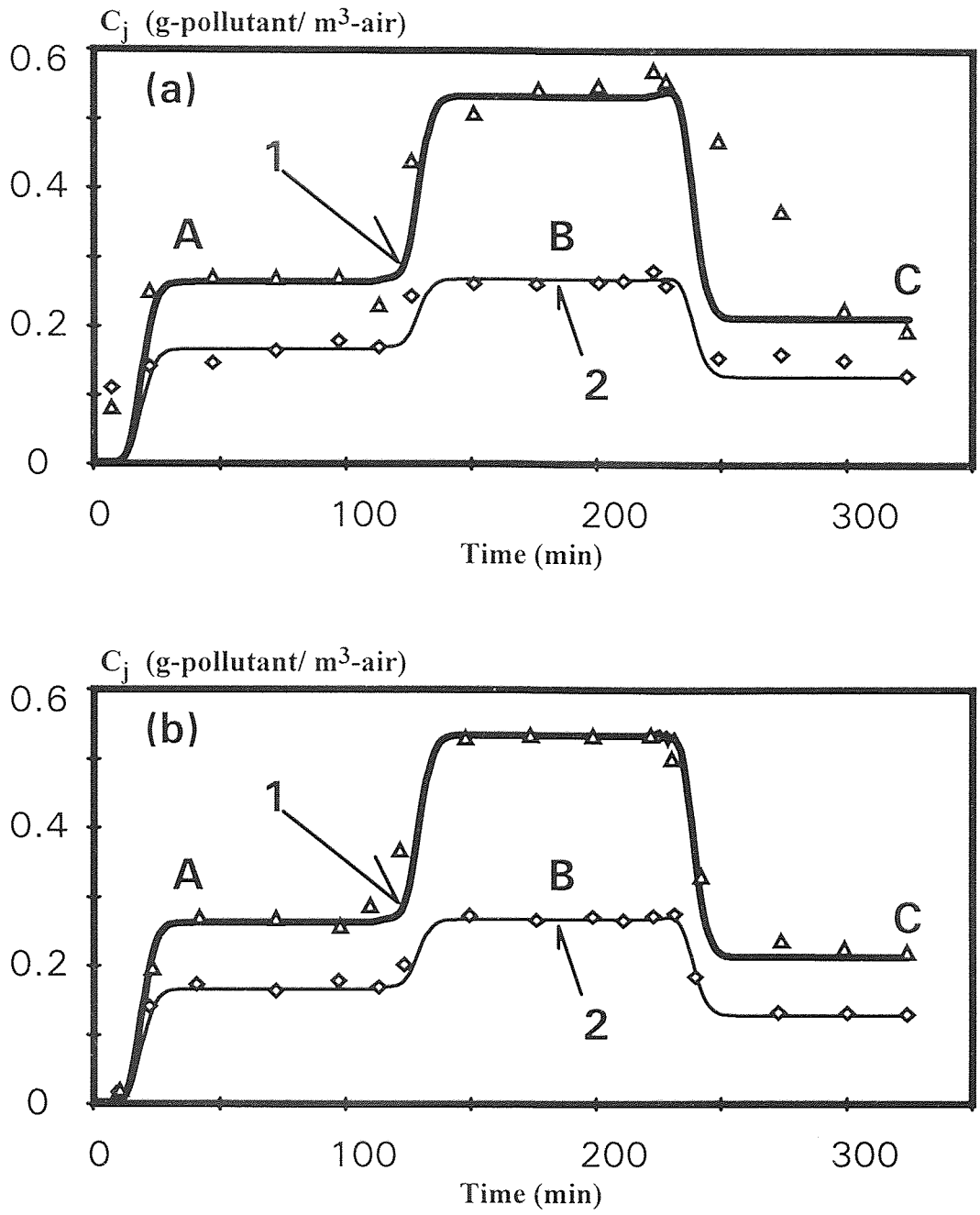

Figure 6.6 Experimental and model-predicted concentration profiles at the outlet (a) and middle point (b) of the column for τ = 1.18 min, F = 0.042 m^3/h, and C_{Bin}(g/m^3) = 0.18, 0.28, 0.12, C_{Tin}(g/m^3) = 0.28, 0.55, 0.19, for **A**, **B**, and **C**, respectively. Benzene: diamonds and curve 2. Toluene: triangles and curve 1.

The experiment, results of which are shown in Figure 6.7 was performed under constant residence time, as that shown in Figure 6.6 but there was a significant difference. Here, the column was originally fed with an airstream carrying benzene only (condition A). After equilibrium was reached, toluene was introduced in the airstream and -at the same time- the benzene concentration was increased (condition B). In this case, the model-predicted concentration profile under condition A does not involve any assumption (since there was only one compound), and the agreement with the data is very good. Under condition B, the agreement is poor, especially for the case of toluene. It appears that, when competition is ignored the model predicts lower benzene and higher toluene concentrations during transients. This is something difficult to explain since at high benzene concentrations the model underpredicts concentration during transients even in cases where benzene is the only VOC in the stream (e.g., transition from region A to B in Figure A-2.13). However, one could possibly argue that the overprediction of toluene concentrations during transients may indicate a preferential toluene adsorption.

Experiments similar to the one discussed in conjunction with Figure 6.7 were also performed under other conditions, and the results are reported in Figures A-2.13 and A-2.14. Upon introduction of toluene (transition from region B to C) Figure A-2.13 exhibits the same features with Figure 6.7. Once again, one can observe the significant overshoot in the outlet concentration upon a substantial decrease in the concentration of a pollutant in the inlet stream (benzene, transition from region B to C in Figure A-2.13(a)). Figure A-2.14(a) exhibits some interesting features. The inlet benzene concentration remains constant in regions A and B while toluene is introduced (transition from A to B). The data suggest that the introduction of toluene does not affect benzene adsorption while once again, the model overpredicts the toluene transient concentrations. The transition from region C to D in Figure A-2.14(a) seems to be the only indication which is consistent with the existence of competitive inhibition as the non-competitive model underpredicts the gas phase concentrations of both pollutants during transients.

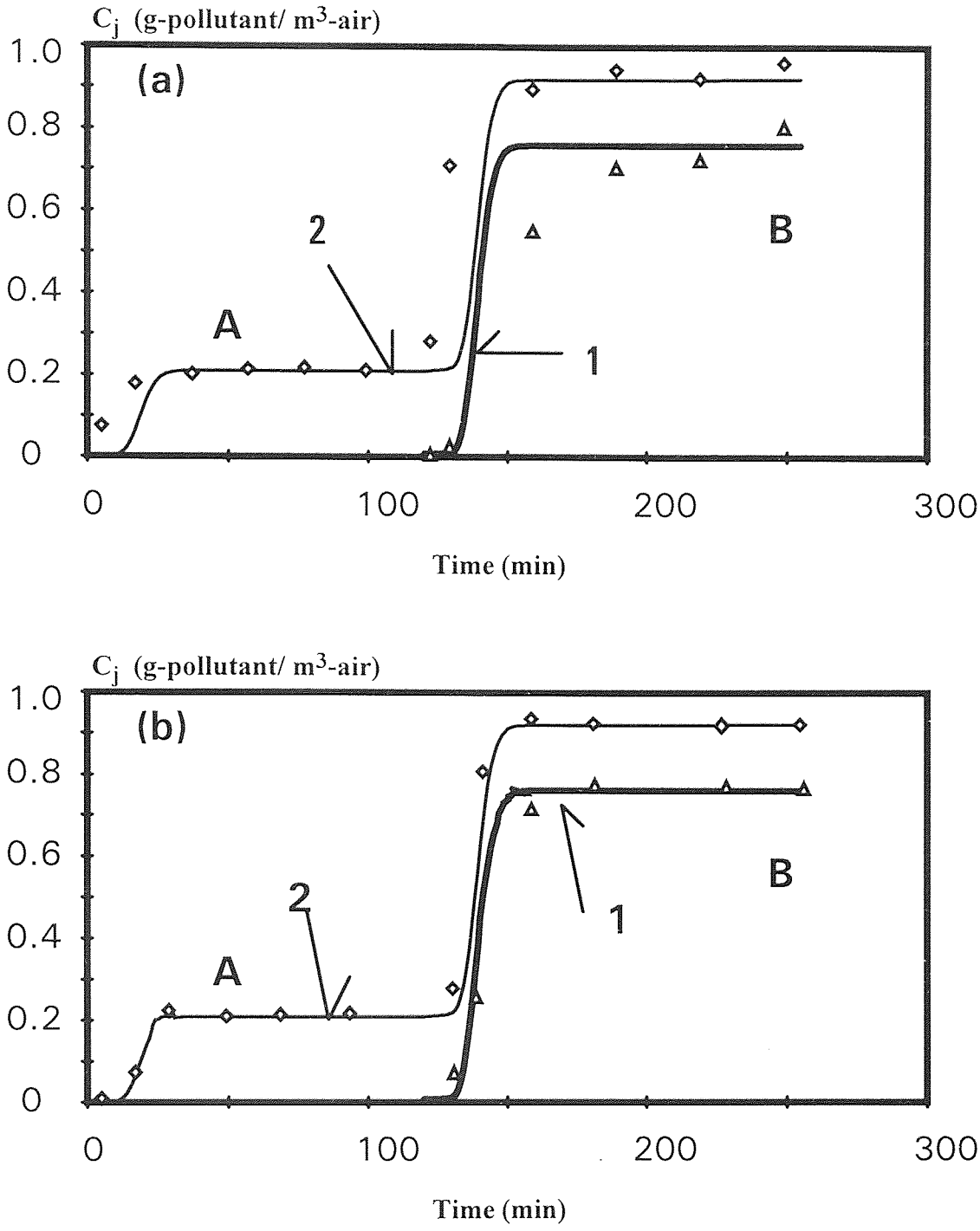

Figure 6.7 Experimental and model-predicted concentration profiles at the outlet (a) and middle point (b) of the column for τ = 1.23 min, F = 0.041 m^3/h, and C_{Bin}(g/m^3) = 0.22, 0.97, C_{Tin}(g/m^3) = 0.0, 0.81, for **A**, and **B**, respectively. Benzene: diamonds and curve 2. Toluene: triangles and curve 1.

Figure A-2.15 shows results from an experiment performed under extremely high concentrations. Initially, the column was supplied with an airstream carrying toluene only at 38 g/m^3. After equilibrium, the toluene concentration was decreased to 8 g/m^3 and -simultaneously- benzene was introduced at 15 g/m^3 . Clearly, the model fails completely to describe the data. The model not only does not account for interaction, but is also applied (for single compounds) at concentrations where even the single compound adsorption isotherms are not valid. The data for both toluene and benzene do not seem to make sense. The toluene data show that more than predicted toluene is desorbed. This is not expected because the adsorption isotherm used most likely overpredicts the toluene concentration on the solids. The benzene data should indicate that a smaller than predicted amount is adsorbed on the solids, thus the concentration of benzene in the outlet airstream should reach that at the inlet much faster than what the model predicts. The diagram of Figure A-2.15 shows exactly the opposite.

Figure 6.8 shows results from an experiment during which the concentrations of benzene and toluene in the inlet airstream were kept constant while the residence time was changed. As also mentioned in the preceding section, a change in residence time should not affect concentration profiles, and this is reflected by the data shown in Figure 6.8. The model predictions show a change because (under conditions A) the model failed to predict attainment of steady-state within the time frame of the experiment.

The experimental results obtained with airstreams carrying mixtures of benzene and toluene seem to suggest the following. When a new packing material is used, and is subjected to both benzene and toluene, the data agree in general with what one would expect by either assuming no interaction or competition. However, in cases where the packing is already saturated with one of the compounds, introduction of the second seems to lead to adsorption of the second compound which is higher than anticipated. This is something which needs further investigation.

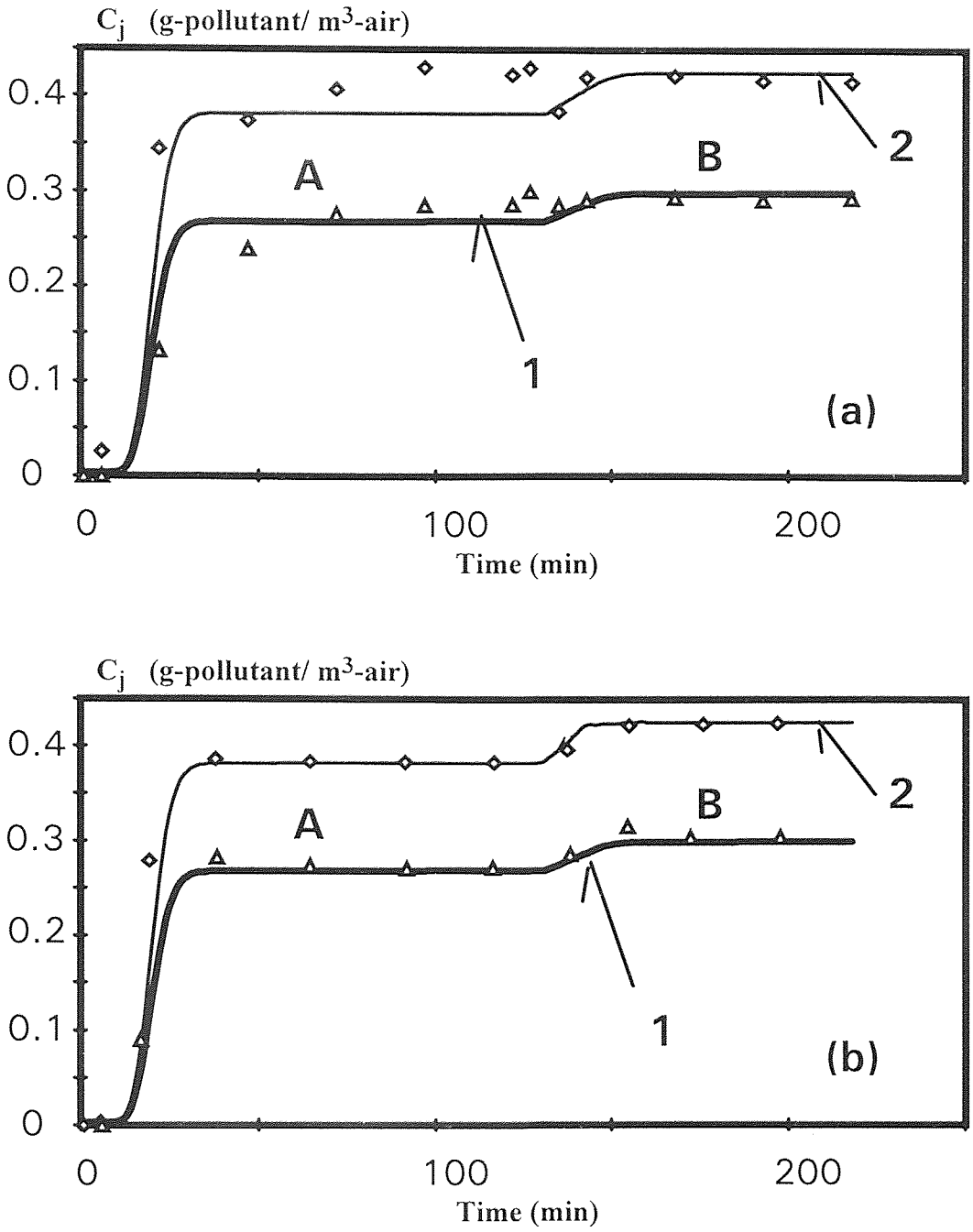

Figure 6.8 Experimental and model-predicted concentration profiles at the outlet (a) and middle point (b) of the column when C_{Bin} (g/m^3) = 0.43 and C_{Tin} (g/m^3) = 0.30. Other conditions τ (min)/F (m^3/h) are 2.70/0.0186 for **A** and 1.81/0.0276 for **B**. Benzene: diamonds and curve 2. Toluene: triangles and curve 1.

CHAPTER 7

CONCLUSIONS AND RECOMMENDATIONS

This study has led to the determination of values of various parameters which are essential for an accurate description of transient biofiltration. The (real) density of a solid packing consisting of peat and perlite (2:3) volume ratio was determined as 0.679×10^6 g-solids/ m^3-solids. The packing was found to have a water holding capacity of 0.601 m^3-water/ m^3-packing (i.e., a porosity of 60%), and a specific surface area of 1961 m^{-1}. The void fraction of the bed was found to be 0.324. With the exception of the specific surface area, the values of the other parameters were found to be close to those estimated (or guessed) in earlier studies with the same packing material [e.g., Shareefdeen and Baltzis (1994)].

Batch adsorption studies of single VOCs have demonstrated that hydrophilic solvents adsorb more readily to the peat and perlite packing material than the hydrophobic solvents. The hydrophilic solvents achieve an equilibrium solids concentration 150 times higher than the equilibrium solids concentration of the hydrophobic solvents, for the same equilibrium gas concentration. This is due to the added absorption of the hydrophilic solvents into the medium present in the pores. All of the solvents were found to follow the Freundlich isotherm with approximately a 99% accuracy. The concentrations of benzene and toluene used in the experiments were low and probably for this reason the adsorption isotherms for these compounds were found to be practically linear.

Batch adsorption studies with mixtures of benzene and toluene revealed that -for the concentration ranges employed in the experiments- the two solvents are involved in a competitive cross-inhibition. The data were successfully described by the Langmuir-

Freundlich equation. The results suggest that benzene inhibits toluene adsorption more than toluene does for benzene.

Column (or flow through) adsorption experiments were also performed with benzene, toluene, and their mixtures. Data from experiments with single VOCs were described with a model which allowed for determination of a correlation for calculating the mass transfer coefficient. This correlation is essentially a modification of an expression earlier proposed by Jones et al. (1993) for the mass transfer coefficient of a solute from a liquid phase to a biofilm. Using this modified correlation, transient data were described (predicted) relatively well. The agreement was found to be better for the case of benzene than for toluene.

Transient data with airstreams containing both benzene and toluene have led to puzzling results. In experiments which started with packing containing no solvent in it, the data followed in general the expected trends, and at low concentrations -when inhibition is not important- they were relatively accurately predicted by the model under the assumption of no interaction. Data which were obtained after the packing was first brought to equilibrium with a solvent suggested that adsorption of a second solvent (compound) is higher than what would be expected under the assumption of no interaction. This result, opposite to what competitive inhibition would imply, is really unexpected and needs further investigation.

In the future, work should be done in the following areas:

1. Adsorption equilibrium isotherms with single VOCs should be determined over a wider concentration range.
2. Detailed desorption experiments should be performed in columns saturated with single VOCs in order to see if adsorption is indeed completely reversible and thus, conclude that there is no amount of VOCs irreversibly adsorbed to the solids.
3. For mixtures batch adsorption experiments with fresh packing should be performed over a wider range of concentration values.

4. Batch adsorption experiments should be performed with packing saturated with benzene and then exposed to toluene and vice versa (saturation with toluene and subsequent exposure to benzene).
5. Column experiments should be performed in ways (possibly with the use of a tracer) which would allow testing the assumption of plug flow of air in the column.
6. A computer code should be developed for describing transient adsorption of interacting (competitive or facilitated) adsorption of solvents.

APPENDIX A1

CALIBRATION CURVES
FOR BENZENE, TOLUENE, ETHANOL AND BUTANOL
(m is the slope determined by linear regression)

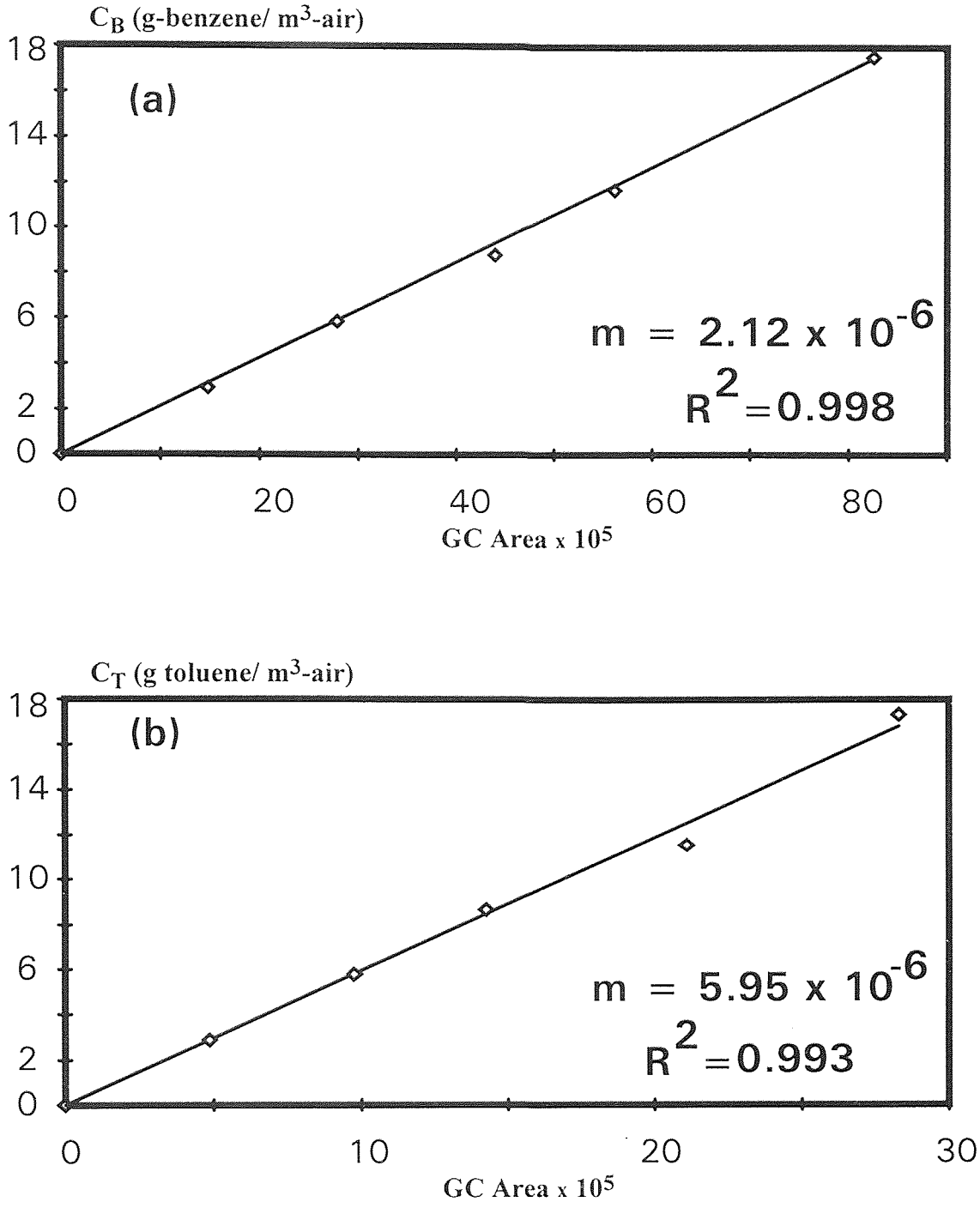

Figure A-1.1 Calibration curves for benzene (a) and toluene (b).

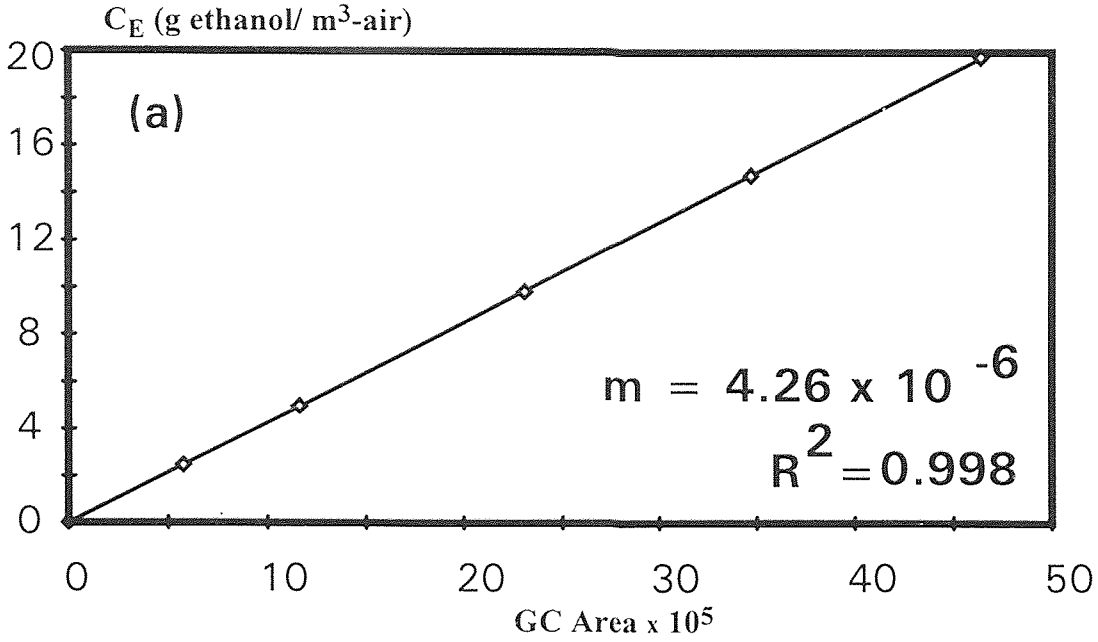

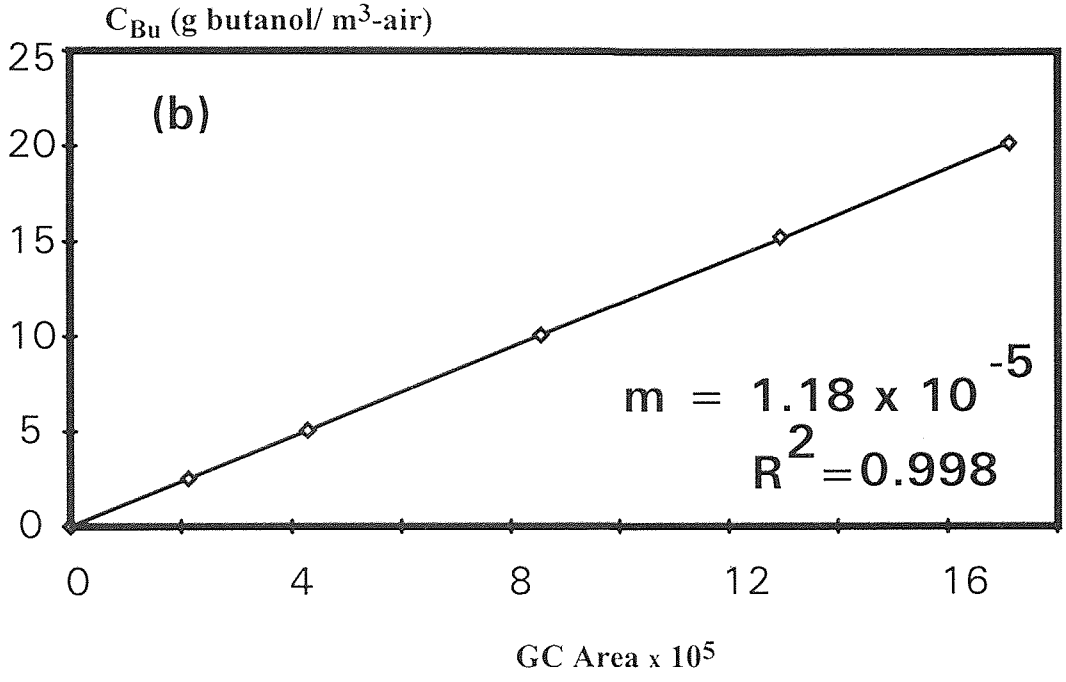

Figure A-1.2 Calibration curves for ethanol (a) and butanol (b).

APPENDIX A2

EXPERIMENTAL AND MODEL-PREDICTED CONCENTRATION PROFILES FROM COLUMN EXPERIMNTS

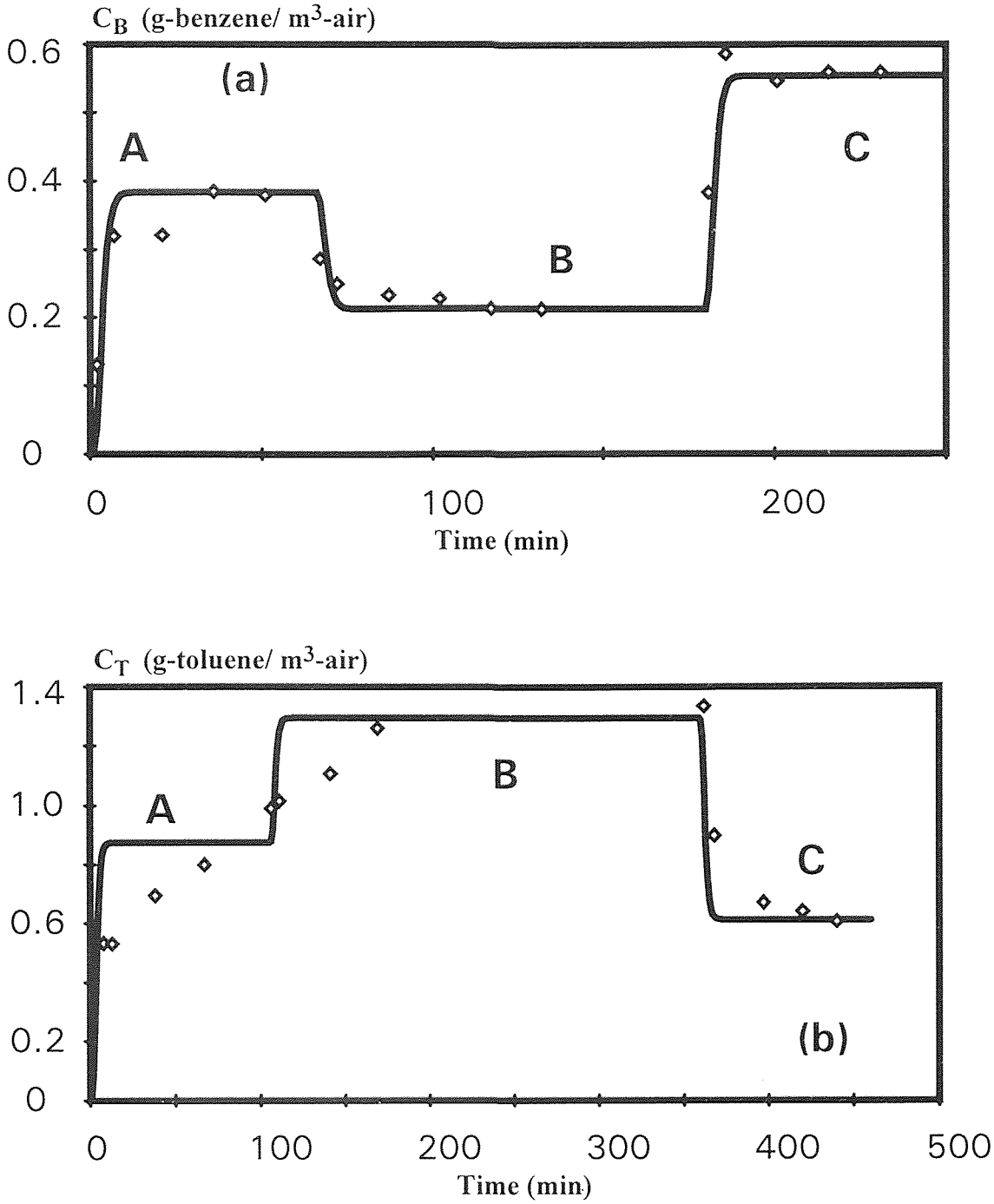

Figure A-2.1 Fitted concentration profiles at port 3 of the column for benzene (a) and toluene (b) under conditions described in Figure 6.1. Port 3 is located at 25% of the volume of the column.

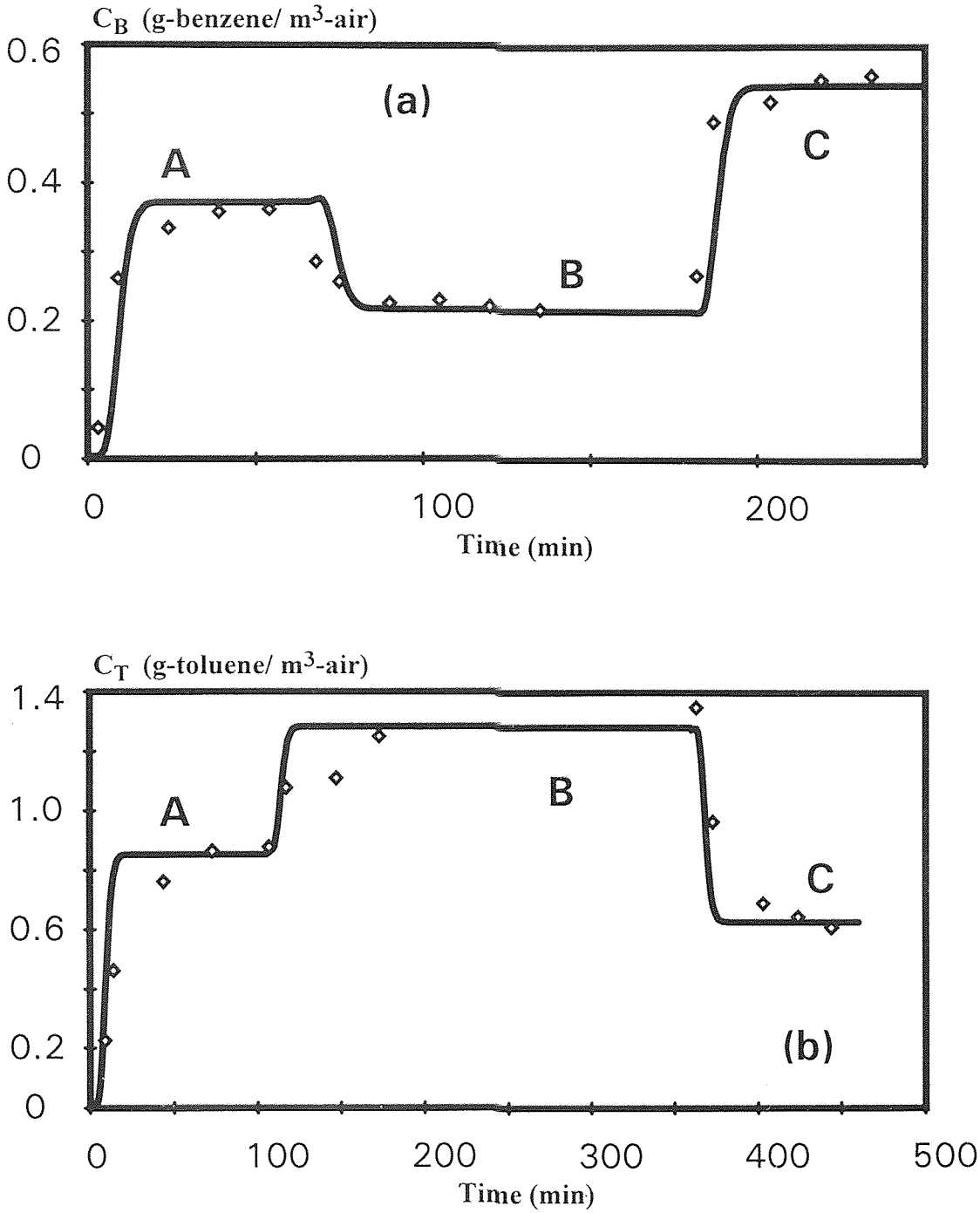

Figure A-2.2 Fitted concentration profiles at port 2 of the column for benzene (a) and toluene (b) under conditions described in Figure 6.1. Port 2 is located at 50% of the volume of the column.

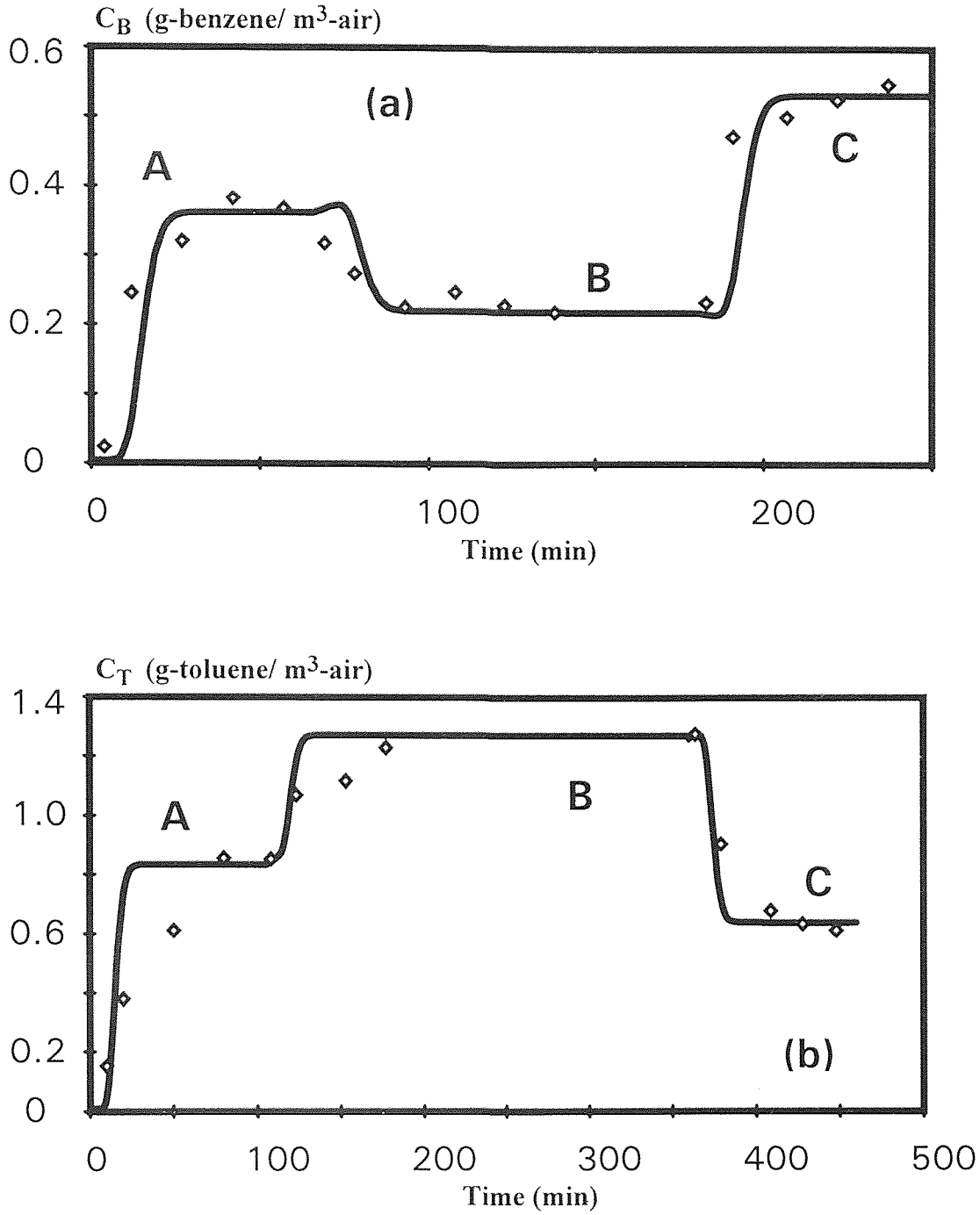

Figure A-2.3 Fitted concentration profiles at port 1 of the column for benzene (a) and toluene (b) under conditions described in Figure 6.1. Port 1 is located at 75% of the volume of the column.

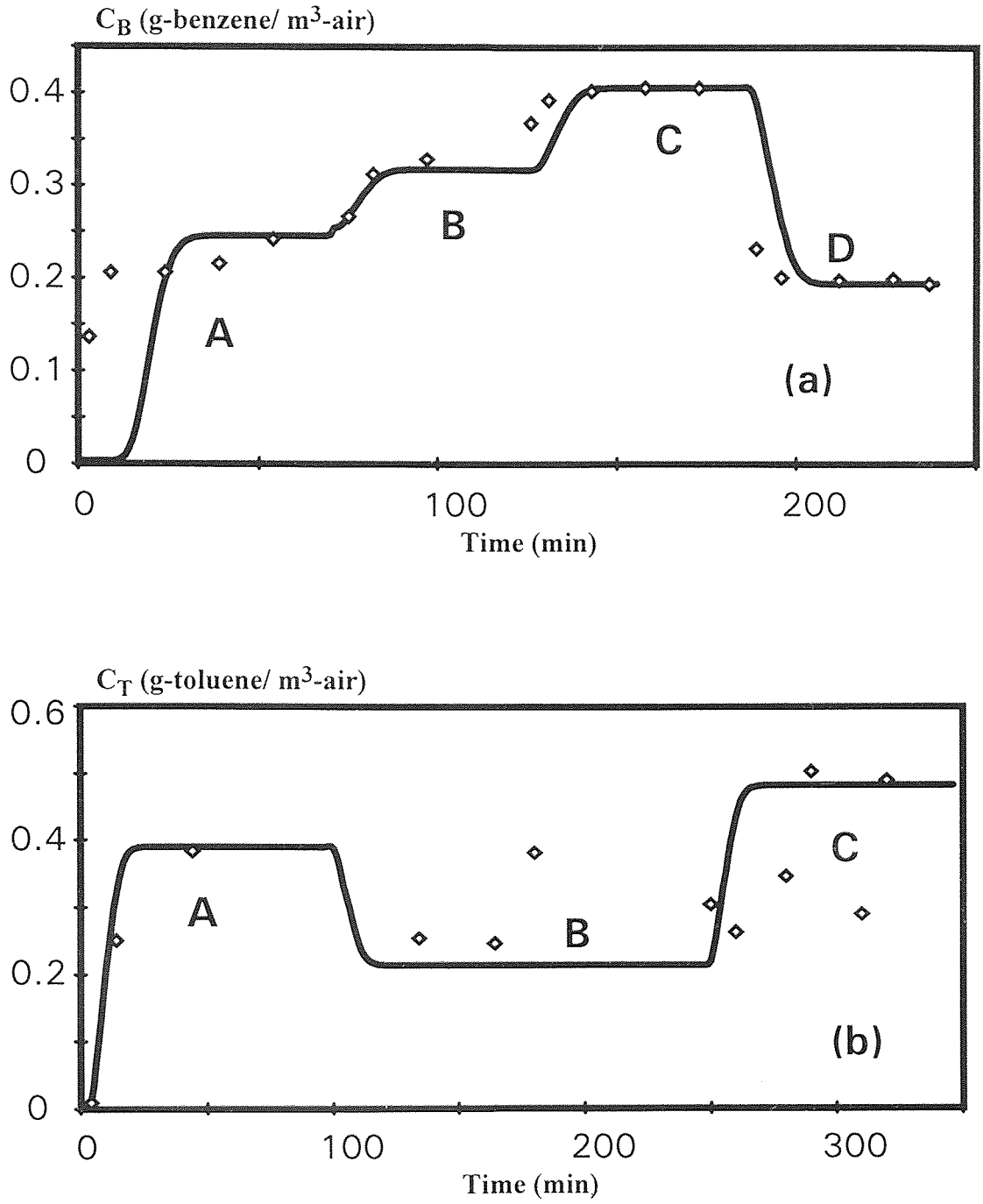

Figure A-2.4 Experimental (symbols) and model-predicted (curves) concentration profiles for benzene (a) and toluene (b) at the middle point of the bed. Conditions for the experiments are same with those in Figure 6.3.

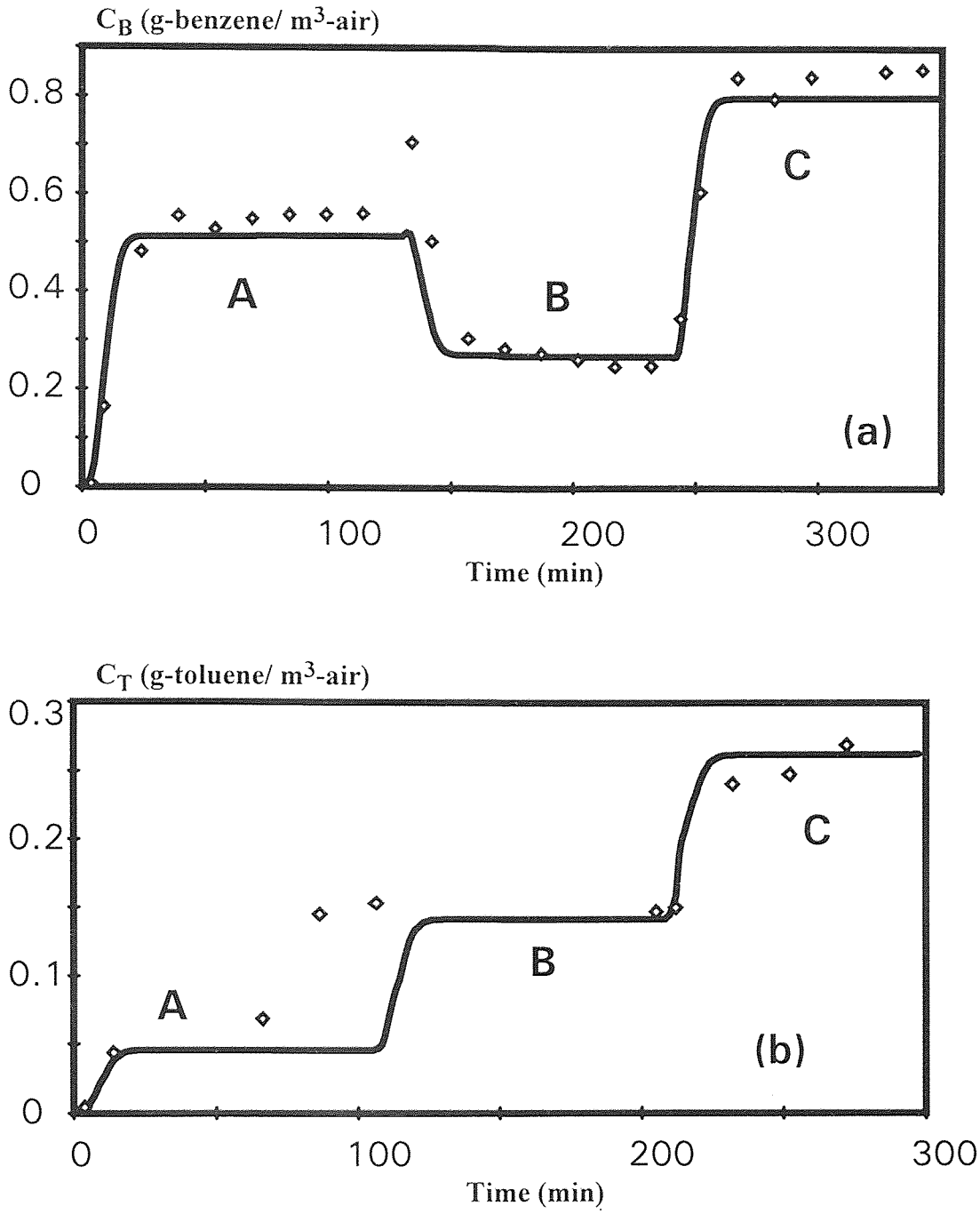

Figure A-2.5 Experimental (symbols) and model-predicted (curves) concentration profiles for benzene (a) and toluene (b) at the middle point of the bed. Conditions for the experiments are same with those in Figure 6.4.

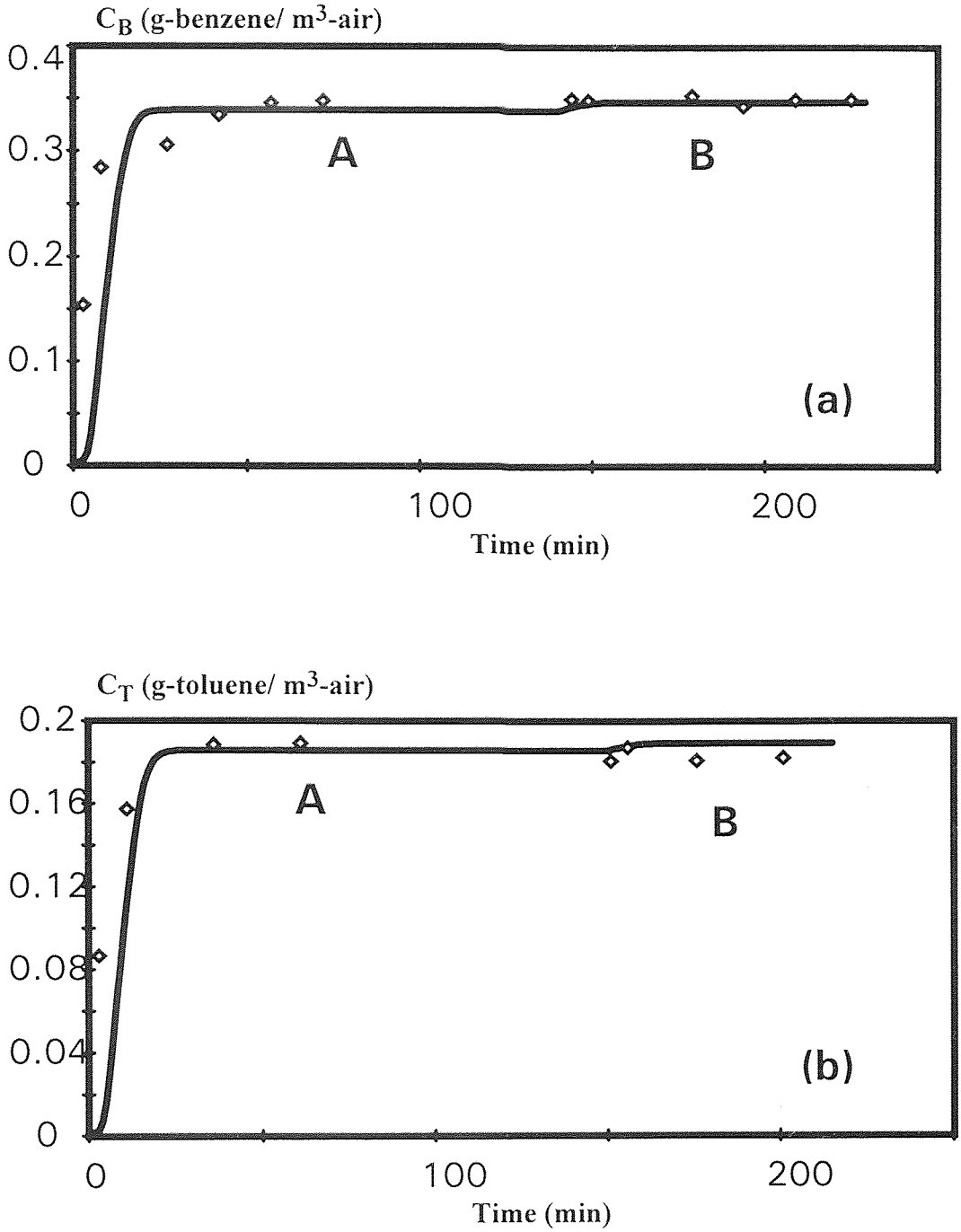

Figure A-2.6 Experimental (symbols) and model-predicted (curves) concentration profiles for benzene (a) and toluene (b) at the middle point of the bed. Conditions for the experiments as same with those in Figure 6.5.

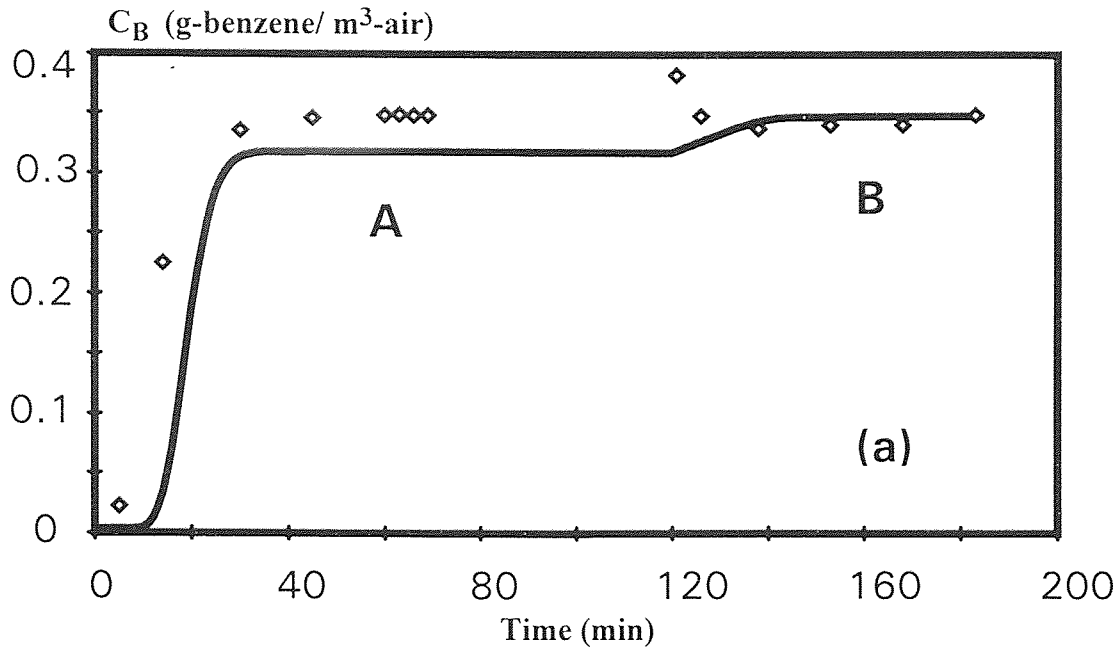

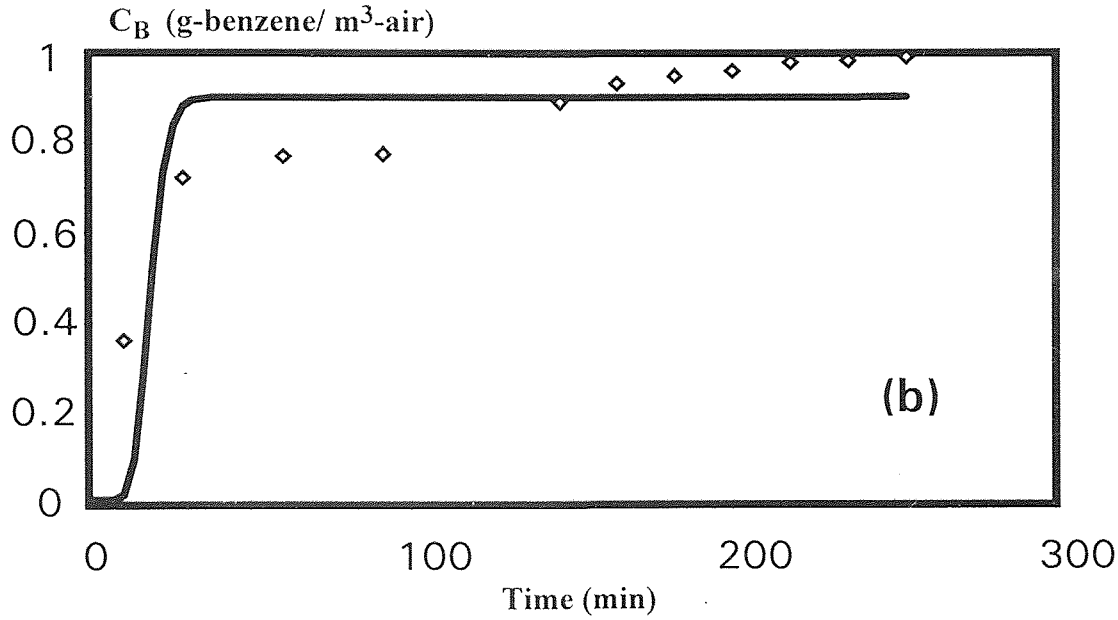

Figure A-2.7 Experimental (symbols) and model-predicted (curves) benzene concentration profiles at the exit of the bed when C_{Bin} (g/m^3) = 0.35 (a) and 1.06 (b). Other conditions are, (a): τ (min)/F (m^3/h), 2.0/0.025 and 0.93/0.054 for A and B, respectively; (b): τ (min)/F (m^3/h), 3.98/ 0.013.

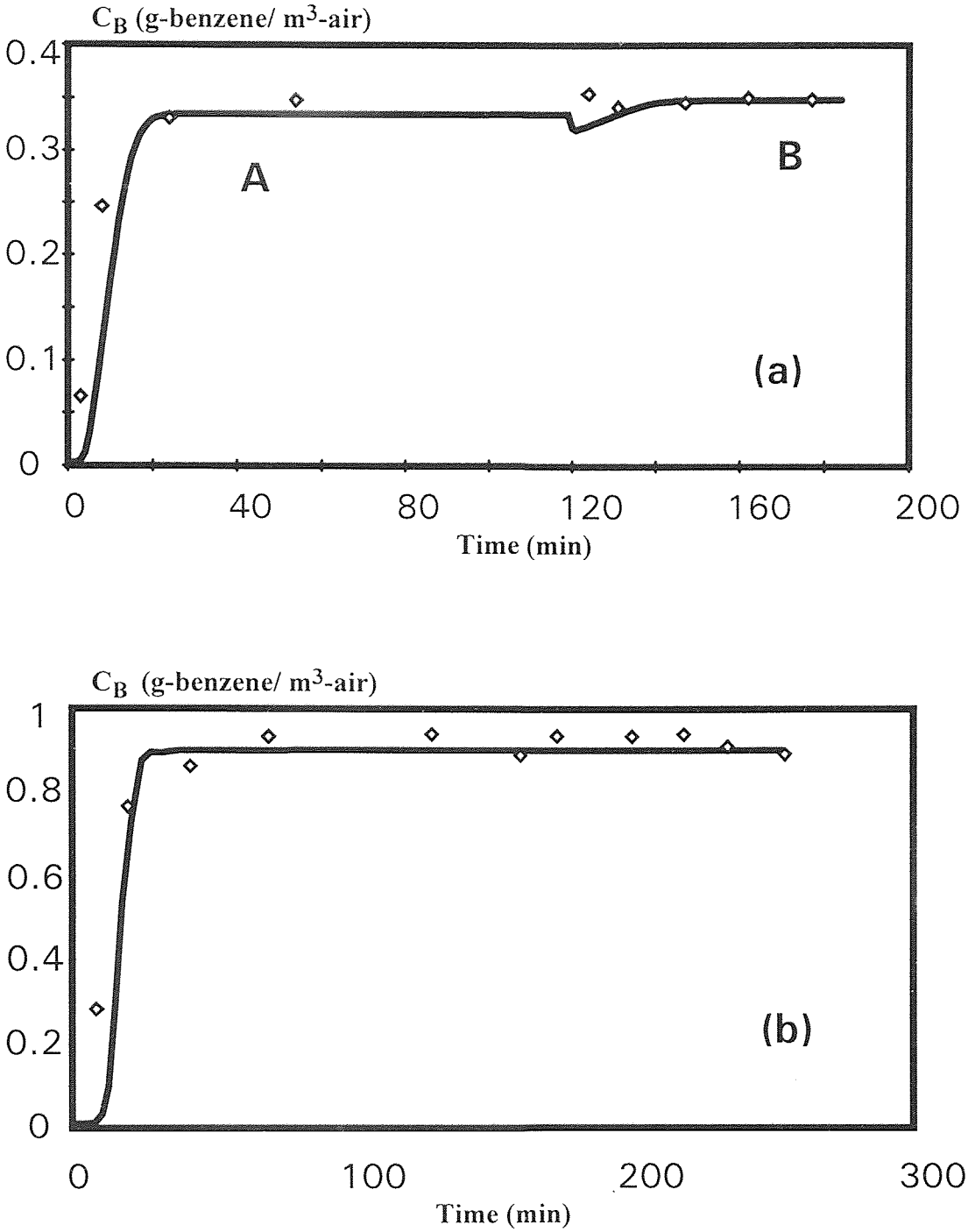

Figure A-2.8 Experimental (symbols) and model-predicted (curves) benzene concentrations profiles at the middle-point of the bed. Conditions are (correspondingly) the same as those in Figure A-2.7.

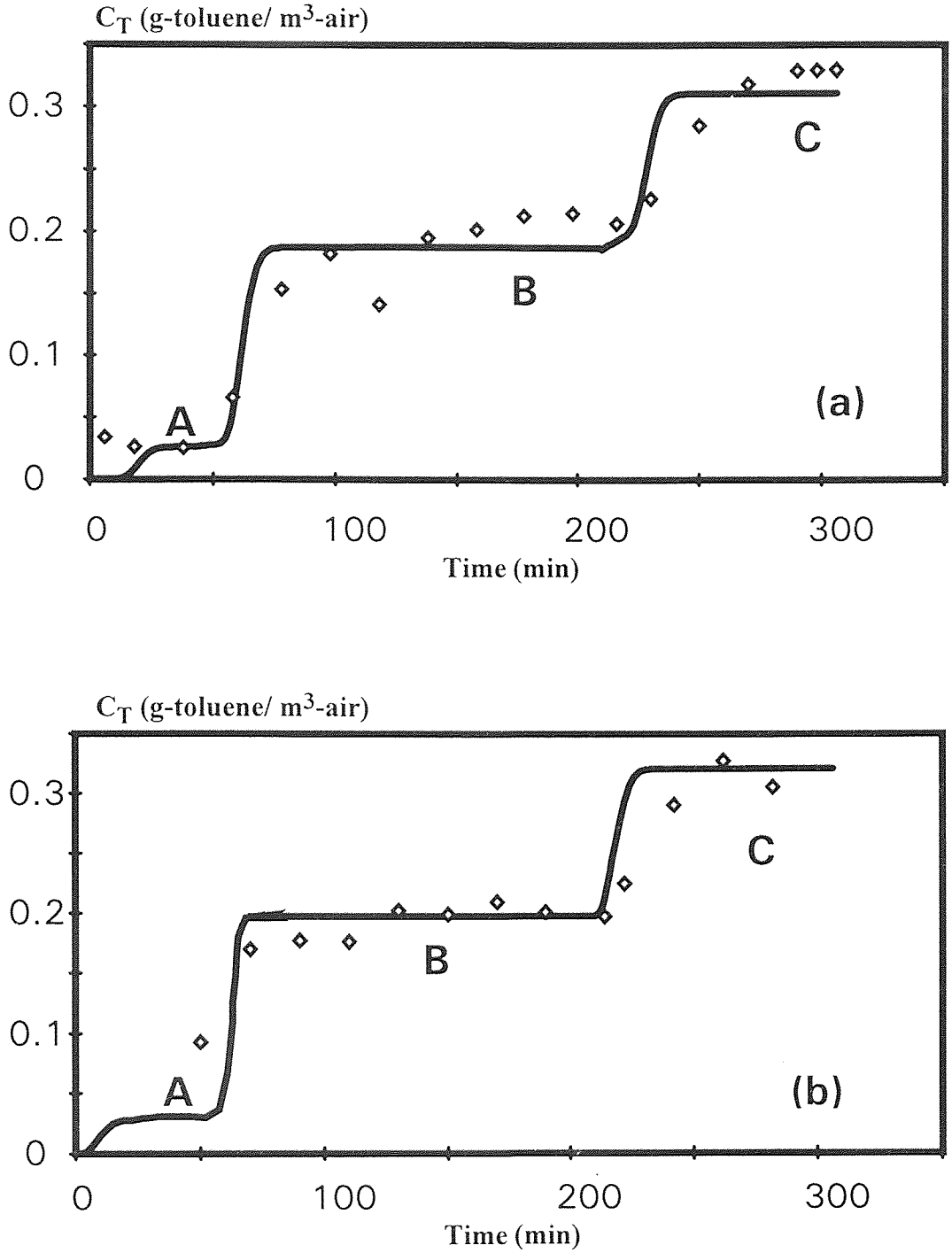

Figure A-2.9 Experimental (symbols) and model-predicted (curves) toluene concentration profiles at the outlet (a) and middle point (b) of the bed when τ= 3.43 min, F = 0.014 m^3/h, and C_{Tin} (g/m^3) = 0.03, 0.21, 0.33, for **A**, **B**, and **C**, respectively.

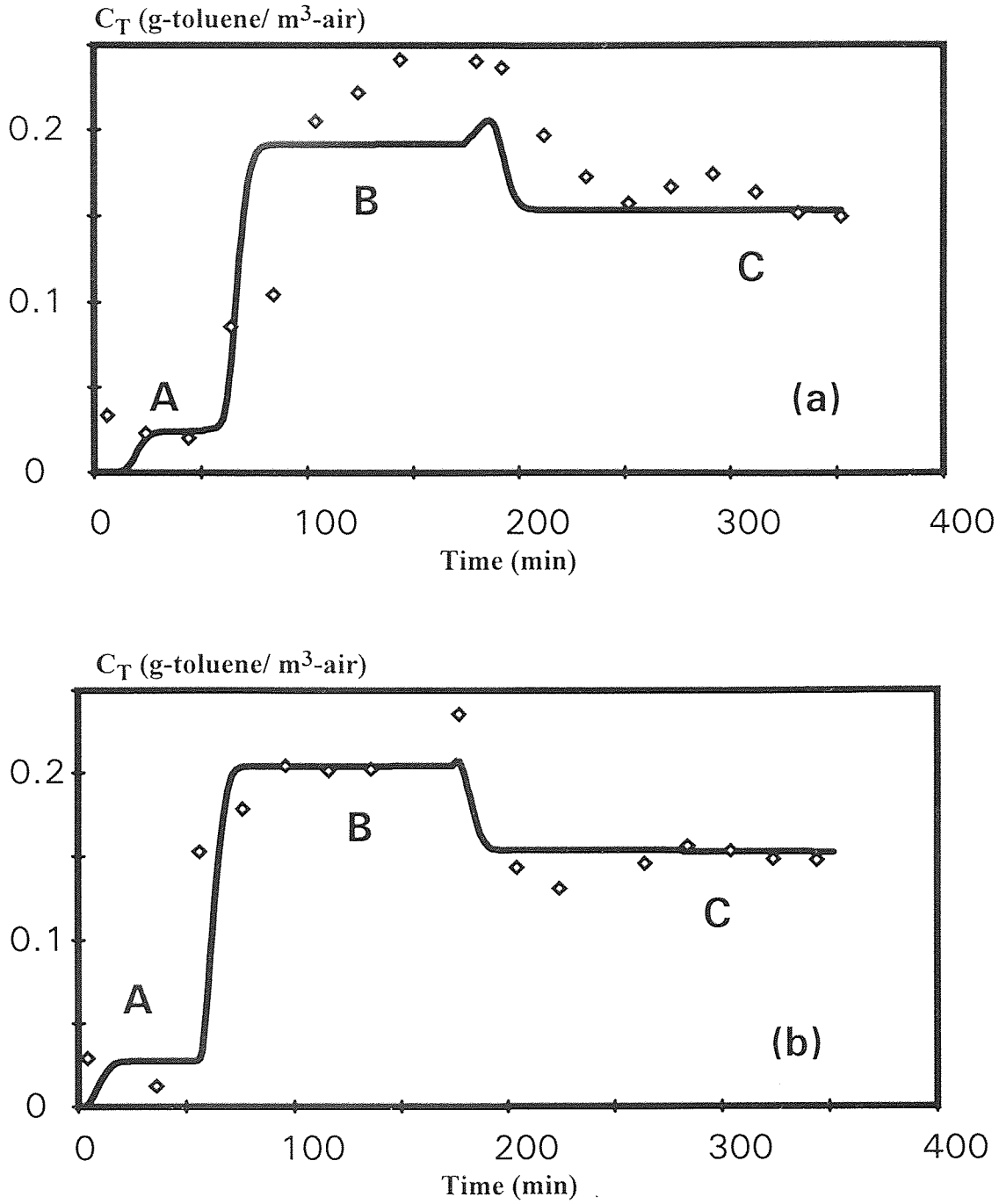

Figure A-2.10 Experimental (symbols) and model-predicted (curves) toluene concentration profiles at the outlet (a) and middle point (b) of the bed when τ= 4.23 min, F = 0.011 m^3/h, and C_{Tin} (g/m^3) = 0.03, 0.22, 0.15, for **A**, **B**, and **C**, respectively.

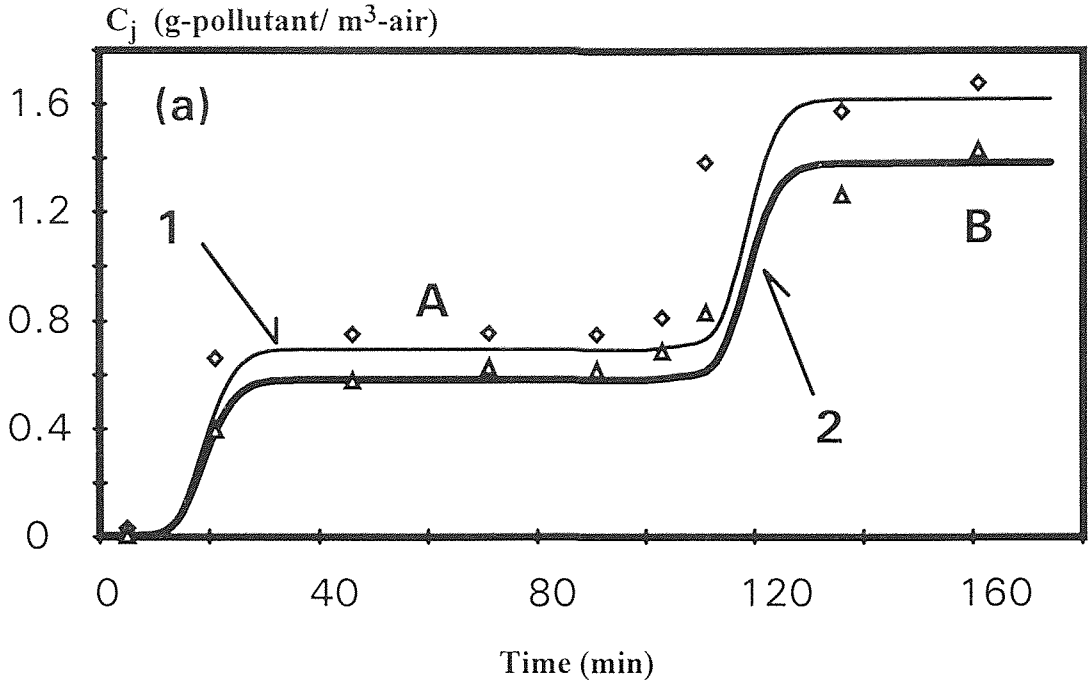

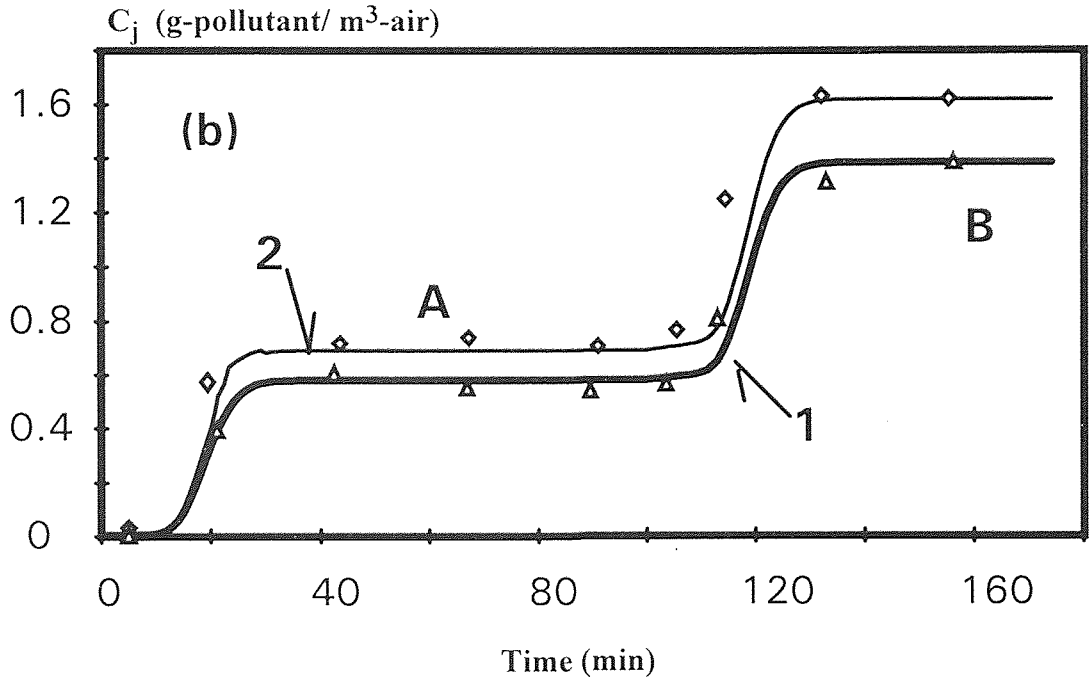

Figure A-2.11 Experimental and model-predicted concentration profiles at the outlet (a) and middle point (b) of the column for τ = 1.59 min, F = 0.032 m^3/h, and inlet concentrations, C_{Bin} (g/m^3) = 0.75, 1.70, C_{Tin} (g/m^3) = 0.63, 1.45, for **A** and **B**, respectively. Benzene: diamonds and curve 2. Toluene: triangles and curve 1.

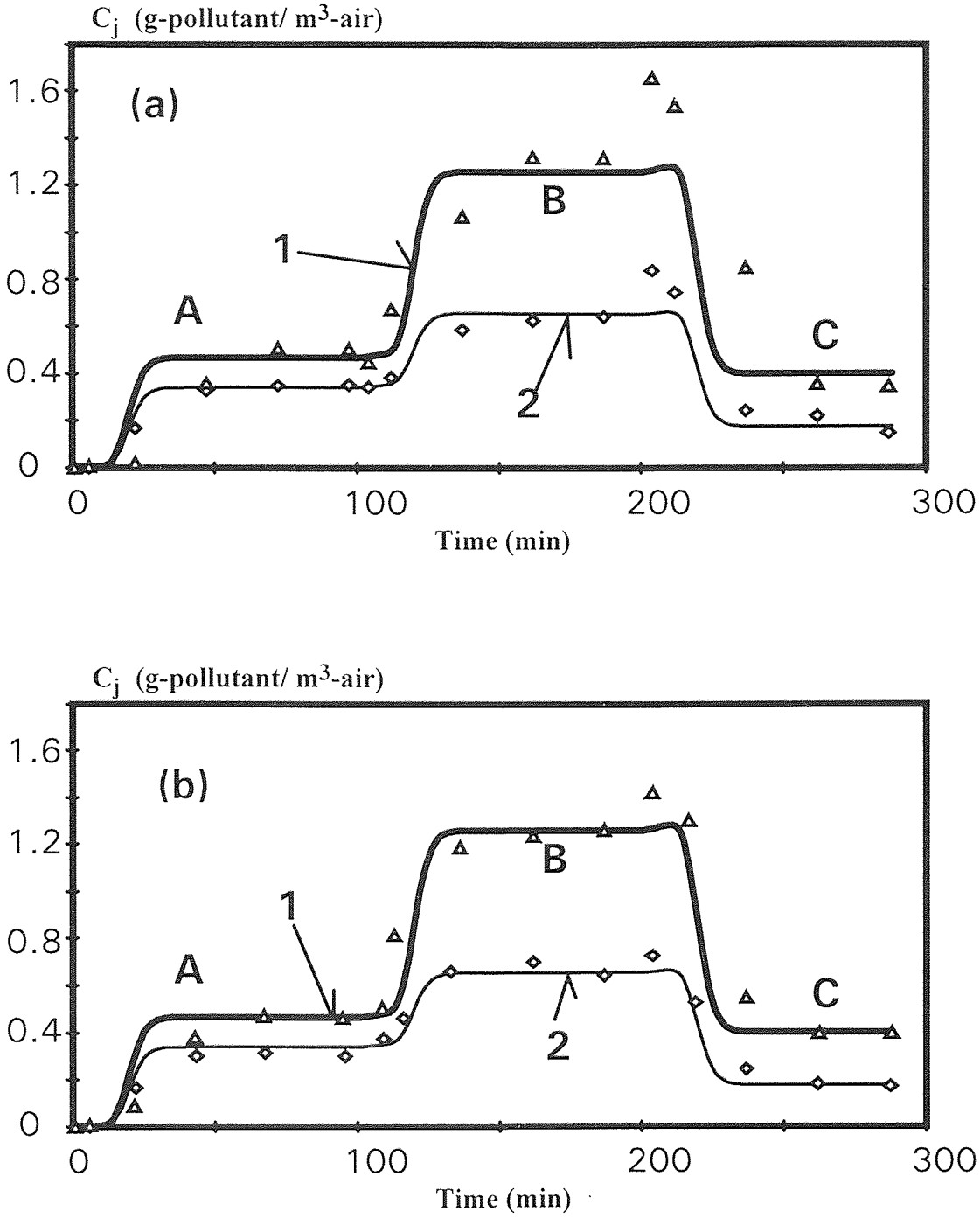

Figure A-2.12 Experimental and model-predicted concentration profiles at the outlet (a) and middle point (b) of the column for τ = 4.41 min; F = 0.011 m^3/h, and C_{Bin} (g/m^3) = 0.37, 0.68, 0.14, C_{Tin} (g/m^3) = 0.50, 1.32, 0.34, for **A**, **B**, and **C**, respectively. Benzene: diamonds and curve 2. Toluene: triangles and curve 1.

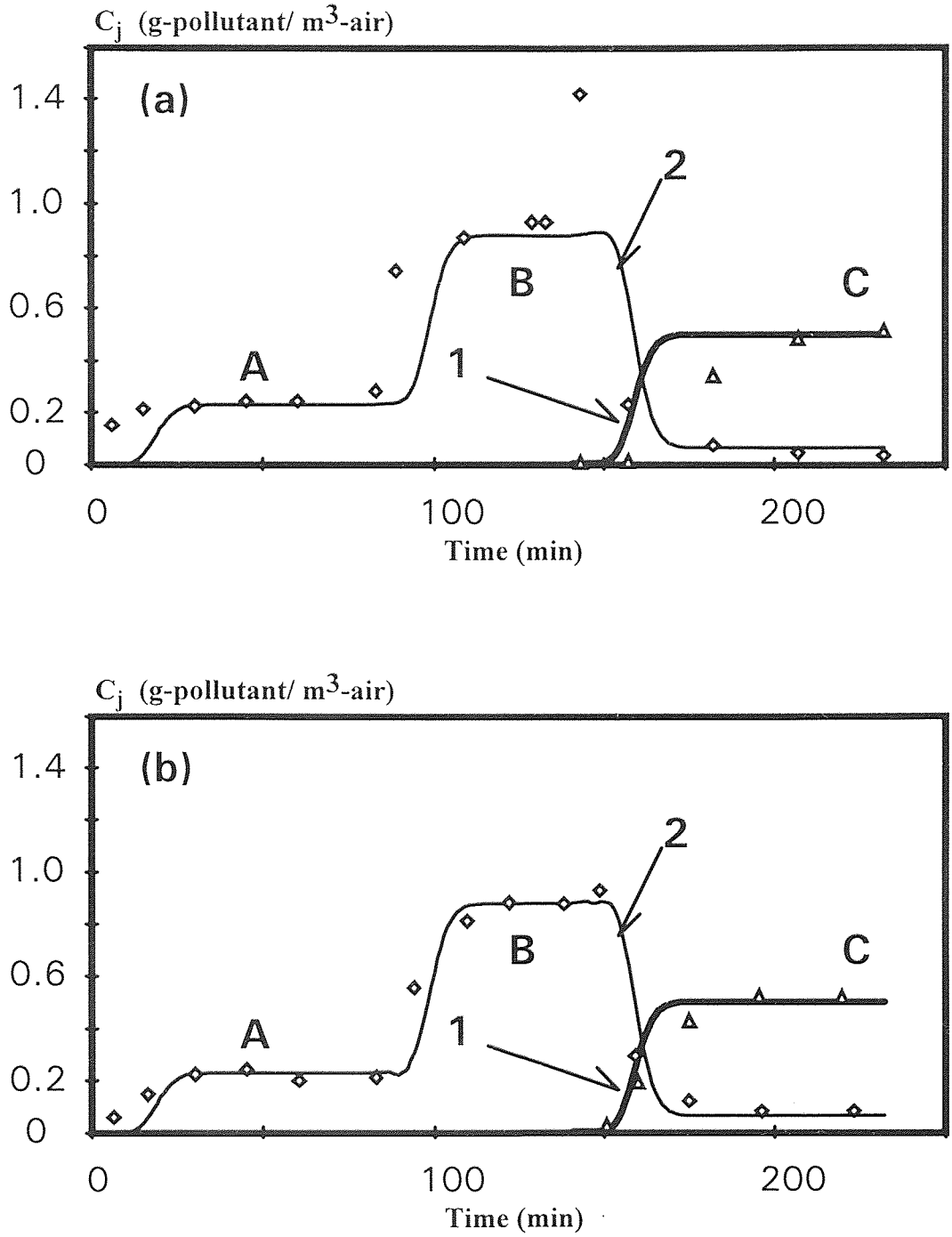

Figure A-2.13 Experimental and model-predicted concentration profiles at the outlet (a) and middle point (b) of the column for τ = 1.06 min, F = 0.047 m^3/h, and C_{Bin} (g/m^3) = 0.24, 0.92, 0.021, C_{Tin} (g/m^3) = 0.0, 0.0, 0.53, for **A**, **B**, and **C**, respectively. Benzene: diamonds and curve 2. Toluene: triangles and curve 1.

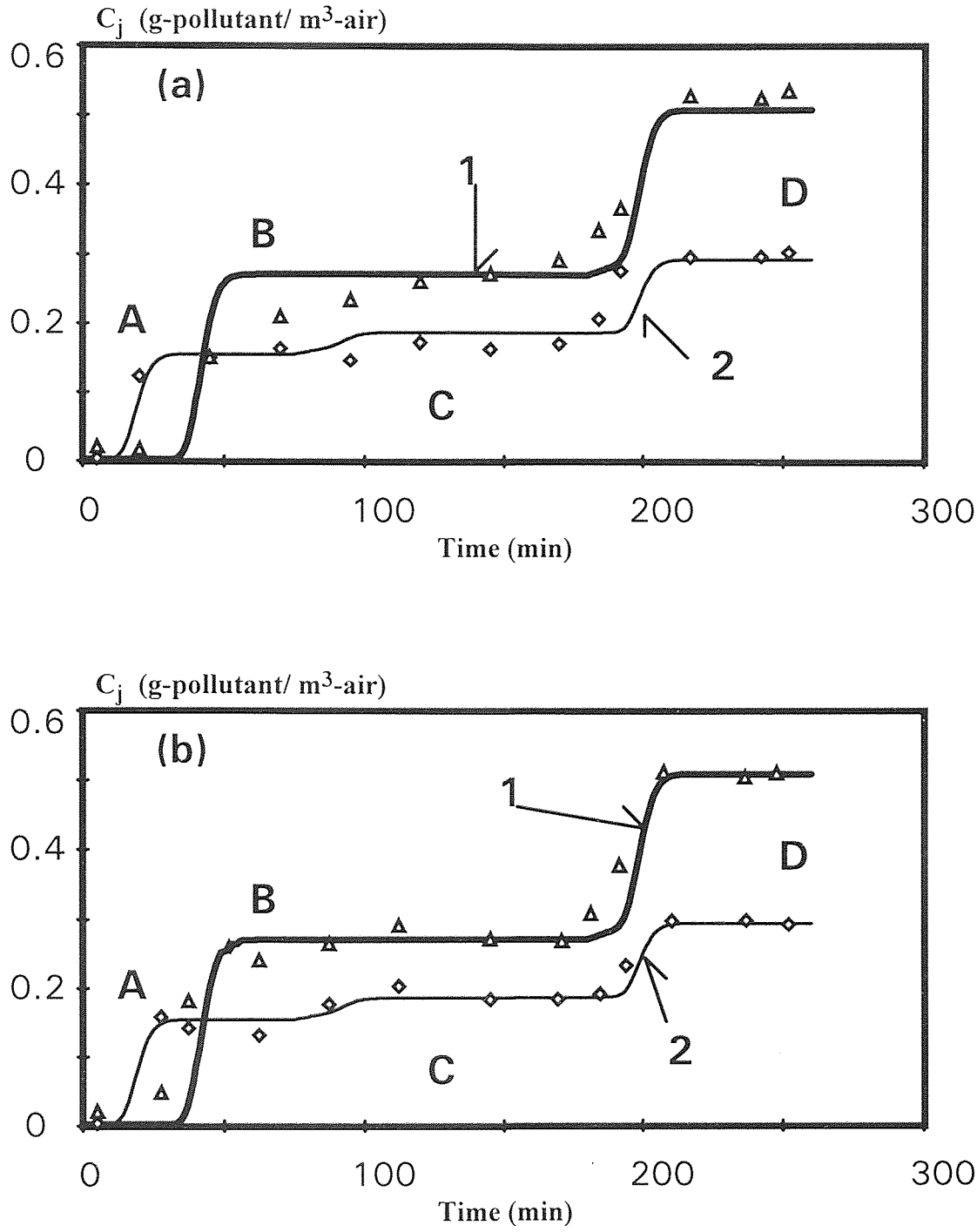

Figure A-2.14 Experimental and model-predicted concentration profiles at the outlet (a) and middle point (b) of the column for τ = 2.33 min, F = 0.021 m^3/h, and C_{Bin} (g/m^3) = 0.17, 0.17, 0.19, 0.31, C_{Tin} (g/m^3) = 0.0, 0.30, 0.30, 0.54, for **A**, **B**, **C**, and **D**, respectively. Benzene: diamonds and curve 2. Toluene: triangles and curve 1.

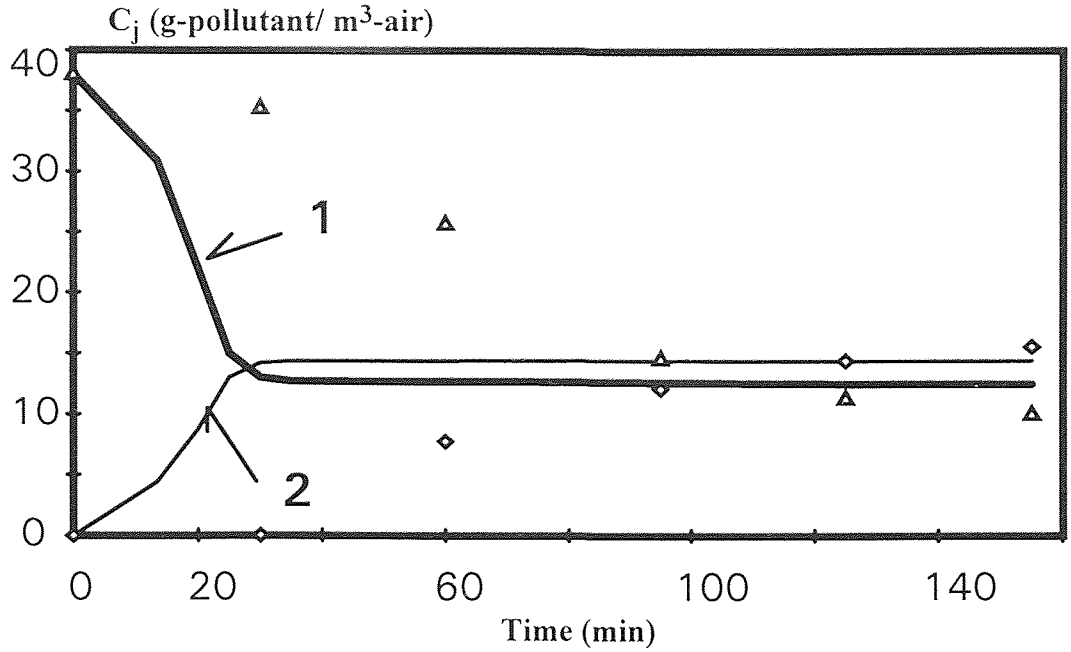

Figure A-2.15 Experimental and model-predicted concentration profiles at the outlet of the column for τ = 6.3 min, F = 0.0079m^3/h, C_{Bin} = 15 g/m^3, C_{Tin}= 8 g/m^3. Originally, the column was at steady-state with an airstream carrying toluene only at 38 g/m^3. Benzene: diamonds and curve 2. Toluene: triangles and curve 1.

APPENDIX B

COMPUTER CODE

```
c*******************************************************
c
c  Purpose     : "Solution of the Transient Biofitration
c                   Model for a Single VOC"
c
c  Method      : ODESSA-Ordinary Differential Equation
c                   Solver with explicit Sensitivity Analysis;
c                   Stiff mode with user supplied jacobian
c                   option is used
c
c  Language    : FORTRAN
c
c  Requirement : ODESSA package which is a part of AUTO
c
c  By          :      Zarook Shareefdeen (1994)
c  Modified by:  Steven Wojdyla (1995)
c*******************************************************
      implicit double precision(a-h,o-z)
      parameter(nt=100)
      parameter(nh=20)
      external fun,dfun,jfun
      dimension par(7),y(3*nh,8),atol(3*nh,8),rtol(3*nh,8),
     1        rwork(5000),iwork(100),neq(2),iopt(3)
      dimension cg(nt,nh+1), co(nt,nh+1), cp(nt,nh+1),
     1        time(nt), ht(nh+1)
c
      common /ef1/ ef1
      common /del/ del
      common /dz / dz
      common /acg01/ acg01,tau
c
      open (5, file = 'trtol.dat', status='old')
      open (6, file = 'trtola.out', status='new')
      open (7, file = 'trtolb.out', status='new')
c
c  conditions of pdes
c
      n=3*nh
      npar=7
      neq(1)=n
      neq(2)=npar
      nsv=npar+1
c
      cond = 0
c  initial conditions of the problem
      if (cond.eq.1) then
            do 30 ih = 1,nh+1
            read (5,*) ht(ih),cg(1,ih),co(1,ih)
            cnfc = 4.7649
            cg(1,ih) = cg(1,ih)*cnfc

   30  continue
```

```
c for start-up only
      else
            do 31 ih = 2,nh+1
            cg(1,ih) = 1.0e-2
            co(1,ih) = 1.0
   31   continue
      endif
c
c
c  film thickness and effectiveness factors are
c  estimated from steady state models and correlations
c  are used
c
      avcg = acg01
      call pdelef ( avcg, del, ef1)
      call prm (1000,ak1,ak2,g,e1,e2,bet,rho)
c
      do 32 ih = 1,nh+1
      cp(1,ih) = cg(1,ih)/rho
   32 continue
c
      do 35 ih = 1,nh
      y(ih,1)      = cg(1,ih+1)
      y(ih+nh,1)   = co(1,ih+1)
      y(ih+2*nh,1) = cp(1,ih+1)
   35 continue
c
      ht(1)  = 0.0
      time(1) = 0.0
      dz     = 1.0/float(nh)
c
c   error control
c
      err=1.d-12
      itol=4
      do 20 i=1,n
      do 20 j=1,nsv
      rtol(i,j)=err
   20 atol(i,j)=err
c
c   parameters for odessa
c
      itask=1
      iopt(1)=0
      iopt(2)=0
      iopt(3)=1
      lrw=5000
      liw=100
      mf=21
c
      do 69 it =1,nt
      cg(it,1) = 1.0
      co(it,1) = 1.0
```

```
      cp(it,1) = cg(it,1)/rho
   69 continue
c
      par(1) = e1
      par(2) = e2
      par(3) = g
      par(4) = ak1
      par(5) = ak2
      par(6) = bet
      par(7) = rho
c
      T      = time(1)
      delta  = 0.016667
      istate = 1
c
      do 60 it = 2,nt
c
      tout   = t + delta
      time(it) = tout
c
      CALL ODESSA(fun,dfun,NEQ,Y,PAR,T,TOUT,ITOL,RTOL,ATOL,
     1   ITASK,ISTATE, IOPT,RWORK,LRW,IWORK,LIW,jfun,MF)
      do 65 ih = 1, nh
      cg (it,ih+1) = y(ih,1)
      co (it,ih+1) = y(ih+nh,1)
      cp (it,ih+1) = y(ih+2*nh,1)
   65 continue
c
c     checking if steady state is reached
c
      d1 = abs (cg(it, nh+1)-cg(it-1, nh+1))
      d2 = abs (co(it, nh+1)-co(it-1, nh+1))
      d3 = abs (cp(it, nh+1)-cp(it-1, nh+1))
      if(d1.le.1.0e-7.and.d2.le.1.0e-7.and.
     &  d3.le.1.0e-5) then
      go to 46
      else
      endif
c
      avcg = cg(it,nh/2)*acg01
c
      call pdelef (avcg, del, ef1)
      call prm (2000,ak1,ak2,g,e1,e2,bet,rho)
      par(4) = ak1
      par(5) = ak2
      if(istate.lt.0)then
      go to 45
      else
      endif
   60 continue
c
c     output your results
c
   46 ntlast = it
```

```
      call print (cg,co,cp,time,ht,ntlast)
      call printxxx (cg,co,cp,time,ht,ntlast)
      write(7,47) tout*tau*24, it, nt
   47 format(//,5x,'Steady state has reached in',f10.3,
     &' hrs',/,5x,'Iterations = ',i10,/,5x,'Maximum
     &  Iterations = ',i10,//)
   45 write(6,*) '  istate=  ',istate
      stop
      end
c*************************************************************************
c print concentration changes along the column time
c*************************************************************************
      subroutine print(cg,co,cp,time,ht,ntlast)
      implicit double precision(a-h,o-z)
      parameter(nt=100)
      parameter(nh=20)
      dimension cg(nt,nh+1), co(nt,nh+1), cp(nt,nh+1),
     1          time(nt), ht(nh+1)
      write (6,84)
      hts = 0
   84 format(//,5x,'Solution of the Transient Model',//)
      do 85 it = 1, ntlast
      write (6,86) time(it)
      hts = 0
   86 format (/, 10x, 'At Time  =  ', f14.3,/)
      write (6,89)
   89 format(//,8x,'h/H',9x,'cg',13x,'co',13x,'cp',//)
      do 95 ih = 1, nh+1
      write (6,96) hts, cg(it,ih), co(it,ih), cp(it,ih)
      hts = hts +.05
   96 format (5x, f7.3,3x,f10.4,5x,f10.4,5x,f10.4)
   95 continue
   85 continue
c
      return
      end
c*************************************************************************
c print concentration changes at the exit of the column with time
c*************************************************************************
      subroutine printx(cg,co,cp,time,ht,ntlast)
      implicit double precision(a-h,o-z)
      parameter(nt=100)
      parameter(nh=20)
      dimension cg(nt,nh+1), co(nt,nh+1), cp(nt,nh+1),
     1          time(nt), ht(nh+1)
      common /acg01/ acg01,tau
      write (7,84)
   84 format(//,5x,'Solution of the Transient Model',//)
      write (7,89)
   89 format(//,8x,'time',9x,'cge',13x,'coe',13x,'cpe',//)
      do 85 it = 1, ntlast
      write (7,96) time(it), cg(it,nh+1), co(it,nh+1), cp(it,nh+1)
   96 format (5x, f7.3,3x,f10.4,5x,f10.4,5x,f10.4)
   97 format (5x, e7.3,3x,e10.4)
```

```
  85 continue
c
      return
      end
c*************************************************************************
c print concentration changes at the selected locations
c*************************************************************************
      subroutine printxxx (cg,co,cp,time,ht,ntlast)
      implicit double precision(a-h,o-z)
      parameter(nt=100)
      parameter(nh=20)
      dimension cg(nt,nh+1), co(nt,nh+1), cp(nt,nh+1),
     1          time(nt), ht(nh+1)
      common /acg01/ acg01,tau
      write (7,84)
  84 format(//,5x,'Solution of the Transient Model',//)
      write (7,89)
  89 format(//,8x,'t (d)',7x,'cg-0.333',7x,'cg-0.666',8x,'cge',//)
c  89 format(//,8x,'t (h)',7x,'cg-0.333',7x,'cg-0.666',8x,'cge',//)
      do 85 it = 1, ntlast
      days = time(it)*tau
c     hours = time(it)*tau
      cg333 = 0.66*(cg(it,8)-cg(it,7))+cg(it,7)
      cg666 = 0.32*(cg(it,13)-cg(it,12))+cg(it,13)
      write (7,96) days, cg333,cg666,cg(it,nh+1)
  96 format (5x, f7.5,3x,f10.4,3x,f10.4,5x,f10.4)
  97 format (5x, e7.5,3x,e10.4)
  85 continue
c
      return
      end
C*************************************************************************
c  this subroutine computes the vectorfield
c*************************************************************************
      subroutine fun(neqn,t,y,par,ydot)
      IMPLICIT DOUBLE PRECISION (A-H,O-Z)
      dimension y(neqn),ydot(neqn),par(7)
      common /por/ por
      common /dz / dz
      common /fp / an
c
      nh = neqn/3
c
      do 10 i = 1,nh
      y1   = par(1)*par(2)*y(i)*y(i+nh)
      y2   = 1.+par(1)*y(i)+par(1)**2*y(i)**2*par(3)
      y3   = 1+par(2)*y(i+nh)
      fun1 = y1/y2/y3
      fun2 = y(i)-par(7)*(y(i+2*nh))**an
c
      if (i.eq.1)then
      der1  = (y(i)-1)/dz
      else
      der1  = (y(i)-y(i-1))/dz
```

```
      endif
c
      ydot(i)= -der1/por-par(4)*fun1-par(6)*fun2
 10   continue
c
      do 20 i = nh+1, 2*nh
      y1   = par(1)*par(2)*y(i-nh)*y(i)
      y2   = 1.+par(1)*y(i-nh)+par(1)**2*y(i-nh)**2*par(3)
      y3   = 1+par(2)*y(i)
      fun1 = y1/y2/y3
c
      if (i.eq.(nh+1))then
      der2  = (y(i)-1)/dz
      else
      der2  = (y(i)-y(i-1))/dz
      endif
c
      ydot(i)= -der2/por-par(5)*fun1
 20   continue
c
      do 30 i = 2*nh+1,3*nh
      fun2 = y(i-2*nh)-par(7)*(y(i))**an
      ydot(i)= par(6)*fun2
 30   continue
c
      RETURN
      END
C*******************************************************************************
c  this subroutine computes the jacobian
c  of the vectorfield
c*******************************************************************************
      subroutine jfun(neqn,t,y,par,ml,mu,pd,nrpd)
      implicit double precision (a-h,o-z)
c
      dimension y(neqn),pd(nrpd,neqn),par(7)
c
      common /por/ por
      common /dz / dz
      common /fp/ an
c
      nh = neqn/3
c
c
c  jacobian of the vectorfield
c
      do 9 i=1,neqn
      do 9 j=1,neqn
   9  pd(i,j)=0.
c
c for i = 1
c
      i    = 1
      y1   = par(1)*par(2)*y(i)*y(i+nh)
      y2   = 1.+par(1)*y(i)+par(1)**2*y(i)**2*par(3)
```

```
      y3   = 1+par(2)*y(i+nh)
      y4   = y1*y3*par(1)*(1.+2.*par(1)*y(i)*par(3))
      dfyi = (y1*y2*y3/y(i)-y4)/y2**2/y3**2
      pd(1,1) = -1/por/dz-par(4)*dfyi-par(6)
c
      dfyn = (y1*y2*y3/y(1+nh)-y1*y2*par(2))/y2**2/y3**2
      pd(1, nh+1) = -par(4)*dfyn
      pd(1,2*nh+1) = par(6)*par(7)*an*(y(i+2*nh))**(an-1)
c
c for i = 2, nh
c
      do 10 i = 2, nh
      pd (i, i-1) = 1/por/dz
c
      y1   = par(1)*par(2)*y(i)*y(i+nh)
      y2   = 1.+par(1)*y(i)+par(1)**2*y(i)**2*par(3)
      y3   = 1+par(2)*y(i+nh)
      y4   = y1*y3*par(1)*(1.+2.*par(1)*y(i)*par(3))
      dfyi = (y1*y2*y3/y(i)-y4)/y2**2/y3**2
c
      pd(i,i) = -1/por/dz-par(4)*dfyi-par(6)
c
      dfyn = (y1*y2*y3/y(i+nh)-y1*y2*par(2))/y2**2/y3**2
      pd(i, nh+i) = -par(4)*dfyn
c
      pd(i,2*nh+i) = par(6)*par(7)*an*(y(i+2*nh))**(an-1)
  10  continue
c
c for i = nh+1
c correct i value dont change....
c
      i    = 1
      y1   = par(1)*par(2)*y(i)*y(i+nh)
      y2   = 1.+par(1)*y(i)+par(1)**2*y(i)**2*par(3)
      y3   = 1+par(2)*y(i+nh)
      y4   = y1*y3*par(1)*(1.+2.*par(1)*y(i)*par(3))
      dfyi = (y1*y2*y3/y(i)-y4)/y2**2/y3**2
      pd(nh+1,1) = -par(5)*dfyi
c
      dfyn = (y1*y2*y3/y(1+nh)-y1*y2*par(2))/y2**2/y3**2
      pd(nh+1, nh+1) = -1/por/dz-par(5)*dfyn
c
c
c for i = nh+2 to 2*nh
c
      do 20 i = nh+2, 2*nh
      pd (i, i-1) = 1/por/dz
c
      y1   = par(1)*par(2)*y(i-nh)*y(i)
      y2   = 1.+par(1)*y(i-nh)+par(1)**2*y(i-nh)**2*par(3)
      y3   = 1+par(2)*y(i)
      y4   = y1*y3*par(1)*(1.+2.*par(1)*y(i-nh)*par(3))
      dfyi = (y1*y2*y3/y(i-nh)-y4)/y2**2/y3**2
c
```

```
      pd(i,i-nh) = -par(5)*dfyi
c
      dfyn = (y1*y2*y3/y(i)-y1*y2*par(2))/y2**2/y3**2
      pd(i, i) = -1/por/dz-par(5)*dfyn
 20   continue
c
c
c
c for i = 2*nh+1 to 3*nh
c
      do 30 i = 2*nh+1, 3*nh
      pd (i, i-2*nh) = par(6)
      pd (i,i) = -par(6)*par(7)*an*(y(i))**(an-1)
 30   continue
c
      RETURN
      END
C*********************************************************************
      subroutine dfun(neqn,t,y,par,dfdp,jpar)
c*****************************************
c     partial derivatives wrt. parameters of interest
c
      implicit double precision(a-h,o-z)
      dimension y(neqn),par(20),dfdp(20)
      return
      end
c*********************************************************************
c-----------------------------------------------------
c    dummy subroutines
c-----------------------------------------------------
      subroutine bcnd
      return
      end
      subroutine fopt
      return
      end
      subroutine icnd
      return
      end
c*********************************************************
       subroutine prm (index,ak1,ak2,g,e1,e2,bet,rho)
       implicit double precision (a-h,o-z)
       common /por/ por
       common /del/ del
       common /ef1/ ef1
       common /acg01/ acg01,tau
       common /fp/ an
c
c 1-benzene-compound
c 2-oxygen
c
c       del = del*1e-6
c
            del = 0.0
```

```
      b0    = 0.0
c
c      xv   = b0/1000
          xv  = 0.0

c      fd   = 1-0.43*xv**0.92/(11.19+0.27*xv**0.99)
          fd = 0.0
c
      call compm (fd,  df1, ay1, ay2, akii1,
     &  akss1, amu1,amm1)
c
      amm2 =  34.4
c      df2  = 2.41e-9 *3600.*fd
      df2 = 0.0

c      akss2 = 0.26
          akss2 = 1.0e-14
c
          ACG01 = 1.056
      aug   = 0.01258
          vv    = 834.4855e-6
c
c in days
c
      tau   = vv/aug/24.0
c in hours
c          tau = vv/aug
c
      acg02 = 275
c
      ef2  = ef1
c      alp  = 0.3
          alp = 0.0
      por  = 0.324
      aka  = 0.00231
      rp   = 0.679e6
c
c  Freundlich Isotherm,
c
      akd  = 3.71e-5
      an   = 0.983
c
c      sur = 40.0/alp
          sur = 184.8
c
      if (index. eq. 1000) then
      CALL SVARI(sur,b0,vv,df1,df2,ay1,ay2,AKII1,AKSS1,
     &  del,amu1,akss2,acg01,acg02,aug, amm1,amm2,
     &  ef1, ef2, alp, por, aka, an, rp, akd)
      else
      endif
c
c      ak1=ef1*alp*sur*del*b0*vv*amu1/ay1/aug/acg01/por
c      ak2=ef2*alp*sur*del*b0*vv*amu1/ay2/aug/acg02/por
```

```
c      g =akss1/akii1
c      e1=acg01/amm1/akss1
c      e2=acg02/amm2/akss2
          ak1 = 0.0
          ak2 = 0.0
          g = 0.0
          e1 = 0.0
          e2 = 0.0
c
      factor = 1.0
c
      bet = aka*(1-alp)*sur*vv/aug/por*factor
c
      rho = acg01**(an-1)*(por/rp/akd/(1-por))**an
c
      if (index. eq. 1000)then
      write(6,123)
      WRITE(6,1)
    1  FORMAT (10x,'Parameters Estimated from the Data Above', /)
      WRITE(6,2) ak1, ak2
      WRITE(6,3) e1, e2
    2  FORMAT (' ', ' ak1   =  ',e14.3,3x,'ak2 = ',3x,f7.3)
    3  FORMAT (' ', ' eps1 =  ',f14.6,3x,'eps2   = ',3x,f7.3)
      WRITE(6,4) g,bet
      WRITE(6,5) rho
    4  FORMAT (' ', ' g =  ',e14.3,5x,'bet =', f10.6,/)
    5  FORMAT (' ', ' rho =  ',e14.3,3x,/)
      write(6,123)
      else
      endif
  123  FORMAT(' _____',/)
      return
      end
c*****************************************************************
     subroutine pdelef (avcg, del, ef1)
     implicit double precision (a-h,o-z)
c     del = 1.513*avcg+33.35
c     ef1 = 0.031*avcg+0.190
     del = 1.0e-14
     ef1 = 1.0e-14
     return
     end
C*****************************************************************
      subroutine compm (fd,  df1, ay1, ay2, akii1,
     &  akss1, amu1,amm1)
      implicit double precision (a-h,o-z)
c
c      df1   = 1.0315e-9 *3600.*fd
          df1 = 0.0
c      ay1   = 0.71
c      ay2   = 0.341
          ay1 = 1.0e-10
          ay2 = 1.0e-10
c      akii1 = 78.94
```

```
c      akss1 = 11.03
         akii1 = 1.0e-10
         akss1 = 1.0e-10
c      amu1  = 1.50
         amu1 = 1.0e-10
       amm1 = 0.27

c
       return
       end
c*****************************************************************
       Subroutine SVARI(sur,b0,vv,df1,df2,ay1,ay2,AKII1,AKSS1,
     &  del,amu1,akss2,acg01,acg02,aug, amm1,amm2,
     &  ef1, ef2, alp, por, aka, an, rp, akd)
c
       write(6,123)
       WRITE(6,1)
    1  FORMAT (5x,/, ' Input data for Transient Biofilter Model',/)
       WRITE(6,19) Aug
   19  format (' ', 'Gas Flow Rate (m3/hr)       = ', e14.3)
       WRITE(6,3) vv*1e6
    3  FORMAT (' ', 'Volume of the column(cm3)   = ', f14.3)
       WRITE(6,4) SUR
    4  FORMAT (' ', 'Biolayer Sur.Area( m2/m3)   = ', f14.3)
       write(6,44) b0
   44  format (' ', 'Biomass Conc. (g/m3)        = ', e14.3)
       WRITE(6,5) del*1e3
    5  FORMAT (' ', 'Film thickness (mm)         = ', f14.3)
       WRITE(6,2) ACG01
       WRITE(6,22) ACG02
    2  FORMAT (' ', 'Inlet conc. (g/m3 of air)(m) = ', f14.3)
   22  FORMAT (' ', 'Inlet conc. (g/m3 of air)(o) = ', f14.3)
       write(6,31) ay1
   31  format (' ', 'Yield Coefficient (1)       = ', f14.3)
       write(6,32) ay2
   32  format (' ', 'Yield Coefficient (o)       = ', f14.3)
       WRITE(6,51) df1*1e9/3600
       WRITE(6,54) df2*1e9/3600
   51  format (' ', 'Diff. Coefficient (1)*1e9   = ', f14.3)
   54  format (' ', 'Diff. Coefficient (o)*1e9   = ', f14.3)
       WRITE(6,56) amm1
   56  FORMAT (' ', 'Dist. Coeff.       (1)     = ', e14.3)
       WRITE(6,566) amm2
  566  FORMAT (' ', 'Dist. Coeff.       (o)     = ', e14.3)
       WRITE(6,567) ef1
  567  FORMAT (' ', 'ef-factor (1)               = ', e14.3)
       WRITE(6,568) ef2
  568  FORMAT (' ', 'ef-factor (2)               = ', e14.3)
       WRITE(6,569) por
  569  FORMAT (' ', 'porosity                    = ', e14.3)
       WRITE(6,570) aka
  570  FORMAT (' ', 'mass transfer coef.         = ', e14.3)
       WRITE(6,571) akd
  571  FORMAT (' ', 'adsorption parameter (akd)  = ', e14.3)
```

```
      WRITE(6,572) an
  572   FORMAT (' ', 'adsorption parameter (an)    = ', e14.3)
      WRITE(6,573) rp/1e6
  573   FORMAT (' ', 'particle density (g/cm3)     = ', e14.3)
      WRITE(6,574) alp
  574   FORMAT (' ', '% area covered by biomass    = ', e14.3)
      write(6,123)
      write(6,*) '          Andrews and other  Parameters'
      WRITE(6,6) akii1,akss1,amu1, akss2
    6   format(' ',/, ' Ki1 (g/m3) = ',e14.3,3x,'Ks1 (g/m3) = ', f7.3,
     &  /,' Sp. Growth Rate-1 (1/hr)=',f14.3,3x,/,' ',
     &  'aKd (g/m3) = ', f7.3,/)
      write(6,123)
  123   FORMAT(' ____________________________________________________________',/)
      return
      end
c*****************************************************************
```

APPENDIX C

TABLES OF MASS TRANSFER COEFFICIENT VALUES

Table C-1 Values for Mass Transfer Coefficient (Runs with benzene only).

Residence Time (min)	Air Flow Rate (m^3/h)	q (m/h)	k_a (m/h)
2.2	0.0229	11.67	0.001451
2.5	0.0249	12.68	0.001405
1.0	0.0498	25.37	0.001762
4.9	0.0102	5.20	0.001184
1.3	0.0376	19.15	0.001643
3.4	0.0147	7.49	0.001300
2.0	0.0249	12.68	0.001484
0.9	0.0540	27.51	0.001789
4.0	0.0120	6.11	0.001235

Table C-2 Values for Mass Transfer Coefficient (Runs with toluene only).

Residence Time (min)	Air Flow Rate (m^3/h)	q (m/h)	k_a (m/h)
1.6	0.0315	16.05	0.001550
0.8	0.0615	31.33	0.001858
4.8	0.0100	5.09	0.001181
0.8	0.0615	31.33	0.001858
2.1	0.0220	11.21	0.001482
2.3	0.0215	10.95	0.001428
3.4	0.0140	7.13	0.001300
4.2	0.0110	5.60	0.001217

Table C-3 Values for Mass Transfer Coefficient (Runs with benzene/toluene mixtures).

Residence Time (min)	Air Flow Rate (m^3/h)	q (m/h)	k_a (m/h)
1.59	0.0319	16.25	0.001572
1.18	0.0424	21.60	0.001693
1.23	0.0407	20.73	0.001676
1.06	0.0472	24.04	0.001739
2.33	0.0215	10.95	0.001428
4.41	0.0114	5.81	0.001218
2.70	0.0186	9.48	0.001377
1.81	0.0276	14.06	0.001521
6.29	0.0126	6.42	0.001250
2.14	0.0230	11.72	0.001459

REFERENCES

Androutsopoulou, H., 1994. *A Study of the Biofiltration Process Under Shock-Loading Conditions*, MS Thesis, New Jersey Institute of Technology, Newark NJ.

Baltzis, B.C. and S.M. Wojdyla. 1995a. "Towards a Better Understanding of Biofiltration of VOC Mixtures," pp. 131-138 in *Proceedings of the 1995 Conference on Biofiltration (an Air Pollution Control Technology)*, D.S. Hodge and F.E. Reynolds Jr. (eds.), Tustin CA.

Baltzis, B.C. and S.M. Wojdyla. 1995b. "Characteristics of Biofiltration of Hydrophilic VOC Mixtures," pp. 322-331 (vol. B) in *Proceedings of the 4th Conference on Environmental Science and Technology,* Th. Lekkas (ed.), University of the Aegean Press, Lesvos, Greece (1995).

Baltzis, B.C. and Z. Shareefdeen. 1994. "Biofiltration of VOC Mixtures: Modeling and Pilot Scale Experimental Verification," *Proceedings of the 87th Annual A&WMA Meeting, Cincinnati, OH*, Paper No. 94-TA260.10P.

Banerjee, K. 1988. *Sorption and Desorption of Organic Compounds by Flyash.* PhD Thesis, New Jersey Institute of Technology, Newark, NJ.

Cohen, M.L. 1996. *CSensitivity Analysis and Design Calculations with Biofiltration Models*. MS Thesis, New Jersey Institute of Technology, Newark, NJ.

Devinny, J.S. 1995 "Host Presentation: Topics for Research in Biofiltration," pp. vi-xiii in *Proceedings of the 1995 Conference on Biofiltration (an Air Pollution Control Technology)*, D.S. Hodge and F.E. Reynolds Jr. (eds.), Tustin CA.

Doedel, E.J. 1986. *AUTO: Software for Continuation and Bifurcation Problems in ODEs*. CIT Press, Pasadena, CA.

Environmental Protection Agency. 1986. *Test methods for evaluating solid waste*, vol IA. SW-846. 3rd ed. US EPA, Washington D.C.

Fritz, W., W. Merk, and E.U. Schlunder. 1981. "Competitive Adsorption of Two Dissolved Organics onto Activated Carbon-II," *Chem. Eng. Sci.* **36**: 731-741.

Golshan-Shirazi, S., Huang, J.X., and G.A. Guiochon. 1991. "Comparison of an Experimental Competitive Isotherm and the Levan-Vermeulen Model and Prediction of Band Profiles in a Case of Selectivity Reversal," *Anal. Chem.* **63**: 1147-1154.

Hodge, D.S. 1995. "Determination of Mathematical Model Constants Using Specially Designed Mini-Column Biofilters," pp. 53-70 in *Proceedings of the 1995 Conference on Biofiltration (an Air Pollution Control Technology)*, D.S. Hodge and F.E. Reynolds Jr. (eds.), Tustin CA.

Jacobson, J.M., J.H. Frenz, and C. Horvath. 1987. "Measurement of Competitive Adsorption Isotherms by Frontal Chromatography," *Ind. Eng. Chem. Res.* **26**: 43-50.

Jennings, P.A. 1975, *A Mathematical Model for Biological Activity in Expanded Bed Adsorption Columns*, PhD Thesis, University of Illinois, Urbana Champaign.

Jones, W.L., J.D. Dockery, C.R. Vogel, and P.J. Sturman. 1993. "Diffusion and Reaction within Porous Packing Media: A Phenomenological Model," *Biotechnol. Bioeng.* **41**: 947-956.

Kataoka, T., H. Yoshida, and T. Yamada. 1973. "Liquid Phase Mass Transfer in Ion Exchange Based on the Hydraulic Radius Model," *J. Chem. Eng. of Japan* **6**(2): 172-177.

Kinniburgh, D.G. 1986. "General Purpose Adsorption Isotherms," *Environ. Sci. & Technol.* **20**(9):895-904.

Leson, G. and A.M. Winer. 1991. "Biofiltration: An Innovative Air Pollution Control Technology for VOC Emissions," *J. Air & Waste Manage. Assoc.* **41**(8): 1045-1054.

Moretti, E.C. and N. Mukhopadhyay. 1993. "VOC Control: Current Practices and Future Trends," *Chem. Eng. Progress* **89**(7): 20-26.

Onda, K., H. Takeuchi, and Y. Okumoto. 1968. "Mass Transfer Coefficients Between Gas and Liquid Phases in Packed Columns," *J. Chem. Eng. of Japan* **1**(1): 56-62.

Ottengraf, S.P.P, J.J.P. Meesters, A.H.C. van den Oever, and H.R. Rozema. 1986. "Biological Elimination of Volatile Xenobiotic Compounds in Biofilters," *Bioprocess Eng.* **1**: 61-69.

Ottengraf, S.P.P. and A.H.C. van den Oever. 1983. "Kinetics of Organic Compound Removal from Waste Gases with a Biological Filter," *Biotechnol. Bioeng.* **25**: 3089-3102.

Perry R.H. and D. Green, 1984. *Perry's Chemical Engineers' Handbook*, Sixth Edition, McGraw-Hill Inc., New York.

Pinnette, J.R., C.A. Dwinal, M.D. Giggey, and G.E. Hendry. 1995a. "Design Implications of the Biofilter Heat and Moisture Balance," pp. 85-98 in *Proceedings of the 1995 Conference on Biofiltration (an Air Pollution Control Technology)*, D.S. Hodge and F.E. Reynolds Jr. (eds.), Tustin CA.

Pinnette, J.R., C.A. Dwinal, and M.D. Giggey. 1995b. "Porosity of Biofilter Media," pp. 207-216 in *Proceedings of the 1995 Conference on Biofiltration (an Air Pollution Control Technology)*, D.S. Hodge and F.E. Reynolds Jr. (eds.), Tustin CA.

Robinson, S.M., W.D. Arnold, and C.H. Byers. 1991. "Multicomponent Ion-Exchange Equilibria in Chabazite Zeolite," pp. 133-152. In: D.W. Tedder, and F.G. Pokland, (eds.), *Emerging Technologies in Hazardous Waste Management II.* ACS Symposium Series **468**. American Chemical Society, Washington, DC.

Rogers, L, J.C. McFarlane, and A.J. Cross. 1980. "Adsorption and Desorption of Benzene in Two Soils and Montmorillonite Clay," *Environ. Sci. & Technol.* **14**(4): 457-461.

Seed, L.P. and R.L. Corsi. 1994. "Biofiltration of BTEX-Contaminated Gas Streams; Laboratory Studies," *Proceedings of the 87th Annual A&WMA Meeting, Cincinnati, OH,* Paper No. 94-RA115A.01.

Shareefdeen, Z., 1994. *Engineering Analysis of a Packed-Bed Biofilter for Removal of Volatile Organic Compound(VOC) Emissions*, PhD Thesis, New Jersey Institute of Technology, Newark NJ.

Shareefdeen, Z., B.C. Baltzis, Y. Oh, and R. Bartha. 1993. "Biofiltration of Methanol Vapor," *Biotechnol. Bioeng.* **41**: 512-524.

Shareefdeen, Z. and B.C. Baltzis. 1994. "Biofiltration of Toluene Vapor Under Steady-State and Transient Conditions: Theory and Experimental Results," *Chem. Eng. Sci.* **49**: 4347-4360.

Stuart, B.J., G.F. Bowlen, and D.S. Kosson. 1991. "Competitive Sorption of Benzene, Toluene and Xylenes onto Soil," *Environmental Progress* **10**(2): 104-109.

Tahraoui, K., R. Samson, and D. Rho. 1994. "Biodegradation of BTX from Waste Gases in a Biofilter Reactor," *Proceedings of the 87th Annual A&WMA Meeting, Cincinnati, OH*, Paper No. 94-TA260.07P.

Thibodeaux, L. J. 1979. *Chemo-Dynamics: Environmental Movement of Chemicals in Air, Water, and Soil.*, John Wiley & Sons, New York.

Weber, Jr., W.J. and E.H. Smith. 1987. "Simulation and Design Models for Adsorption Processes," *Environ. Sci. & Technol.* **21**(11): 1040-1050.

Yen, C. and P.C. Singer. 1984. "Competitive Adsorption of Phenols on Activated Carbon," *J. Env. Eng.* **110**(5): 976-989.

Zilli, M., A. Converti, A. Lodi, M. Del Borghi, and G. Ferraiolo. 1993. "Phenol Removal from Waste Gases with a Biological Filter by *Pseudomonas putida*," *Biotechnol. Bioeng.* **41**: 693-699.

Ziminski, R.W. and J. Yavorsky. 1994. "Control of Hazardous Air Pollutants Using a Commercial Biofilter," *Proceedings of the 87th Annual A&WMA Meeting, Cincinnati, OH,* Paper No. WA74A.02.